University of Stavanger

Faculty of Science and Technology

MASTER'S THESIS

Study program/Specialization: Marine and Offshore Technology	Spring semester, 2021 Open
Writer: Erik Dahl Fidje	Erik Dahl Fidje ..... (Writer's signature)
Supervisor: Prof. Yihan Xing	
Thesis title: Development of roll stabilization on a large zero-energy freighter-ship using sails.	
Credits (ECTS): 30	
Keywords: Roll stabilization Seakeeping capabilities Bilge keel ANSYS AQWA Response Amplitude Operator Added mass	Pages: 93 + Enclosure: 2 **Stavanger,** **June 14th 2021**

Preface and acknowledgments

This thesis was completed in the spring of 2021 as a final project of the Master of Science degree in Marine and Offshore Technology course at the University of Stavanger.

The theme of this thesis is an optimization of roll stabilization for a large vessel using sails. The objective is to improve the methods of designing ships utilizing sails as means of propulsion.

I want to offer my appreciation to my supervisor, Professor Yihan Xing from the University of Stavanger, for the proposal of this exciting and educational thesis. Additionally, I want to thank him for his guidance, encouragement, and expert advice throughout this duration.

I would also like to thank my fellow students for their encouraging words and pleasant working environment throughout the entirety of the past two years. Additionally, I want to thank my family for always supporting me.

Stavanger, June 2021

Erik Dahl Fidje

Abstract

In recent years, research for creating climate-friendly solutions has become more desired. As the transport of cargo by sea is heavily utilized and will continue to be so, this is an area that can be improved. During this thesis, the main focus will be on analyzing the effect of roll motion mitigation and investigating the optimal solution to reduce roll motion for a large cargo ship using sails as means of propulsion.

For the analysis, simulations will be performed using the ANSYS AQWA hydrodynamic diffraction and including an additional matrix to obtain the correct RAO (Response Amplitude Operator) values. Different alpha values are compared to showcase the potential effect of the viscous damping created by the keels. The RAO values that are obtained through the simulations will be presented and discussed. These simulations showcase that the efficiency of the keels increases when a more considerable alpha value is presented. Most of the simulations during this thesis are simulated with an alpha value of 0,01. Values of 0,02 and 0,05 are also presented as potential higher values of damping.

Research is showing that utilizing bilge keels become more effective when traveling at lower speeds and will due to this be the primary solution when analyzing roll mitigation. The simulations show that the bilge keels are becoming more effective when the ship´s heeling is increased. The keel with the higher aspect ratio is more effective, yet limitations in the size of the keel could prove vital if navigating shallower water become of interest. Due to this, a less wide keel could prove beneficial, even though a wider keel mitigates more roll motion.

The keels created for this study reduces the roll motion by 9% up to 30%, depending on the geometry of the keel, where the reduction increases with further heeling on the ship hull. The conclusion is that for a large freighter using sails as means of propulsion, bilge keels will be most effective as the cruising speed of the vessel will be lower than the traditional freighter ships.

Contents

List of Figures

List of Tables

1. Introduction

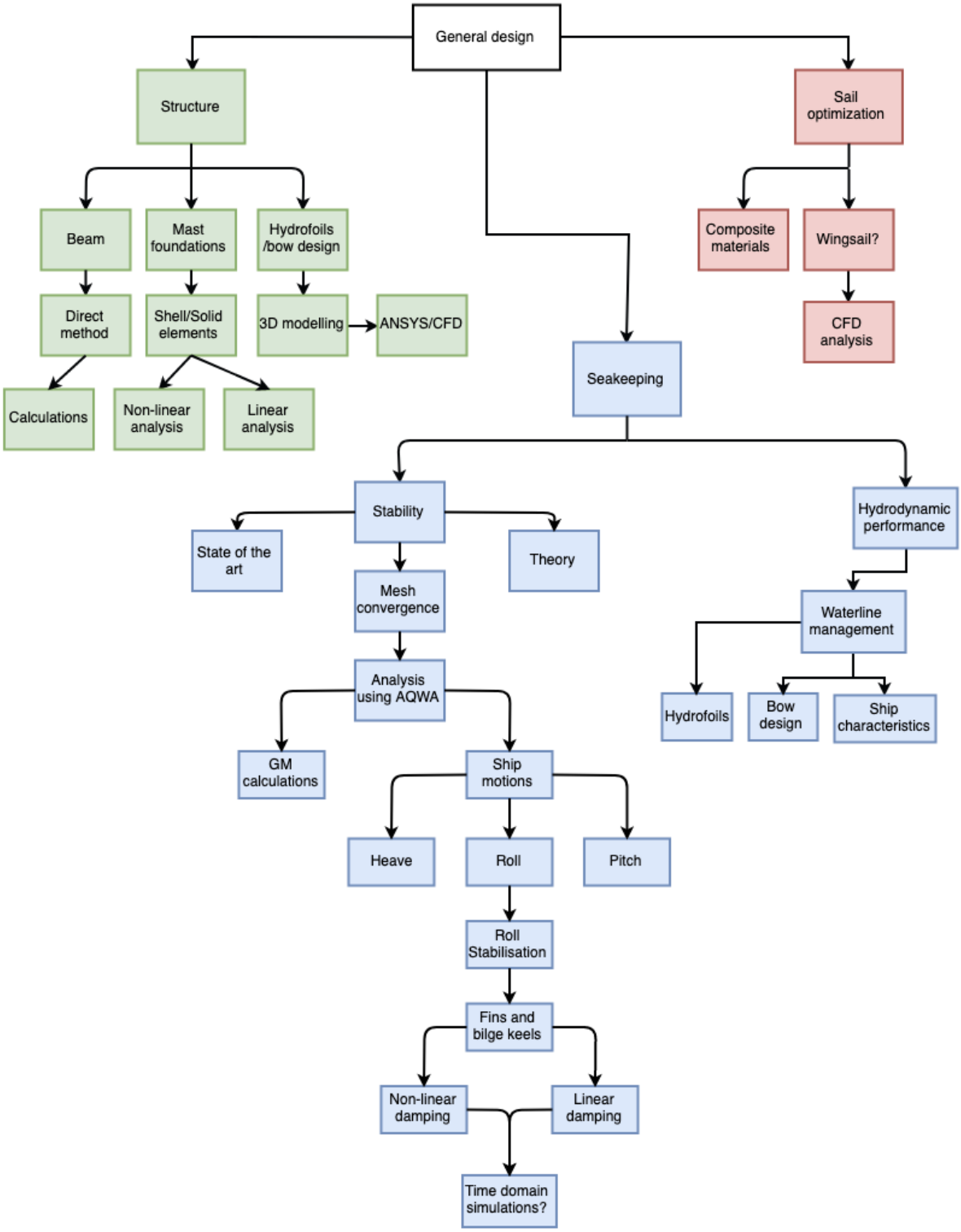

Figure 1.1 - Flowchart

This flowchart represents some key factors that will be discussed during this thesis. During the early stages of the semester, three different approaches are discussed, and it is decided to focus heavily on the stability regarding roll motion. The green and red routes shown in the figure above are not being focused on, and the path that will be followed during this thesis is the blue "Seakeeping → Stability." If time is available, time-domain simulations will be examined.

1.1 Background and Motivation

1.1.1. Motivation

As the focus on climate-friendly products has increased immensely in the last years, environmentally friendly solutions for transporting goods by sea are lacking. Around 11 billion tons of goods are transported by sea every year, as stated in [1]. Transporting goods by sea has opened many opportunities regarding trading between different nations and will have to continue. Hence, stopping this transport is not an acceptable solution.
Due to this, there is a vast potential to decrease the carbon footprint from goods transported by sea by providing an environmentally friendly solution for this transport.

In this project, looking at key features that are important when designing a zero-energy cargo-ship, could prove beneficial for other designs to come.

1.1.2. State of the Art

There is currently not a ship at the market which can transport goods at low emissions. However, there are a few that is under development.

The Oceanbird is predicted to deliver the first vessel by the end of 2024. Having sails that will reach up to 80 meters high when fully extended, they are looking to decrease the total emissions by about 90%. This cargo ship will transport up to a total of 7000 cars every trip. This solution is great for the climate, yet there are downsides. While reducing the emissions significantly, the transport duration will be increased by four full days, from 8 to 12, stated in this article[2]. This is because the vessel will not reach the speeds of a conventional cargo ship currently used. Figure 1.2 is presented in [3].

Figure 1.2 - Oceanbird

The UT Wind Challenger is also a project where the research has been going on since 2009 and mainly focuses on creating the sails provided to cargo ships. The sails mainly consist of aluminum and reinforced plastic material which makes the sails very rigid. They were expecting to deliver these sails during 2016 but have yet to be put into reality. Increased knowledge of the environmental difficulties of fuel will perhaps increase the interest significantly. Companies are more willing than previously to invest in climate-friendly solutions[4]. Figure 1.3 is presented in [5].

Figure 1.3 - UT Challenger

Roll stabilization:

Anti-roll tanks are used quite often when the goal is to reduce roll motion. One of the main advantages of anti-roll tanks is that they will reduce the roll motion while the vessel is not moving forward. This because the anti-roll tanks do not require any forward speed to be functioning. Anti-roll tanks operate in the way that most of the water will be trapped on the opposite side of the rolling motion[6][7][8]. An example of an Anti-roll tank is given in Figure 1.4 below.

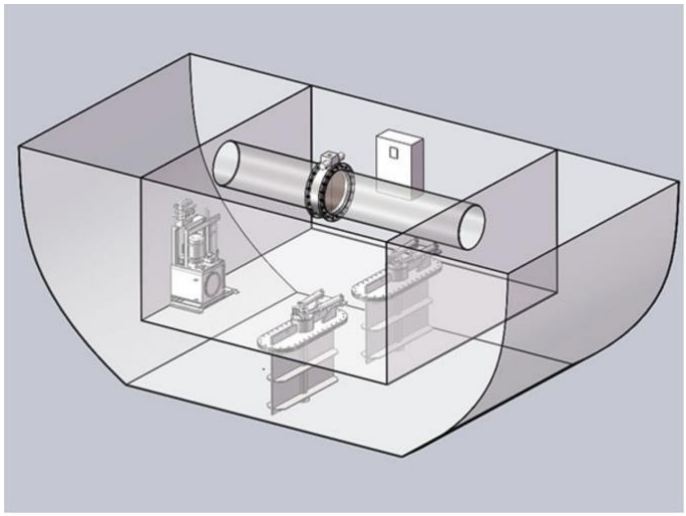

Figure 1.4 - Anti-roll tank[9]

Fins and bilge keels:

Stabilizer fins and bilge keels are often used with smaller ships utilizing sails. This is done by adding a geometry to reduce roll motion due to increased added mass in the roll direction. The fins and bilge keels are attached to the hull of the ship. Stabilizer fins can be active and passive, where the active fin has a mechanical part controlling the fin, and the passive does not.

Rotor sails:

Rotor sails are one of the solutions that have been used in recent years. Some cargo ships have been attached with pillars that rotate. The rotation creates an effect called the “Magnus effect.” This effect will propel the vessel forwards as a result of wind turning the pillar. Fuel consumption will be minimized when the conditions are favorable. Presented in this article[10].

1.1.3. Objective

During this project, there will be a closer look at some of the general vital factors that will make a ship like this perform at a high standard, introducing key factors such as; Seakeeping capabilities, sail performance and structural design. Many different elements are essential when designing a vessel, but for the purposes of this project and the time that is at disposal, seakeeping will be the main focus.

When analyzing the seakeeping capabilities of a ship, some key features arise. One of these features is roll stability. When designing a large vessel using sails as means of propulsion, the roll will be heavily affected by the force created by the wind. The sails will have a large area affected by the wind at a high altitude. This creates a significant moment force which will add to the roll moment created by the waves and wind on the ship's foundation. So, for a vessel using sails, it is essential to analyze the roll stabilization. Hence, this project will go deeper into the roll motion of a large ship with sails and also which methods will be practical regarding the reduction of potential roll motion of a vessel this size.
So, one of the main questions that will be answered during this thesis is;
What will be the most efficient roll reduction solution on a large ship using sails as means of propulsion?

1.1.4. Scope of the project

Firstly, in chapter 1, an introduction to the thesis will be presented. This will consist of background and motivation, state of the art, and also the objective of the thesis.
In chapter 2, the theory will be the subject. This will provide a general and vital insight into the approach that is being used during this thesis and also during simulations using Ansys software.
In chapter 3, the numerical method and methodology will be discussed. This will consist of the design variables, mesh convergence, and also the procedure of running the simulations using the additional matrix.

In chapter 4, the analysis will be presented. The study will consist of simulations without keel and simulations with different keel configurations.

In chapter 5, the conclusion and future recommendations will be presented and what can be done to bolster the analysis or take the work further.

2. Theory

2.1. Seakeeping

Seakeeping is the vessel´s ability to perform well in rough sea conditions. It is critical for a ship to withstand different type of waves/sea states but even though the vessel can withstand the waves does not mean it has good seakeeping capabilities. To be efficient, it has to maintain most of its speed and momentum when traveling through rough sea. This seakeeping capability is mainly affected by three components[11]:

- The incoming waves that will affect the ship
- Ships characteristics. (length, width, height, hull size)
- Ship motions, which is how the vessel will respond to the incoming waves and how the ship´s motion is affected by the wind.

There are generally multiple tools for predicting a ship's seakeeping capability. These tools are as following[12]:

- Model tests are usually performed using a large water tank.
- Measurements performed on a full-scale vessel traveling at sea.
- Computations in the frequency domain, using an alternative software program to determine the response of the vessel. This could be a program such as Ansys AQWA
- Computations in the time domain, which is a way to compute the response of a ship at a given point in time.

- Computations in the statistical domain, which are computations of significant seakeeping values in irregular sea. This could, for example, be exceeding limits such as motions or loads.

Seakeeping can also be referred to as “Safety at sea.” The ship's seakeeping capabilities can be seen as the ship's capability to survive all hazards, including rough sea states. Improving the ship´s seakeeping competence will increase the possibility of the ship´s return unharmed, explained in[13].

2.1.1. Roll stabilization

Roll motion of a vessel is a behavior that is important when talking about seakeeping capabilities. If the ship has too much roll motion, the ship will not be able to perform appropriately, and in the worst-case scenario, the vessel can capsize. If too much roll motion is the case, some modifications of the ship is necessary.
There are different ways to mitigate roll motion, and most of them use methods that oppose the roll motion.
As roll motion has low inherent damping, it is possible to increase the damping forces to reduce roll motion significantly. The reason for this is that the maximum roll motion amplitudes occur close to the natural frequency. On the other hand, for other motions where the inherent damping is high, the maximum motion amplitudes will occur where the frequency is close to 0. It is, therefore, more beneficial to increase the damping where the natural frequency is close to the high motion amplitudes, in this case, roll motion[14][15].

- Bilge keels are keels that are mounted at the turn of the bilge on a ship. As the keels have no mechanical parts, they are easy to mount and easy to maintain. They require the same maintenance as the hull. They have been widely tested and are proved to be very effective at reducing roll motion at lower cruise speeds. Below a picture of a bilge keel is presented in Figure 2.1.

Figure 2.1 - Bilge keel[16].

- Stabilizer fins are fins that are mounted on the hull of a ship. These fins generate a force that will create added mass. This added mass will mitigate some of the roll motion of the ship. As shown in Figure 2.2, the fin force will be opposite of the roll motion. The force created by the fins is determined by the angle and the speed of the vessel.

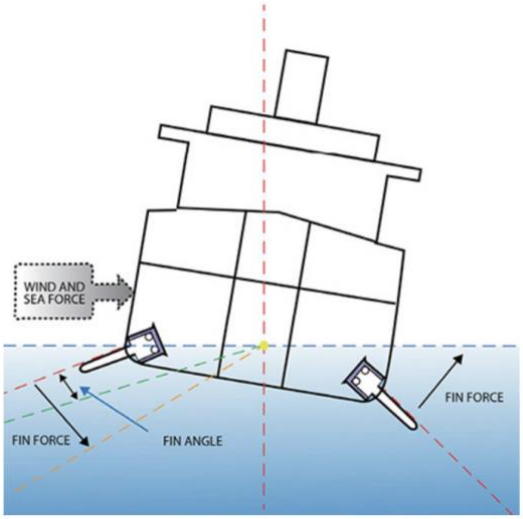

Figure 2.2 - Showing stabilizer fin forces[17].

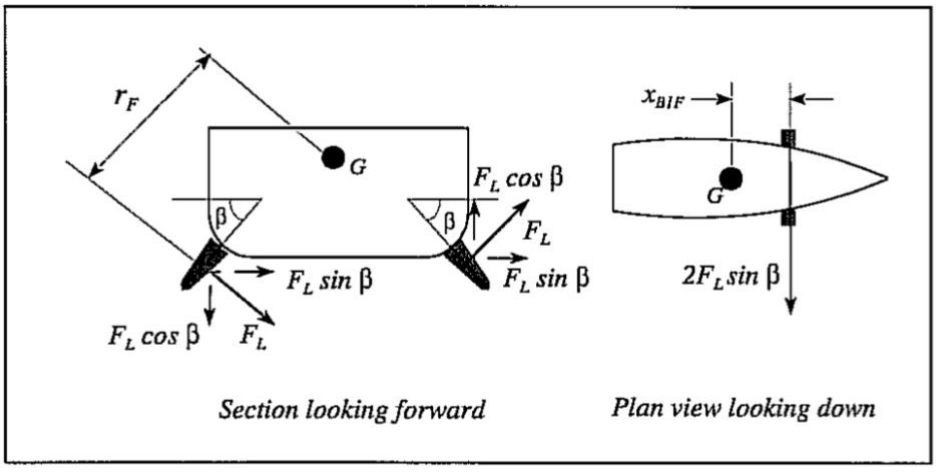

Figure 2.3 - More detailed version showing fin forces[14].

The force which will negate the roll motion is the resultant lift force applied by the stabilizer fins. The lift force generated by a single fin can be found using a formula for lift force given below[14][18].

$$F_L = C_L * \frac{1}{2} * \rho * U^2 * A_F \quad (1)$$

The lift forces will then result in a roll moment which will mitigate roll motion for the ship as the roll moment will always be working in the opposite direction of the roll motion. (equation 2).

$$2 * F_L * r_F \quad (2)$$

- Active vs. Passive system

  There is also the opportunity to use an active system compared to a passive approach mentioned above. The active system will have a moving part or a controlled mechanical surface to produce the anti-roll movement. Some examples of this could be anti-rolling tanks inside the ship, active fins, or a moving weight that will act opposite the rolling motion. The active systems are usually more effective, but the downside is that it is usually more expensive[19].

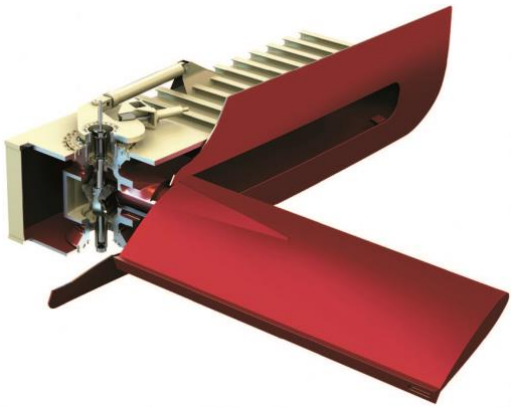

Figure 2.4 - Example of an active fin[20]

To give a perspective on the effectiveness of the different systems, a table from the book "Basic Ship Theory" provides an overview, shown in Table 2.1. It is evident that the active systems provide more roll reduction yet are more expensive when installed.

Table 2.1 - Comparison of different roll stabilization systems[21].

Type	Active Fins	Passive Tanks	Active Tanks	Bilge Keel
Percentage Roll Reduction	90%	60-70%	no data	35%
Effective at very low speeds	No	Yes	Yes	Yes
Increase in ship resistance	When in operation	No	No	No
Auxiliary Power requirement	Small	Nil	Large	Nil
Vulnerable to damage	Not when retracted	No	No	Yes
First Cost	High	Moderate	High	Low
Maintenance	Normal Mechanical	Low	Normal Mechanical	Often High

2.1.2. Hydrostatic

The hydrostatic of a ship is a measure of the stability of the vessel. Parameters such as metacentric height (GM) will heavily affect the roll motion of the ship. If a GM value becomes too low, the vessel can capsize[22]. If a GM value that is too high is obtained, the ship will have a shorter period of roll, which is acceptable but not preferred. The roll period is directly linked with the GM value, so having a desired GM is desirable[23][24].

$$\mathrm{GM} = \mathrm{BM} + \mathrm{KB} - \mathrm{KG} \qquad (3)$$

Where,

GM = Metacentric height

BM = Metacentric radius

KB = Keel to the center of buoyancy

KG = Keel to the center of gravity

When a ship utilizes sails as a means of propulsion, a sail force will affect the vessel. This will create a roll angle, dependent on how large this force is. The ship is rotating around the center of flotation (LCF). The LCF is defined as the center of the waterplane area. When the vessel is heeling, this waterplane area will change; hence the center of flotation will be shifted[25]. This center of flotation is being calculated through the AQWA software.

The longitudinal metacentric height and transverse metacentric height is calculated through AQWA using these equations:

$$\overline{GM_L} = \frac{I_{YY}}{\nabla} \tag{4}$$

$$\overline{GM_T} = \frac{I_{XX}}{\nabla} \tag{5}$$

The stiffness matrix is also found through AQWA software. AQWA uses these equations to measure the stiffness matrix[13], whereas the stiffness matrix is presented in Table 2.2.

Table 2.2 - Stiffness matrix, AQWA

$$\begin{matrix} 0 & 0 & 0 & 0 & 0 & 0 \\ 0 & 0 & 0 & 0 & 0 & 0 \\ 0 & 0 & K_{33} & K_{34} & K_{35} & 0 \\ 0 & 0 & K_{43} & K_{44} & K_{45} & K_{46} \\ 0 & 0 & K_{53} & K_{54} & K_{55} & K_{56} \\ 0 & 0 & 0 & 0 & 0 & 0 \end{matrix}$$

$$K_{33} = -\rho g \int_{S_0} n_3 dS = \rho g A \tag{6}$$

$$K_{34} = K_{43} = -\rho g \int_{S_0} (Y - Y_g) n_3 dS \tag{7}$$

$$K_{35} = K_{53} = \rho g \int_{S_0} (X - X_g) n_3 dS \tag{8}$$

$$K_{44} = -\rho g \int_{S_0} (Y - Y_g)^2 n_3 dS + \rho g (Z_B - Z_g) \nabla \tag{9}$$

$$K_{45} = K_{54} = -\rho g \int_{S_0} (X - X_g)(Y - Y_g) n_3 dS \tag{10}$$

$$K_{55} = -\rho g \int_{S_0} (X - X_g)^2 n_3 dS + \rho g (Z_B - Z_g) \nabla \tag{11}$$

$$K_{46} = -\rho g (X_B - X_g) \nabla \tag{12}$$

$$K_{56} = -\rho g (Y_B - Y_g) \nabla \tag{13}$$

2.2. Sail optimization

The sail-assisted research has had an increasing interest as the shipping industry has many advantages using this technology[27]. The advantages being less fuel consumption and CO2 emissions. This benefits both the company and the environment. In Figure 2.5, a sail is affected by relative wind speed coming from the North-West direction, if Y-axis is North.

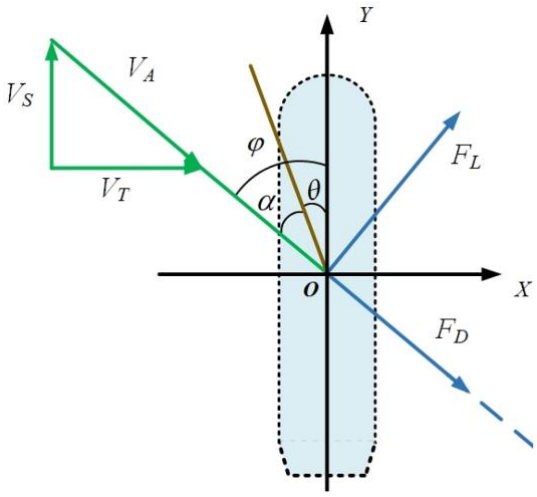

Figure 2.5 - Sail affected by relative wind speed. Showing resulting lift force and drag force[28]

Where;

$V_A = relative\ wind\ speed$

$F_D = drag\ force$

$F_L = lift\ force$

$\alpha = angle\ of\ attack$

$\theta = pitch\ angle$

An approximation of the sail force can be calculated by using the equation:

$$\mathrm{F} = 0.0034 * \mathrm{Area} * \mathrm{Wind\ velocity}^2 \quad (14)$$

From this equation, it is evident that the wind speed is the extensive factor, as it is squared. Changes in the wind speed can be crucial to the sail, and the sail area has to be able to be reduced in case of high wind speeds.

Calculations of wind force corresponding to how much heeling the ship could potentially obtain, could provide helpful. To do so, some equations will simplify this process and estimate how large of a wind force is representative of what heeling the vessel has. These equations are presented in [29].

$$\mathrm{M}_{thrust} = F_{thrust} * d \quad (15)$$

$$Heeling\ angle = \frac{M_{thrust}}{K_{44}} \quad (16)$$

Where,

d is the length from the center of sails to the center of buoyancy.

M_{thrust} is the moment of the thrust generated on the center of gravity, as the center of gravity is oriented at the ship's axis system.

K_{44} is the stiffness of the ship hull in the roll direction. The point of reference for this value is the center of gravity.

2.3. Structural design

Presented in Figure 2.6 is the 6 degrees of motion in respect to a ship. For a large vessel, such as a cargo ship transporting heavy goods, the most critical motions are heave, sway and surge. These motions are referred to as the lateral forces, and these forces will affect the ship's beam.

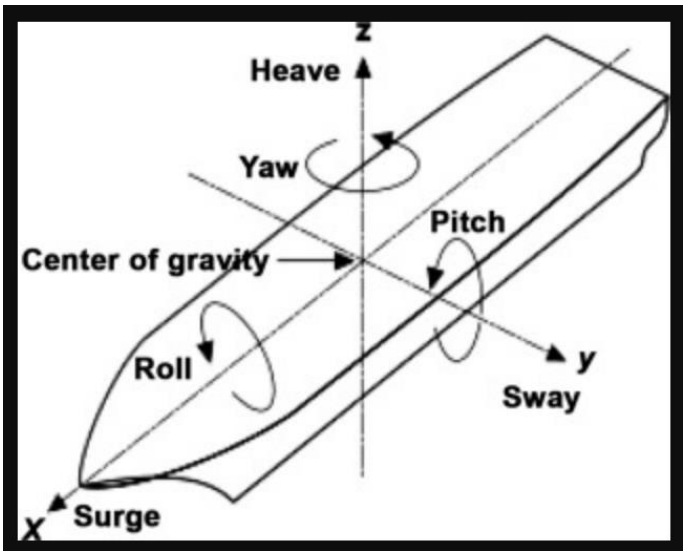

Figure 2.6 - 6 degrees of motion of a ship[30]

During wave crests, the ship will rise due to the heave motion, and at the top of the crest, the vessel will be "split in half." The pitch motion will raise the bow of the ship. This is where the vessel's bow will be at one side of the crest, and the aft will be on the other side. This will cause bending on the ship as the ship has a considerable length. As a result of this, the vessel's beam will be affected by significant torsional forces[31].

The swaying and surging motion can cause twisting of the ship´s hull, depending on the orientation of the vessel when traveling through waves. When traveling head-on, the waves will not cause any sway[32].

2.4. Wave theory

It is essential to mention some of the theories that AQWA is using to calculate simulations correctly. Regular and irregular waves are vital factors here, and under irregular waves, AQWA uses three formulated wave spectra.

2.4.1. Regular Wave

In a regular wave, there is a single wave amplitude and a single frequency. The frequency is a measure of how many times an event occurs in a given unit of time. In Figure 2.7, an example of a regular wave is presented. Note that the amplitude and period are the same on all parts of the wave. This is the simplest wave, but it is rarely viable in a realistic scenario as regular waves rarely occur in ocean waves.

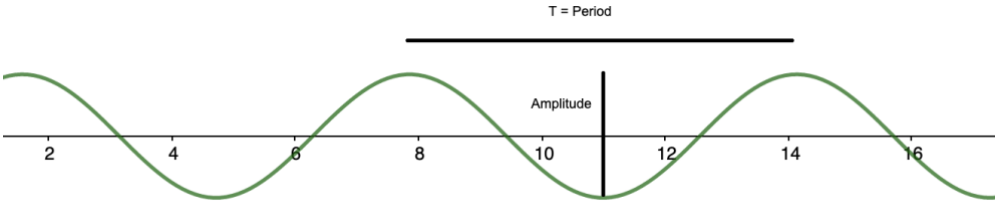

Figure 2.7 - Regular wave

A regular wave can be explained with the equation:

$$\zeta = \zeta_a * \cos(kx - \omega t) \quad (17)$$

Where,

ζ_a is the wave amplitude (m)

k is the wavenumber (rad/m)

ω is the circular wave frequency (rad/s)

2.4.2. Irregular Waves

Given that you have a regular wave, multiple can be combined, creating an irregular wave. The regular waves establish a superposition that displays many layers of regular waves on top of each other. This happens in the ocean, where an unknown number of regular waves create the irregular waves we experience. This superposition is indicated using Figure 2.8 below. Here, eight waves create one irregular wave.

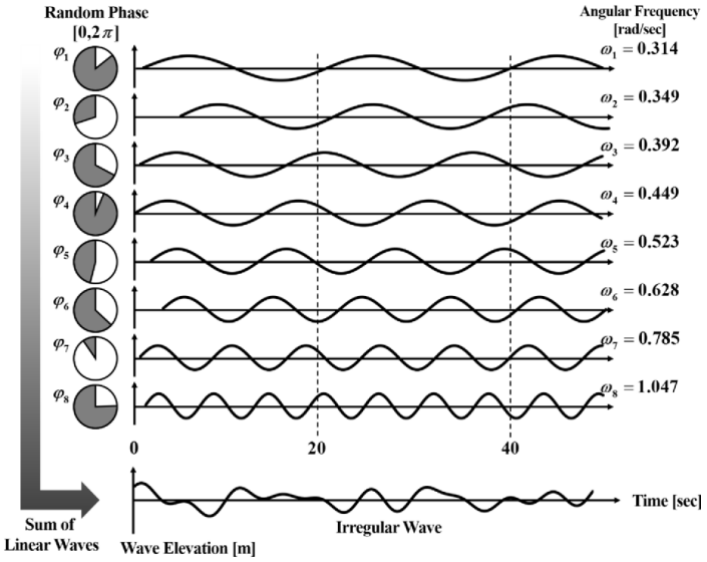

Figure 2.8 - Irregular waves created by superposition[33].

As a result of this, an equation of an irregular wave can be expressed using equation 18.

$$\zeta(t) = \sum_{n=1}^{N} \zeta_{a_n} cos * (k_n * x - \omega_n * t + \epsilon_n) \tag{18}$$

In this equation, the total sum of n waves is calculated to find the irregular wave. The ϵ_n is a random phase angle component in this case.

Wave spectrum is a distribution of wave oscillations at different frequencies. A wave spectrum depends on wind direction, wind speed, the fetch, and how long the storm is present. The further away from shore, the more fetch. Using a wave spectrum is a way to present the severity of the sea state. The standard wave spectra can be expressed using key parameters such as significant wave height H_s, and average periods $\bar{T}$[34].

Figure 2.9 shows an interpretation of a wave spectrum. The wave energy density spectrum on the right side is produced by taking:

$$S_\zeta(\omega) = \frac{1}{2} * \zeta_a^2$$

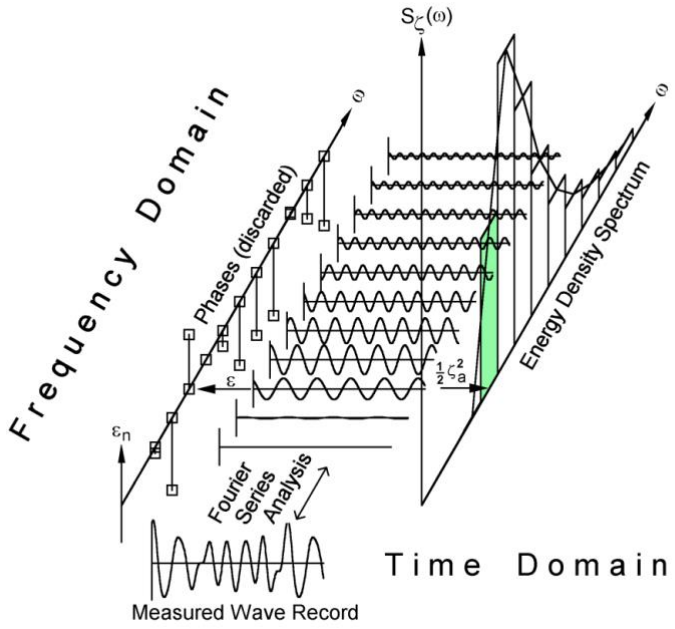

Figure 2.9 - Interpretation of a wave spectrum [UIS].

Which means taking half the amplitude squared. This amplitude is taken from each individual regular wave. The x-axis of the energy density spectrum is frequency. This displays the different frequencies from the regular waves.

2.4.3. Pierson-Moskowitz spectrum

Pierson-Moskowitz is a wave spectrum created by local winds. The spectrum can be expressed by the equation:

$$S_{PM}(w) = \frac{5}{16} * H_s^2 \omega_p^4 \omega^{-5} * \exp\left(-\frac{5}{4}\left(\frac{\omega}{\omega_p}\right)^{-4}\right) \quad (19)$$

Where,

$S_{PM}(\omega)$ is the Pierson-Moskowitz spectrum

H_s is the significant wave height

$\omega_p = \frac{2\pi}{T_p}$ is the angular spectral peak frequency. T_p is the peak period.

2.4.4. JONSWAP spectrum

JONSWAP, short for Joint North Sea Wave Project, was performed in 1968 through 1969. This project was performed to analyze data that was measured at an area that was affected by fetch limited sea state. The JONSWAP spectrum represents the waves generated at a sea state where the sea is not fully developed. The JONSWAP spectrum is an extended version of the Pierson-Moskowitz spectrum above.[34][26]

2.4.5. Gaussian spectrum

The standard Gaussian spectrum can be expressed as:

$$\mathrm{S}(\omega) = \frac{H_s^2}{16\sqrt{2\pi} * \sigma} * e^{\frac{-(\omega-\omega_p)^2}{2\sigma^2}} \quad (20)$$

Where,

$$\sigma \geq 0{,}08 * \omega_p$$

3. Numerical method and methodology

This chapter introduces the different methods that are used during the thesis. These methods have been used to collect data in a reasonable manner. A methodology chapter explains what I did and how. This will create validity and reliability for people that will be reading this thesis[35].

3.1. Research approach

For this thesis, the first approach is to obtain knowledge from other sources so that a good understanding of the desired topic could be achieved. The research that was being read was primarily qualitative data, yet some quantitative data provided its uses during the thesis.
The primary data have been collected through software simulations. These are results that have not been found through reading materials provided by another author. Yet, some data have been gathered from articles and work created by someone else.
As some problems occurred during the simulation stage, some parameters had to be altered to obtain relevant results which seemed logical. These parameters were in no case random, yet some assumptions had to be made.
The AQWA software is widely used, and the values obtained through this software are quite reasonable.

3.2. Methods of data collection

3.2.1. Design variables

For the analysis to be most accurate, a large ship model is used for the study. This ship is approximately 200m long and has a total displacement of 16003 tons[36].

The ship being used to develop an understanding of the roll stability when adding sails to a large vessel is shown in Figure 3.1.

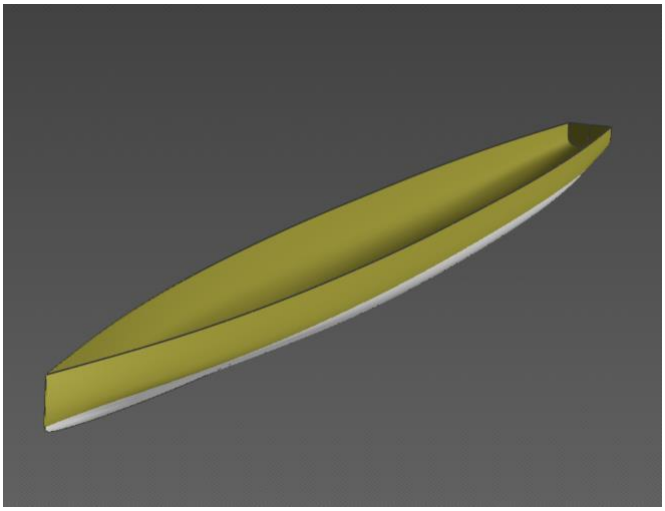

Figure 3.1 - Ship hull

This ship is designed without any purpose of adding sails to its structure, so there are currently no added roll stabilizers.

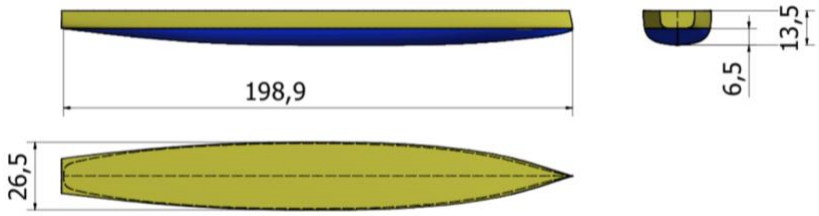

Figure 3.2 - Ship hull seen from above, starboard, and aft.

Table 3.1 - Ship details

	Value	Unit
Transverse GM	7,7	m
Longitudinal GM	565,306	m
Vertical COB	4,059	m
Longitudinal COB	94,321	m
Kxx	8,87	m
Kyy	66,525	m
Kzz	66,525	m

Given the longitudinal GM and the transverse GM, the ship is relatively stable. Longitudinal GM is the metacentric height around the pitch axis, and transverse GM is the metacentric height around the roll axis. As the ship is much longer than it is wide, the longitudinal GM is a lot larger. This is commonly the case for larger vessels.

Keel1:

The keel used for comparison is this keel illustrated in the figures below. This keel will be called Keel1 throughout the thesis.

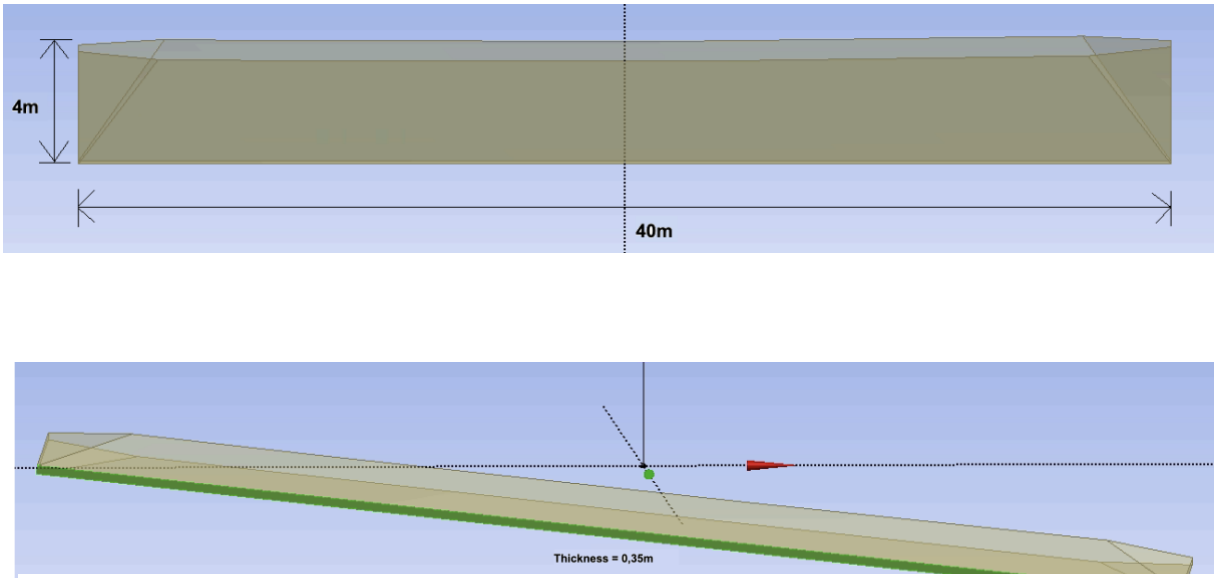

Figure 3.3 - Dimensions of keel1. The thickness connected to the ship hull is 1m. The keel gradually becomes thinner the further away from the ship hull. The green area is the tip of the keel, which is furthest away from the ship hull.

The first bilge keel used has an aspect ratio of 0,2. This is close to the aspect ratio that creates the most possible drag. So, having this high of an aspect ratio will benefit the mitigation in roll motion.

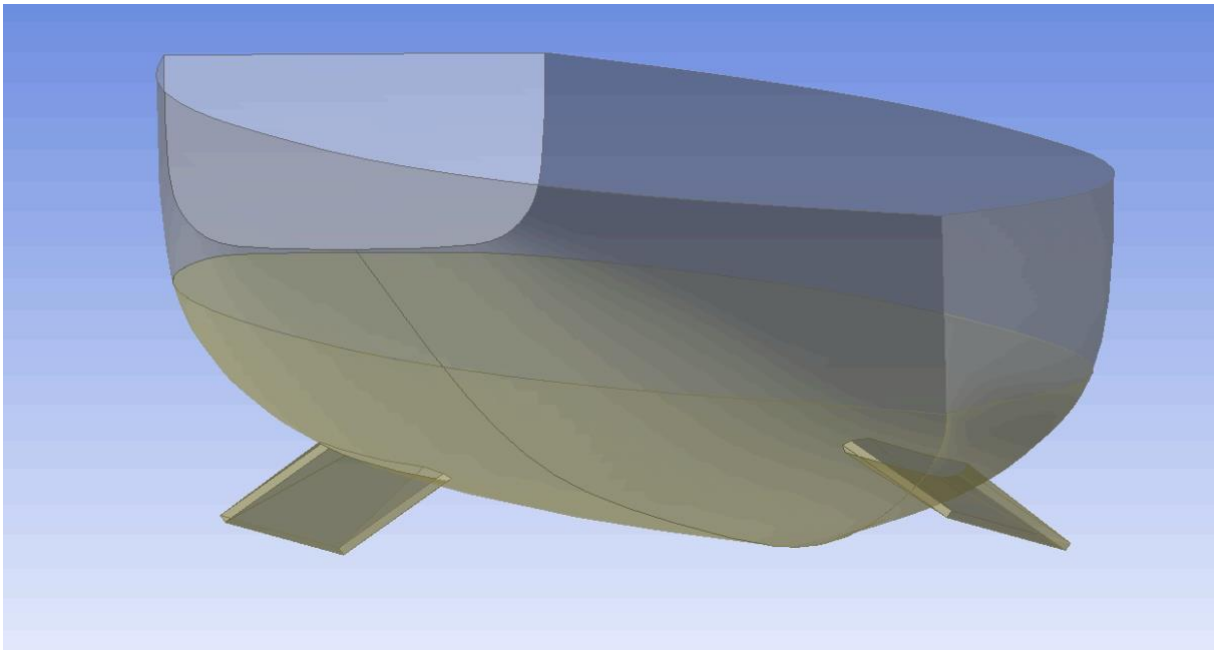

Figure 3.4 - Keel1 mounted on the ship hull

Keel2:

Keel2 is created with the knowledge that the keel is not to be placed outside the parameters given in the figure below, Figure 3.5. This is because the keel can cause problems if navigating shallow waters, as the keels will be the outer part of the ship hull.

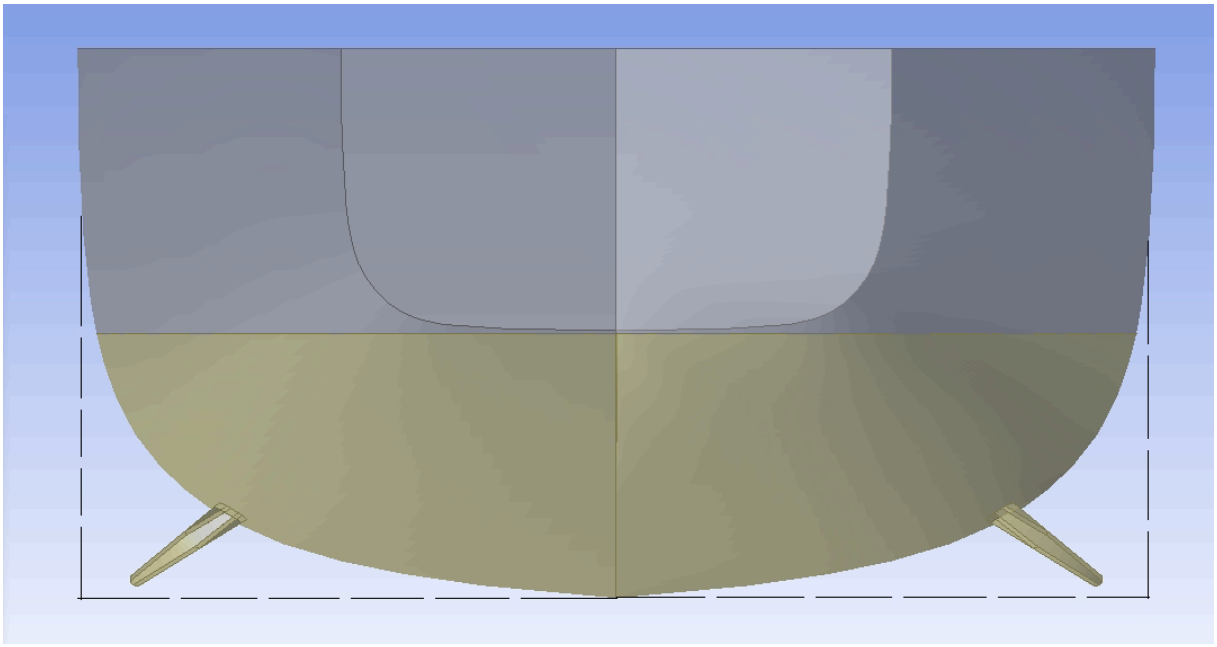

Figure 3.5 – Placement of Keel2 on ship hull. Rectangle area showing limitations.

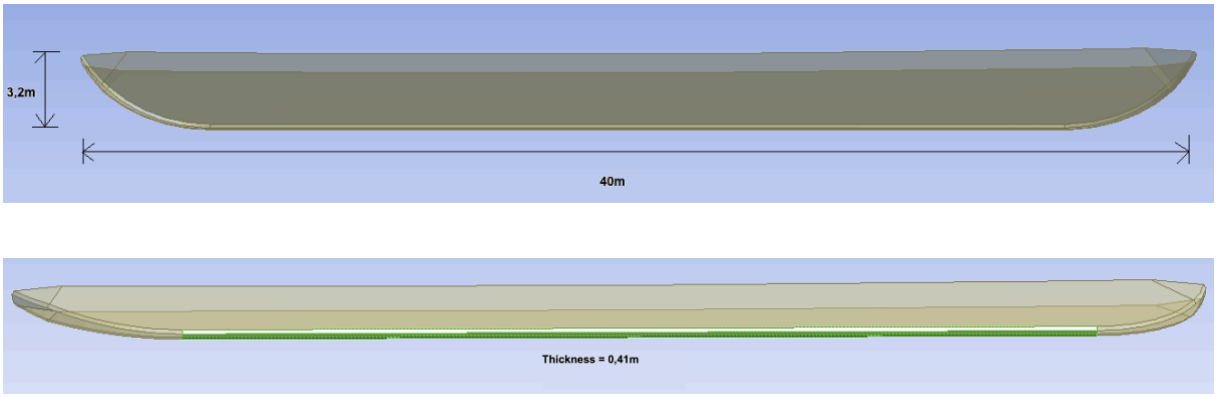

Figure 3.6 - Dimensions of keel2. The thickness at the end of the keel (green area) is 0,41m. The thickness closest to the ship hull is 1m. The keel is gradually becoming thinner the further away from the ship hull.

Keel2 is 40 meters long and is 3,5m deep. This area is less than Keel1 and is predicted to be less effective. The keel is also rounded at the edges. This will create less resistance as the hydrodynamic forces will be reduced.

The aspect ratio of keel2 is 0,16.

The keels are mounted at the exact location as Keel1, and the only difference is the geometry changes. Below, Figure 3.7 is showing keel2 mounted on the ship hull.

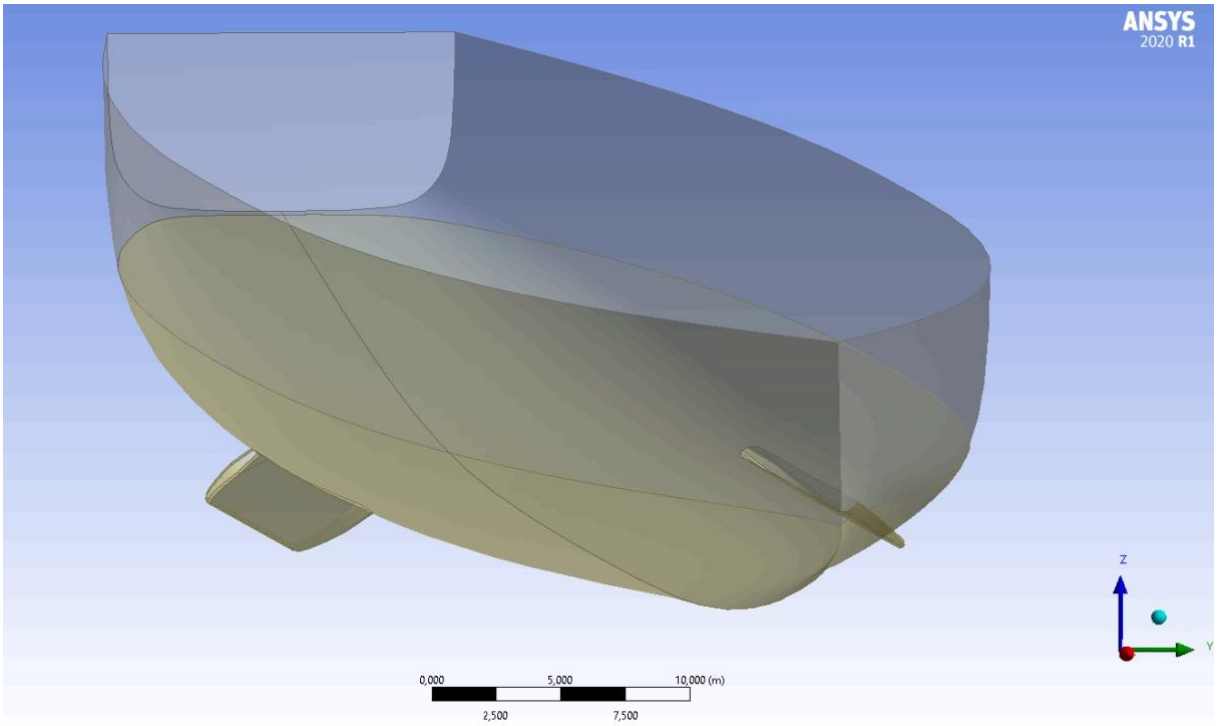

Figure 3.7 - Keel2 mounted on the ship hull

3.2.2. Mesh convergence

To make the results obtained from the simulations reliable, a mesh convergence study is performed to minimize the quantity and maximize quality.

The mesh quality is essential and plays a considerable part when utilizing numerical computations[37]. It is paramount to increase the quality of the mesh, and at the same time, reduce the number of mesh elements. To define the quality of the mesh, a mesh convergence of the model is to be performed. This is done using AQWA, where natural periods of the ship are found using different number of elements. First off, using a mesh with large-sized elements will create a model with few total elements. The natural period of heave, roll, and pitch is extracted from these results and later used to perform a convergence study. To make a mesh convergence trustworthy, multiple number of elements have to be compared. Eventually, the graph will converge, and when it does, the mesh quality at the converge point is appropriate for further analysis. The license currently at hand limits the number of total elements to 40.000. Ten frequencies are used to create the mesh convergence such that AQWA will run the simulation rather quickly. Having 100 frequencies for this mesh convergence requires a lot of hours of simulation. First off, ten frequencies with 1.309 total elements are simulated. After

this, the total number of elements is increased to 2.308, 5.248, 20.936, 32.987, and 35.145, respectively.

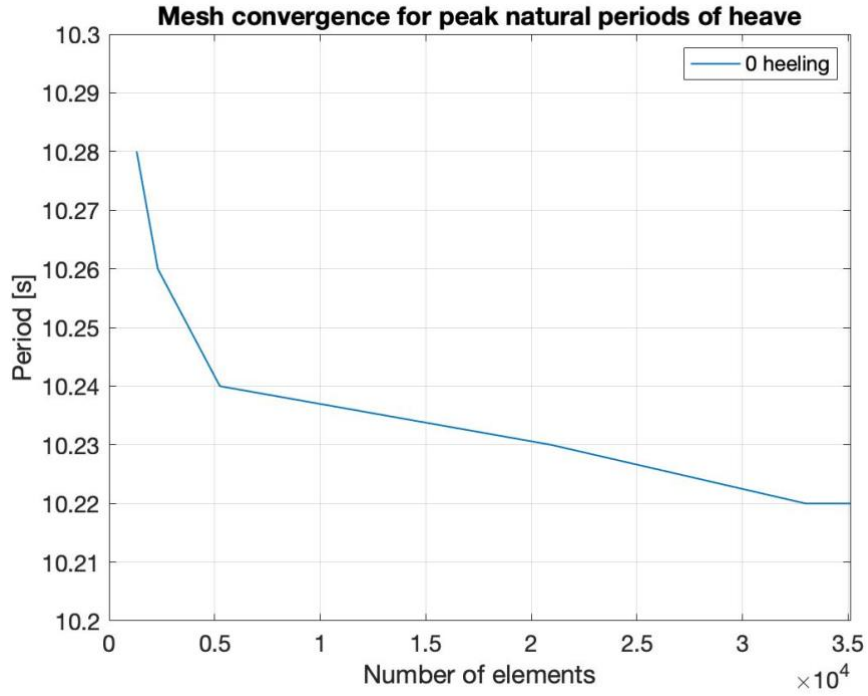

Figure 3.8 - Mesh convergence for peak natural periods of heave.

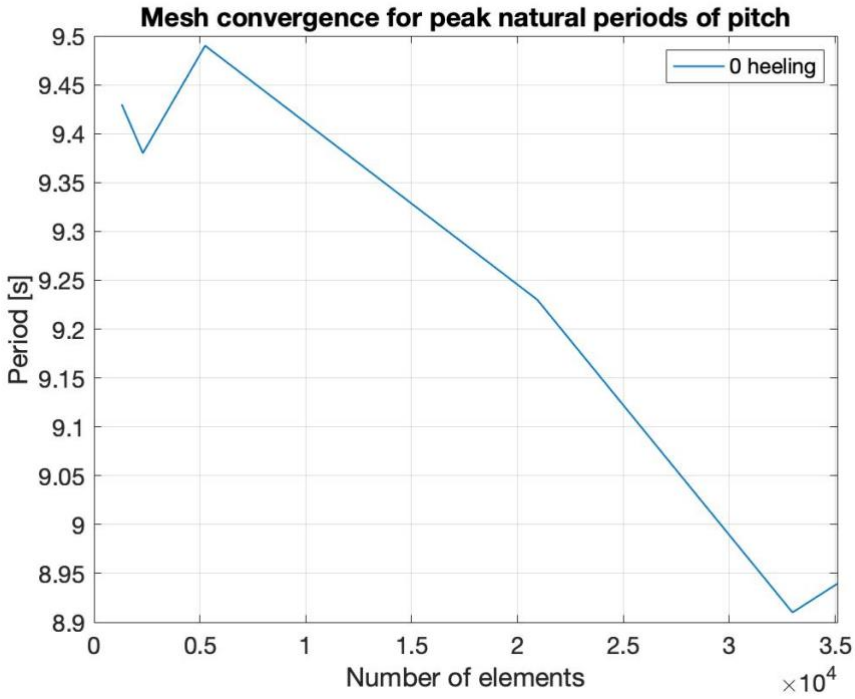

Figure 3.9 - Mesh convergence for peak natural periods of pitch.

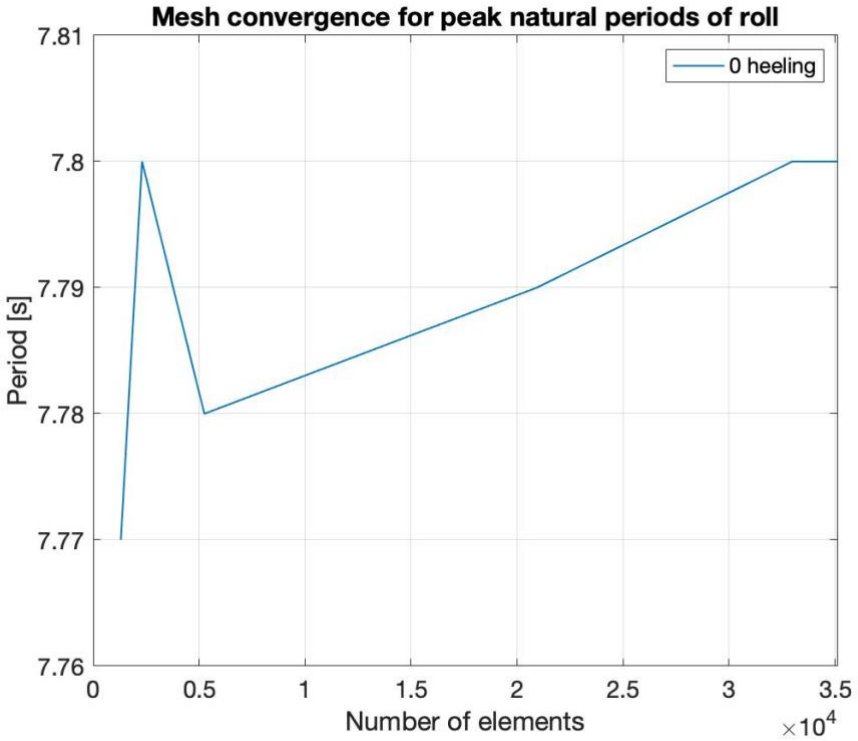

Figure 3.10 - Mesh convergence for peak natural periods of roll.

It is clear from the simulation shown in the pages below, that the peak value of heave, roll, and pitch are converging when using 32.987 or more elements. From peak heave and roll periods, the changes from 20.000 to 33.000 elements are minimal and can be considered converging from 20.000. For peak heave periods, the converging occurs closer to 30.000 elements.

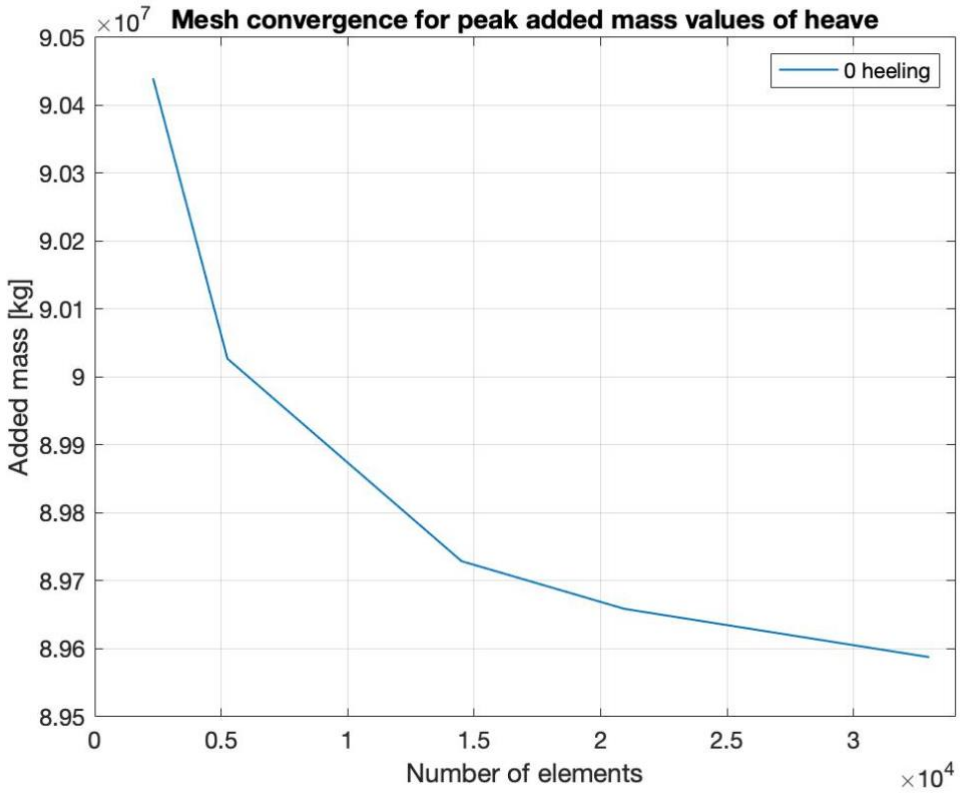

Figure 3.11 - Mesh convergence for peak added mass values of heave.

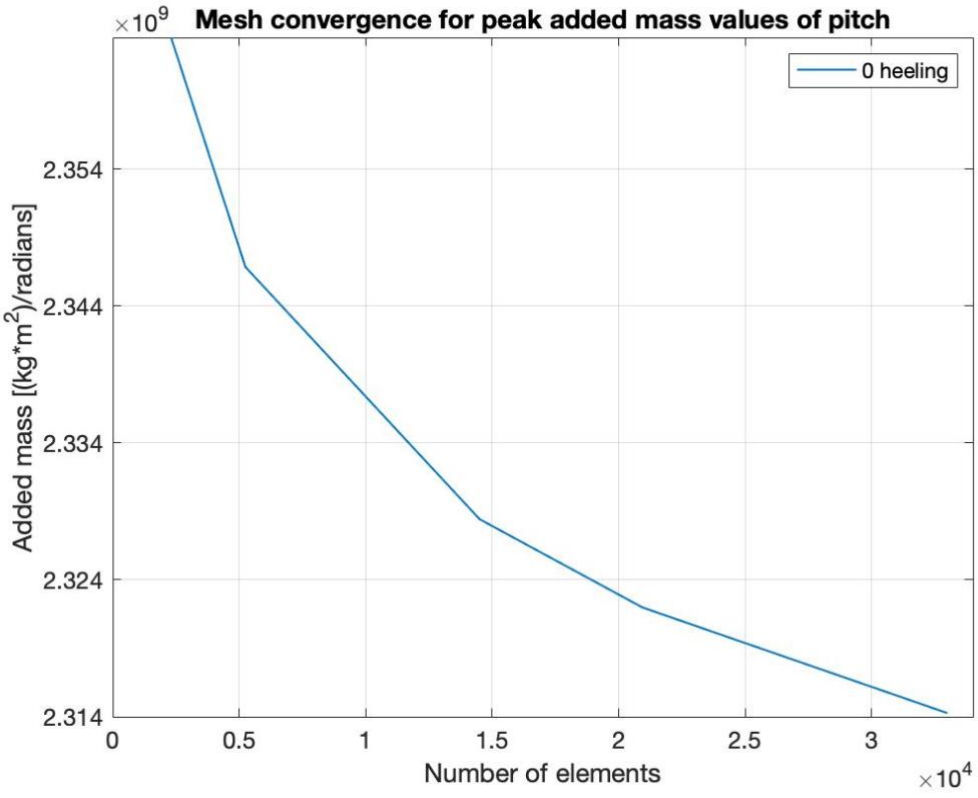

Figure 3.12 - Mesh convergence for peak added mass values of pitch.

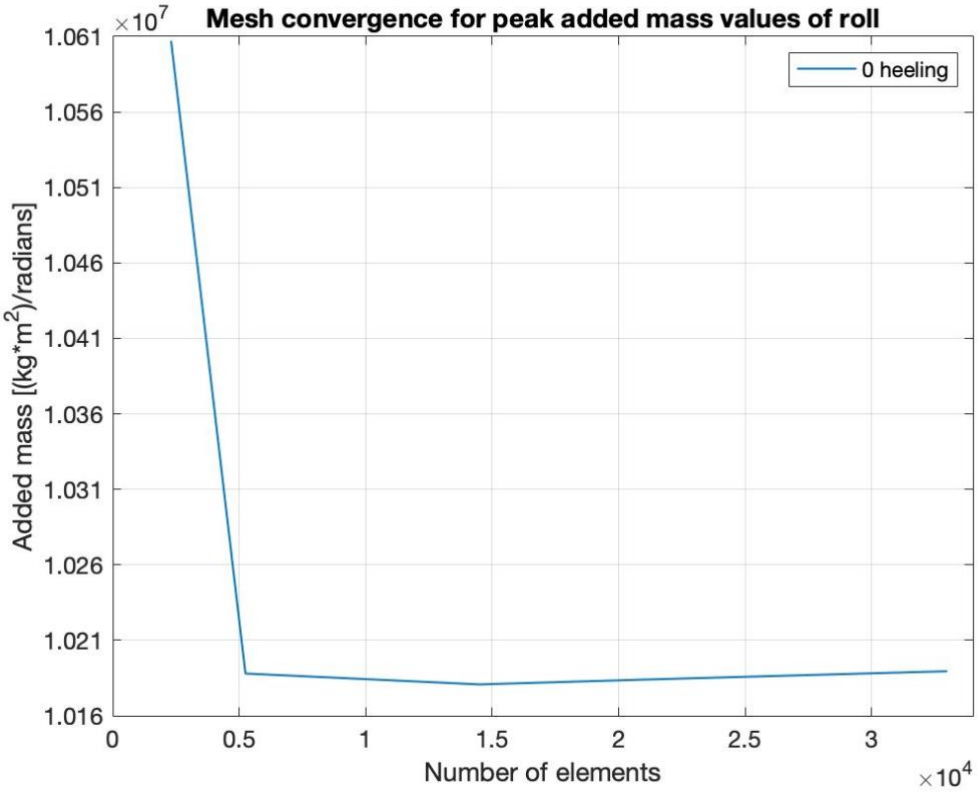

Figure 3.13 - Mesh convergence for peak added mass values of roll.

For the added mass, the convergence occurs at around 14.000 elements. From 14.000 elements to 30.000 elements, the added mass stabilizes. For this case, it is evident that 20.000 elements are adequate for running simulations.

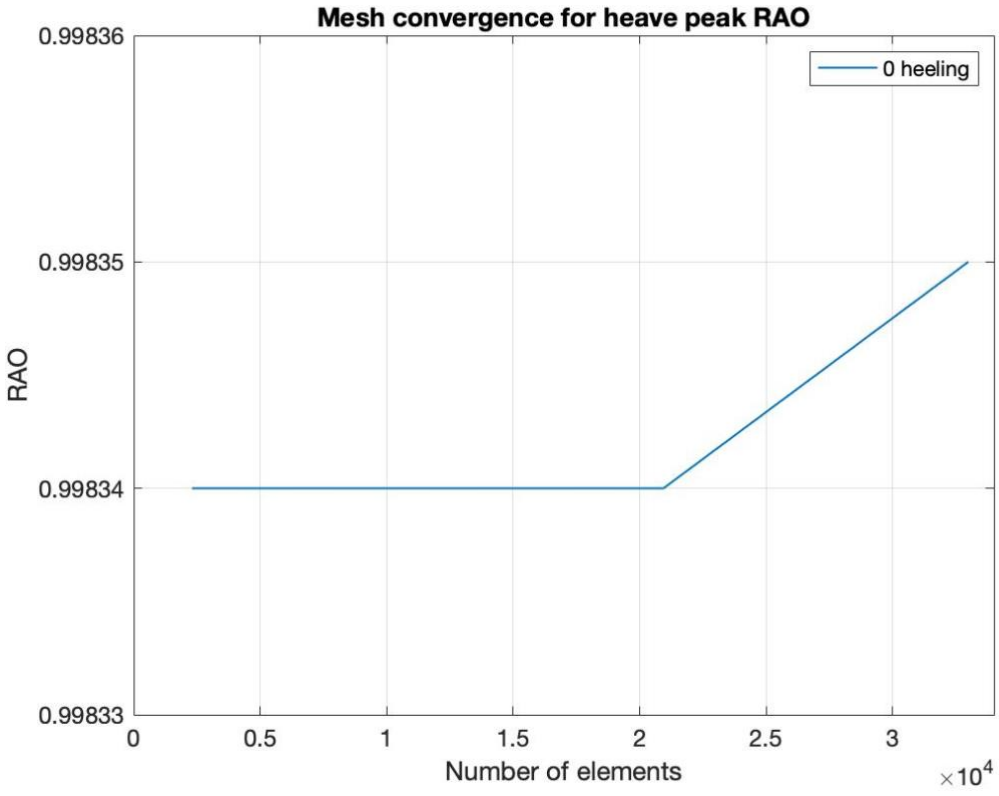

Figure 3.14 - Mesh convergence for heave peak RAO

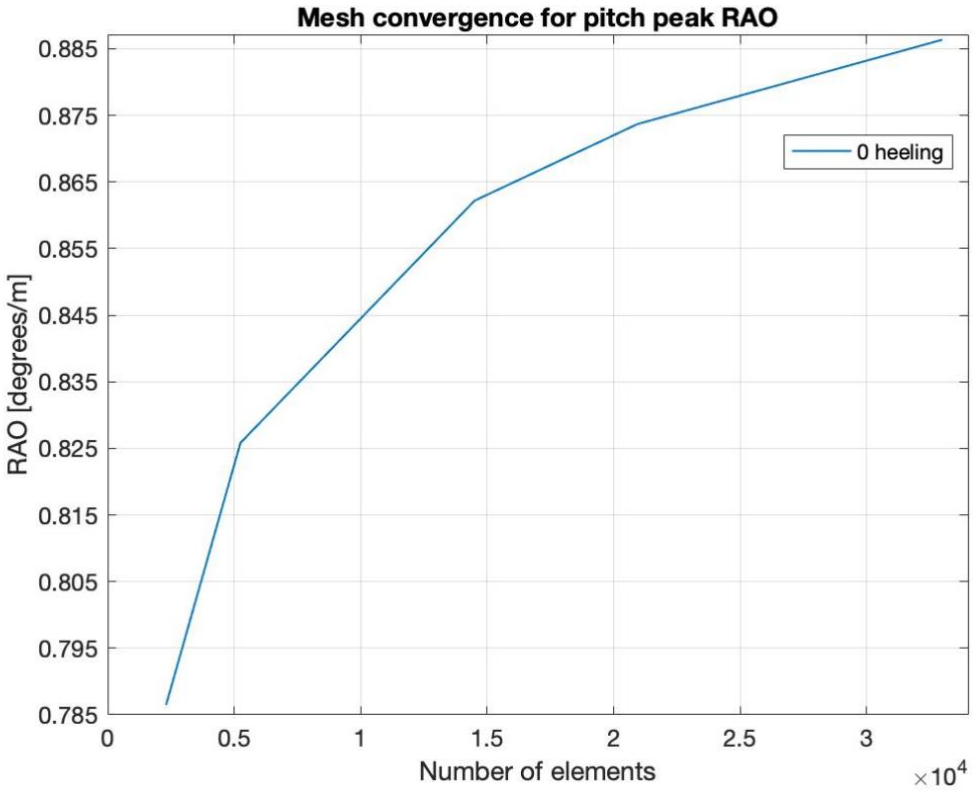

Figure 3.15 - Mesh convergence for pitch peak RAO

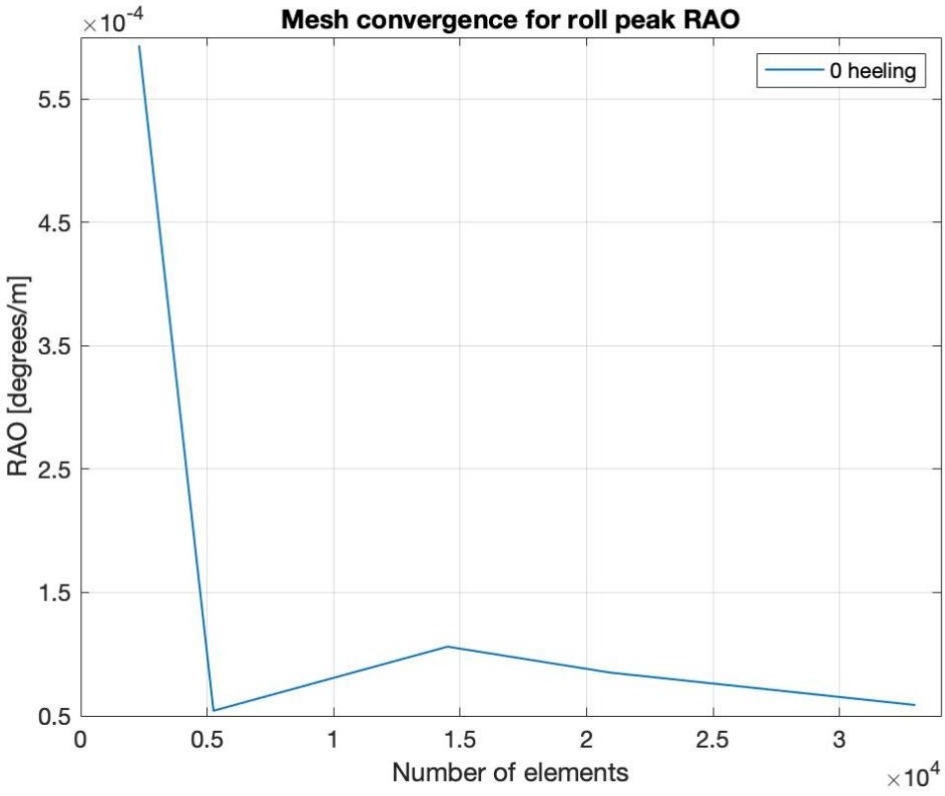

Figure 3.16 - Mesh convergence for roll peak RAO

The converge happens at various locations for the RAO results, but it is safe to say that it has entirely converged after using more than 20.000 elements. Figure 3.14 shows an abrupt change in peak RAO after 20.000 elements. This looks like a severe change in peak RAO, but it is essential to realize that the difference is only 0.00001. Given these results, using 32.987 elements should be the goal. Yet, given that the change is so small after 20.936 elements, it is reasonable to stay at approximately 20.000 elements to reduce simulation length significantly.

3.2.3. ANSYS software

The ANSYS - AQWA software will be used throughout the whole thesis. AQWA will make it possible to run simulations of the ship hull to obtain different essential parameters, such as RAO for roll, pitch, heave, and added mass.

The ANSYS project schematic will consist of a geometry connected with hydrodynamic diffraction. The flowchart will be as shown in Figure 3.17. The hydrodynamic diffraction will simulate the ship hull using ANSYS theory and manual inputs.

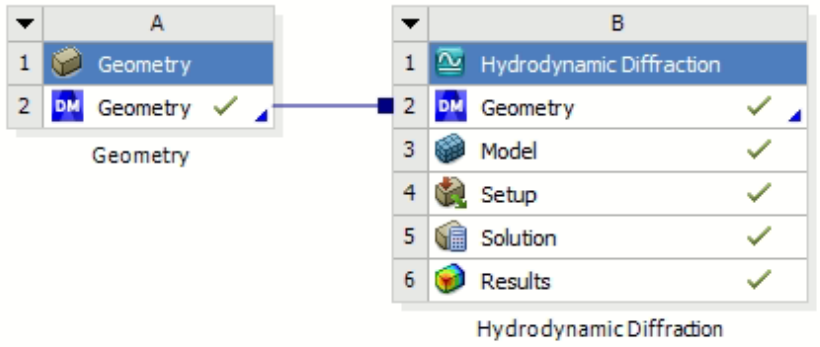

Figure 3.17 - Flowchart Ansys Workbench 2020 R1

The AQWA hydrodynamic diffraction provides the possibility to develop hydrodynamic parameters to create complex motions and response analyses. This software is primarily designed for floating structures such as ships[26].

DesignModeler:

DesignModeler is the 3D modeling program used to change the models used for this analysis. This program is coupled very well together with AQWA and has its geometry already connected through Workbench. As a ship hull is not created from scratch, this program was mainly used to generate the bilge keels and attach these to the already existing model[38].

3.2.4. Additional damping matrix

As the results obtained from the simulations showed illogical results, adding an additional damping matrix is necessary. This supplementary damping matrix is essential as the software does not include the viscous damping created by the added geometry (keels) added to the structure. This function is available through the AQWA software and requires hand calculations to correctly plot the damping matrix[39].

When performing the simulations without a keel, the RAO results received from the simulations are unexpectedly high, especially for the RAO roll angles. After running 12 simulations with different heeling angles between 0-15 degrees, the peak angles of roll resulted, as shown in Figure 3.20. The highest peak at 0-heeling equals to 17,171 degrees roll angle.

The peak roll RAO has the highest peak at 0-heeling and slightly decreases for every added heeling angle. The lowest peak is registered at 15 degrees of heel, which is 12,493 degrees. For this graph, it is essential to remember that the addition angle is added on top of the RAO angle received.

An example is, 5 degrees of heeling has a RAO of 16,971 degrees. The total peak of roll will then result in 16,971 degrees + the additional 5 degrees of heel. This means that the total peak will result in 21,971 degrees.

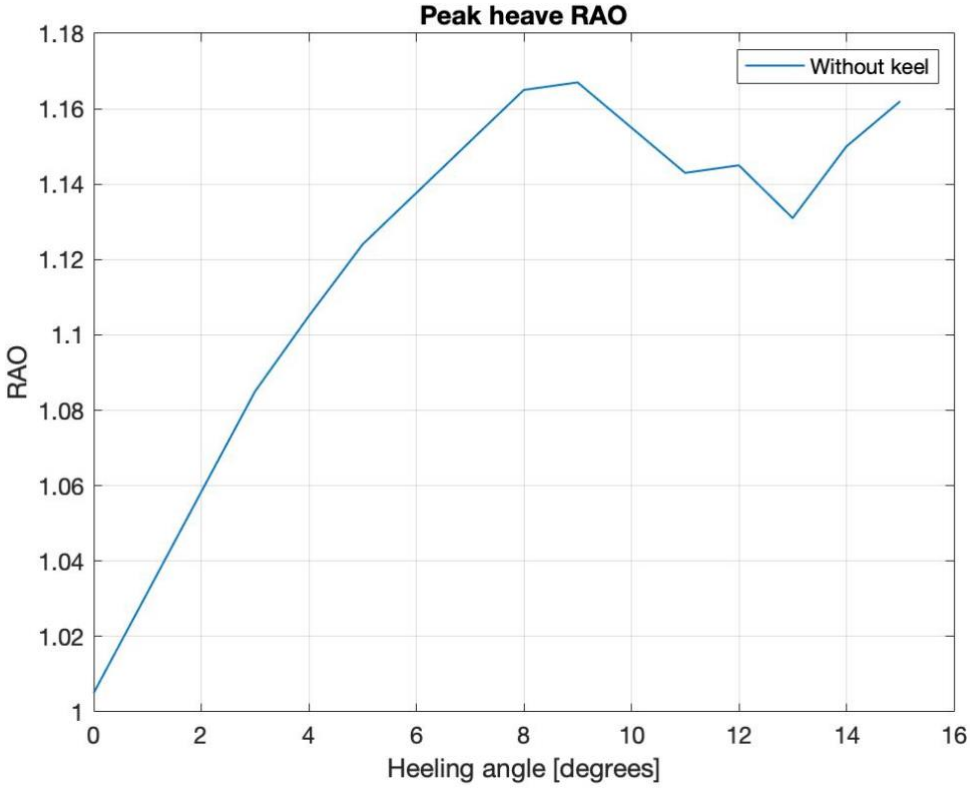

Figure 3.18 - Peak heave RAO, without keel. (Not corrected RAO) 10 knots forward speed.

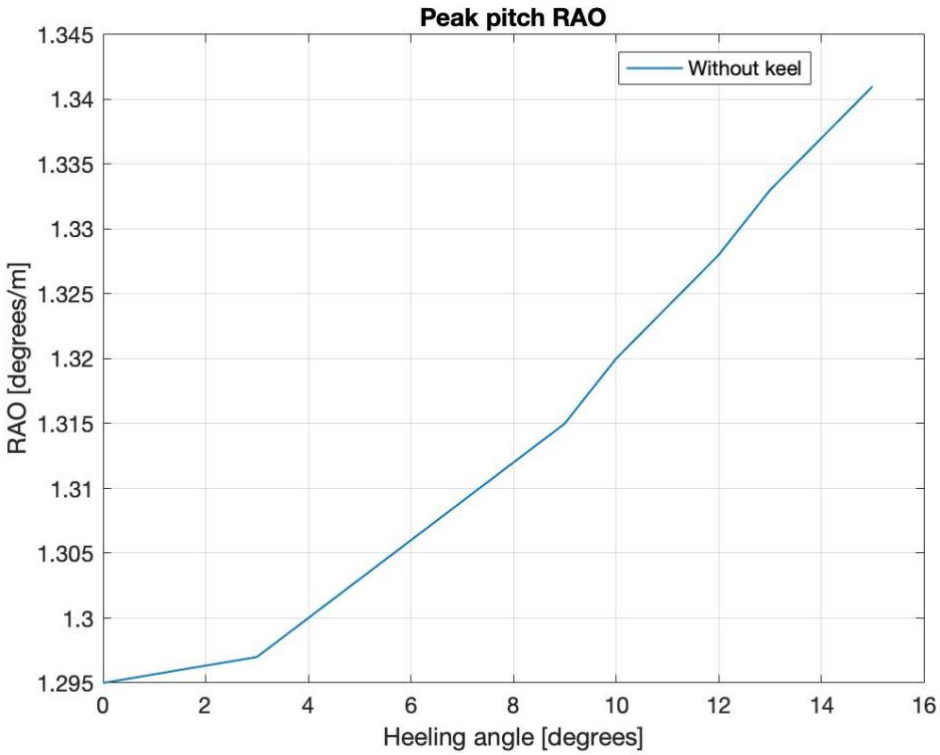

Figure 3.19 - Peak pitch RAO, without keel. (Not corrected RAO) 10 knots forward speed.

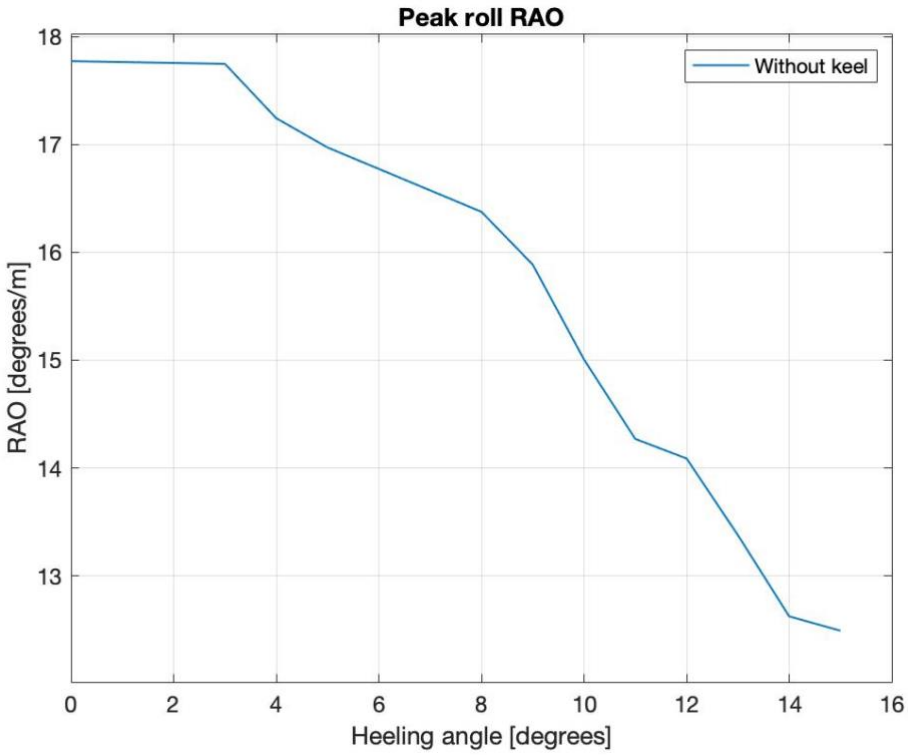

Figure 3.20 - Peak roll RAO, without keel. (Not corrected RAO) 10 knots forward speed.

These values above certainly show high values for roll angle, and some correction has to be made. To figure out what might cause the results to behave this way, some comparison of values must be brought forward.

$$x(t) = \frac{F_0}{m * \sqrt{(2\omega * \omega_0 * \zeta)^2 + (\omega_0^2 - \omega^2)^2}} * \sin(\omega t + \varphi) \quad (21)$$

This equation above decides the RAO for a single degree of freedom. The F_0, ζ and added mass are the values that can be changed to differentiate the RAO. The added mass is integrated into the "m" value. The F_0 is the excitation force. The excitation force is the Froude Krylov force added together with the diffraction force. The excitation force will be higher when adding more area to the ship hull. The reason for this is that the additional area will create a higher diffraction force compared to the ship hull without this area. As the $F_0, m \; and \; \zeta$ are scaled 1:1 in equation 21 above, the changes in either of these parameters will change the outcome of the result equally[40].

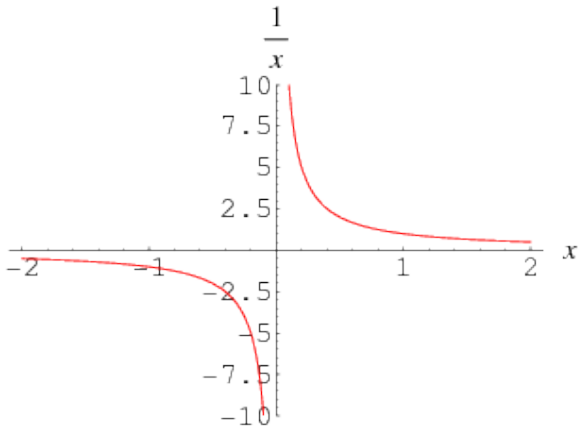

Figure 3.21 – Reciprocal as shown in[41].

If "m" were to be the only parameter that changes significantly, the RAO would follow a reciprocal graph. This means that the RAO would decrease by a considerable amount by minor changes, but the more it changes, the more negligible effect the change will have on the RAO result. This is shown in Figure 3.21.

Figure 3.22 shows that the excitation loads are the loads the wave generates on the structure. This load will increase if the design has more area affected by the waves. The added forces are the diffraction forces the structure will generate/deflect when affected by waves.

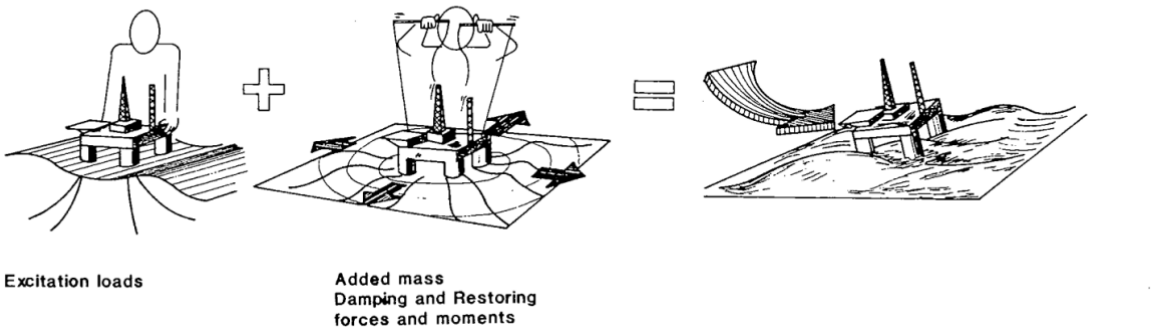

Figure 3.22 - Excitation force[42].

To find out where the fault lies, comparing the excitation force, damping, and added mass with and without keel could be helpful. This comparison was made later in the thesis, so the keel was simulated to compare against "without keel." As this correction of RAO is essential to bring note to early in the process, it is presented here.

To check whether the excitation force has increased noteworthy, a graph is plotted with the Fk (Froude Krylov) + diffraction forces for both with the bilge keel and without, Figure 3.23. The chart shows that the excitation forces have not increased significantly and are approximately equal in both cases.

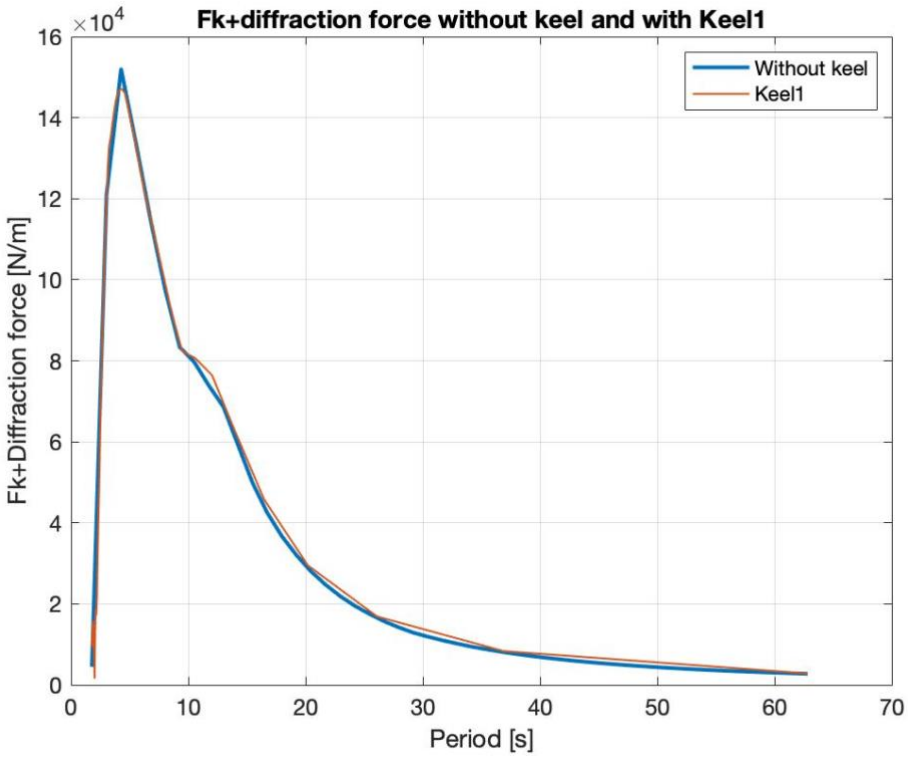

Figure 3.23 – Froude Krylov + Diffraction force comparison for without keel and with Keel1. Waves coming from 90 degrees and ship heeling 0 degrees.

To compare the added mass, ma44 is plotted in a graph for both without keel and with Keel1. To do so, an explanation of ma44 is shown in Table 3.2.

The added mass matrix, where;

- 1 – Surge
- 2 – Sway
- 3 – Heave
- 4 – Roll
- 5 – Pitch
- 6 – Yaw

- The ma24 represents the added mass in sway motion generated by the roll of the ship.

- The ma42 represents the added mass in roll generated by the sway of the ship.

Table 3.2 - Added mass matrix

$$\begin{bmatrix} ma11 & ma12 & ma13 & ma14 & ma15 & ma16 \\ ma21 & ma22 & ma23 & ma24 & ma25 & ma26 \\ ma31 & ma32 & ma33 & ma34 & ma35 & ma36 \\ ma41 & ma42 & ma43 & ma44 & ma45 & ma46 \\ ma51 & ma52 & ma53 & ma54 & ma55 & ma56 \\ ma61 & ma62 & ma63 & ma64 & ma65 & ma66 \end{bmatrix}$$

Plotted below in Figure 3.24 is the added mass for 0-heeling for the scenarios without keel and with Keel1. The added mass with Keel1 is higher than without keel. This is expected in the roll direction as the keels will create higher added mass when rotating around the roll axis. At the low periods, the added mass is about two times the added mass without keel. This will significantly affect the RAO, which is not the case from the simulation results.

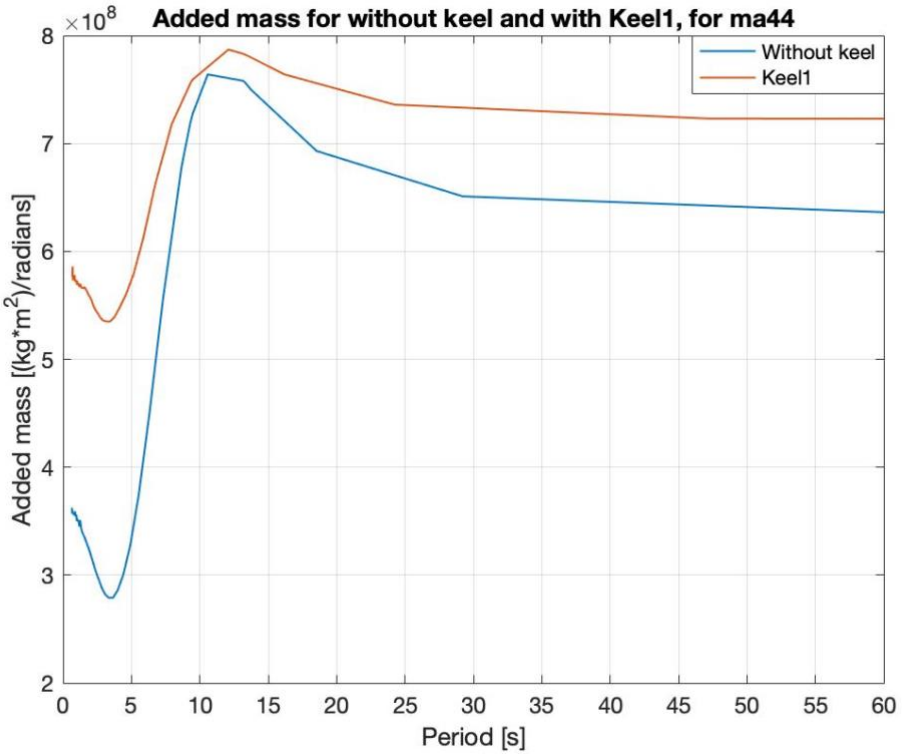

Figure 3.24 - Comparison of added mass when plotting ma44 values for without keel and with Keel1. 0 heeling. 10 knots forward speed.

Lastly, the damping is compared. The damping matrix also functions the same way as the added mass matrix. The most critical damping parameters are the c24, c42, and c44. Below, in Figure 3.25, a comparison of without keel and with Keel1 is presented. This graph shows values from c44. The damping is reducing significantly when adding a bilge keel to the structure. This is odd and might be the reason why the simulation is showing higher RAO results.

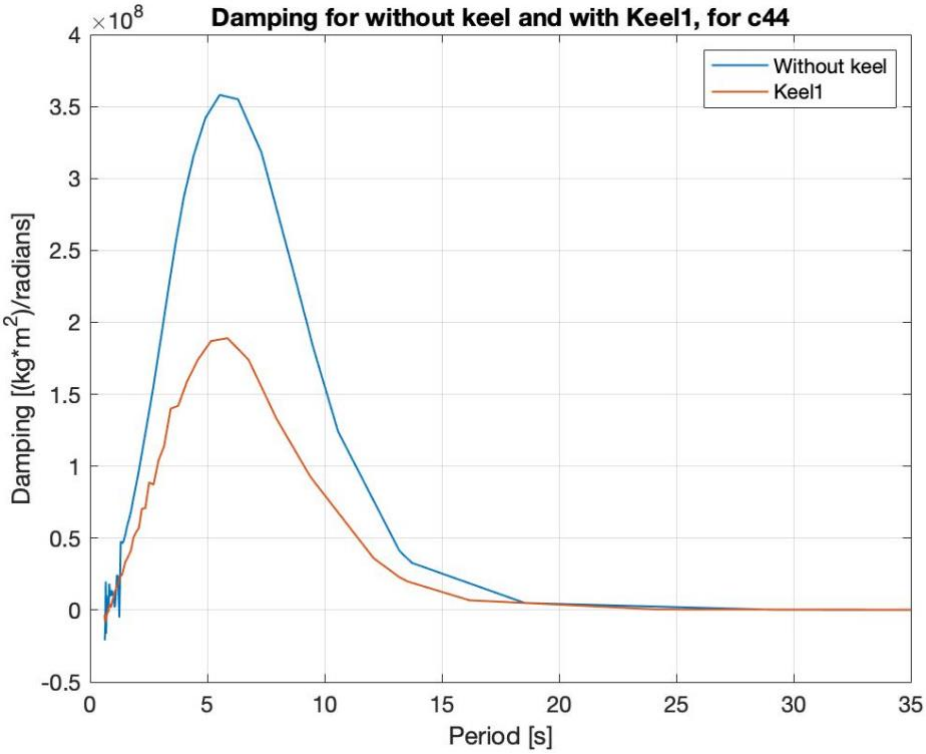

Figure 3.25 - Comparison of damping when plotting the c44 values for without keel and with Keel1. 0 heeling. 10 knots forward speed.

As the excitation force is similar in both cases, it seems like the added mass and damping is the main issue. The added mass with Keel1 is less than with no keel, yet the added mass is higher with the keel. This means that the viscous damping that the keels should provide is not included in the simulations, and some corrections have to be made.

There are some options on how to proceed further with this analysis.

- The first is to linearize the drag term such that the linear damping coefficient will provide the same work that would be provided by the non-linear drag term[43].

- Another approach is to add a non-linear roll damping function to the AQWA analysis. Using this function will, according to Ansys, provide the additional non-linear damping.

- The last approach is to use the "additional damping" function in AQWA. To be able to utilize this function, a matrix has to be found. This matrix will provide the additional damping from the ship. This has to be found using results from the simulation and hand calculations.

To proceed, an approach using the additional damping function is set in motion.
To find the damping matrix that will be added to the "additional damping" function, the mass matrix and added mass matrix have to be found. The beta and stiffness can be neglected in this case. This damping is called Rayleigh damping[44].

$$\mathrm{c} = \alpha * (\mathrm{m} * m_A) + \beta k \tag{22}$$

$$\mathrm{c} = \alpha * (\mathrm{m} * m_A) \tag{23}$$

Where the "m" equals to the mass matrix of the ship shown in Figure 3.26. The ship's axis is oriented at the Center of Gravity, so a mass transformation is unnecessary.

$$M_s = \begin{bmatrix} m & 0 & 0 & 0 & mz_g & -my_g \\ 0 & m & 0 & -mz_g & 0 & mx_g \\ 0 & 0 & m & my_g & -mx_g & 0 \\ 0 & -mz_g & my_g & I_x & -I_{xy} & -I_{xz} \\ -mz_g & 0 & -mx_g & -I_{yx} & I_y & -I_{yz} \\ -my_g & mx_g & 0 & -I_{zx} & -I_{zy} & I_z \end{bmatrix}$$

Figure 3.26 - Mass matrix of a ship[45].

When plotting the parameters, the result becomes the following mass matrix, m:

Table 3.3 - Mass matrix for ship hull

$$\begin{bmatrix} 16077000 & 0 & 0 & 0 & 0 & 0 \\ 0 & 16077000 & 0 & 0 & 0 & 0 \\ 0 & 0 & 16077000 & 0 & 0 & 0 \\ 0 & 0 & 0 & 1{,}1650 * 10^9 & 0 & 0 \\ 0 & 0 & 0 & 0 & 5{,}395 * 10^{10} & 0 \\ 0 & 0 & 0 & 0 & 0 & 5{,}462 * 10^{10} \end{bmatrix}$$

MATLAB is used to calculate the damping matrix. When using the mass matrix above and the infinite added mass (added mass at the lowest frequency), the damping matrix for 0-heeling without keel resulted in this, Table 3.4.

Table 3.4 - Additional damping matrix for 0-heeling without keel, with alpha value = 0.01

1.6394e+05	0.8173	2.7558e+03	7.2631	1798800	96.0720
-0.1815	2.4200e+05	3.0952	-664640	-52.1330	488090
2725	-21.6010	1.0903e+06	-94.0580	-193870000	-9.1418e+03
0.5517	-666750	-149.9500	1.7943e+07	32169	131570
1787800	-7.8505e+03	202710000	-12334	2.4599e+13	579300000
-30.4980	488510	45.4580	87669	-32845000	2.1500e+12

When this additional damping matrix is added to the simulation through ANSYS AQWA, the main focus is the roll angle. When inserting the values into AQWA, only the values that affect the roll angle are added. Assuming that the c22, c24, c42, and c44 values are the values affecting the roll motion.

The result is much more promising. A comparison of the RAO roll angles with the additional matrix and the simulations without the additional matrix is given in Figure 3.27.

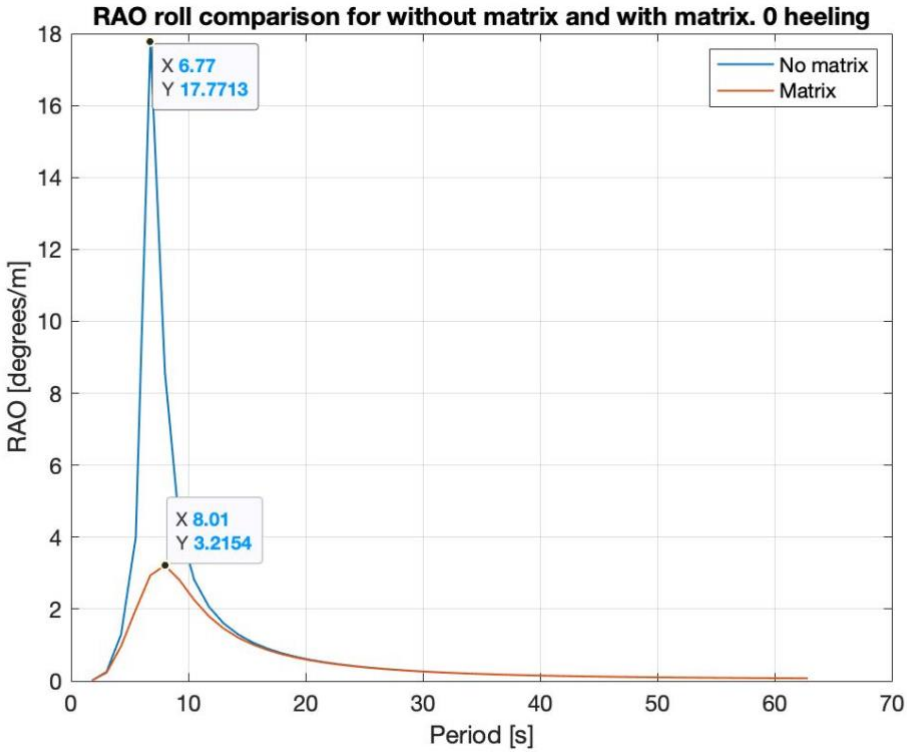

Figure 3.27 - RAO roll comparison for without additional matrix and with additional matrix. 0 heeling and waves coming from 90 degrees. 10 knots forward speed.

The RAO roll angles drastically decrease when adding the additional matrix. After adding the matrix, the RAO roll reduced from a peak of 17,171 degrees to a peak of 3,215 degrees. The heave and pitch angles have minimal changes, but not drastically, as the roll angles are prioritized when adding the matrix to the simulations.

3.2.5. Simulation procedure

When adding the supplementary matrix, the simulations increase in size significantly. The reason for this is that the infinite added mass has to be added to the additional matrix. To find the infinite added mass, the added mass at the lowest frequency is extracted. This is collected from the simulations without an additional matrix. So, the method to obtain the correct RAO is to first run a simulation to export the infinite added mass values, then simulate with the proper

additional matrix using the valid infinite added mass values. This has to be repeated with every single heeling angle, thus very tedious.

4. Analysis and discussion

During this analysis, the main focus will be on analyzing the roll stabilization of a large ship using sails. The roll will be heavily affected by forces generated by the wind, and the total sum of the roll angle will be increased. During this project, the roll of a ship will be analyzed, and preventive measures to compensate for roll angle will be discussed.

4.1. Analysis with sail forces

When sails are added to the ship, the waterline area will be different as the vessel will obtain roll angles due to forces acting on the sails. There will be different scenarios that will affect the ship in various aspects. Having wind forces acting from aft will push the bow downwards. Having wind forces acting from starboard/portside will give the boat roll angle towards port/starboard. Figure 4.1 shows how the waterline area will change when affected by wind from starboard/portside. As explained, the ship will obtain a heeling angle that has to be considered during analysis.

The X-axis is considered in surge direction, Y-axis in sway direction, and Z-axis is heave direction. The simulations will be run with a forward speed of 10 knots.

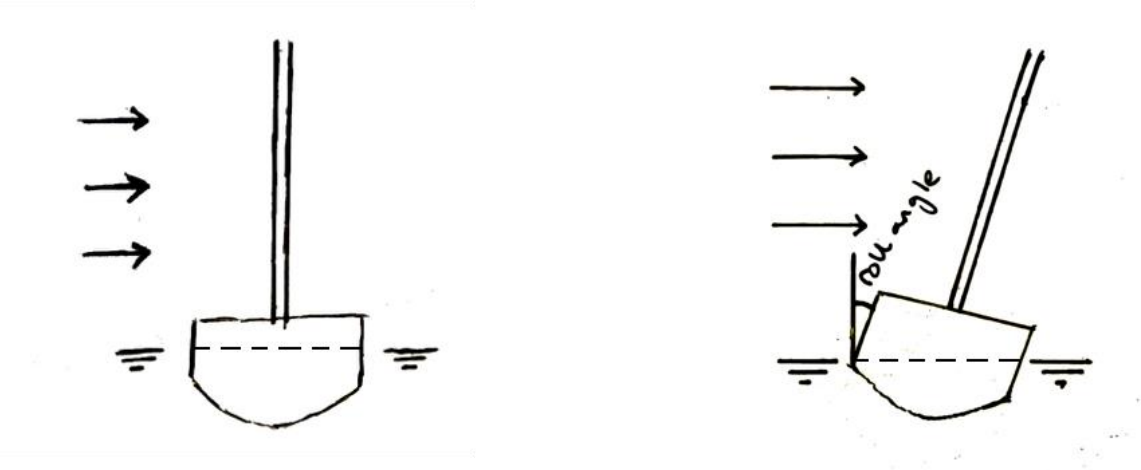

Figure 4.1 - Rotation towards portside on the ship due to wind forces from starboard position. Not an accurate representation.

Figure 4.2 shows an angle that can occur when affected by wind from the aft position. This can lower the bow of the ship, which will result in changes in the waterline area.

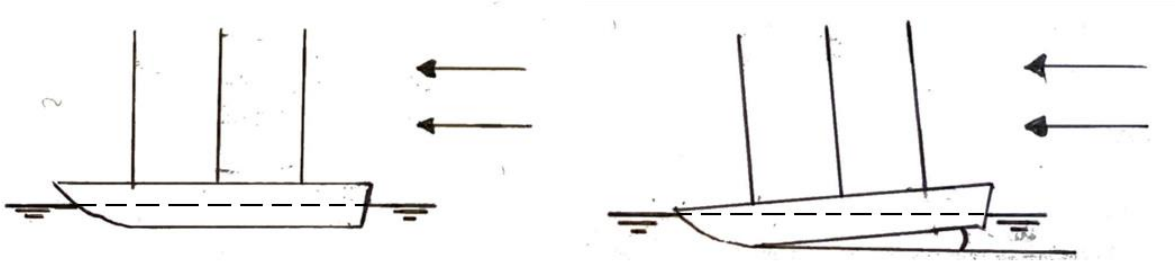

Figure 4.2 - Rotation towards bow due to wind forces from aft position. Not an accurate representation.

The reasonable way to proceed with the analysis is to simulate the ship at different roll angles. It is easier to potentially calculate the corresponding wind force generated by the sails after figuring out possible roll angles. First of all, a rough simulation analysis will be done, where simulating roll angles of 15 degrees, 10 degrees, and 5 degrees. These angles will be simulated on the port/starboard side and also at the bow. The port side and starboard side will be similar, as the ship is symmetric. Given that the ship never sails into a headwind, the aft can be neglected, and the roll angle will not be necessary to simulate at this point.

After performing the mesh convergence, the simulations will now be performed with 50 frequencies at the preferred number of approximately 20000 elements.

4.2. Comparison with another ship

Table 4.1 - Comparison of ship hull vs. S60

	Ship hull	**S60[46]**
Length	195 (m)	122 (m)
Breadth	26 (m)	17,4 (m)
Draft	6,5 (m)	6 (m)
Displaced volume	15612,7 (m^3)	9605 (m^3)

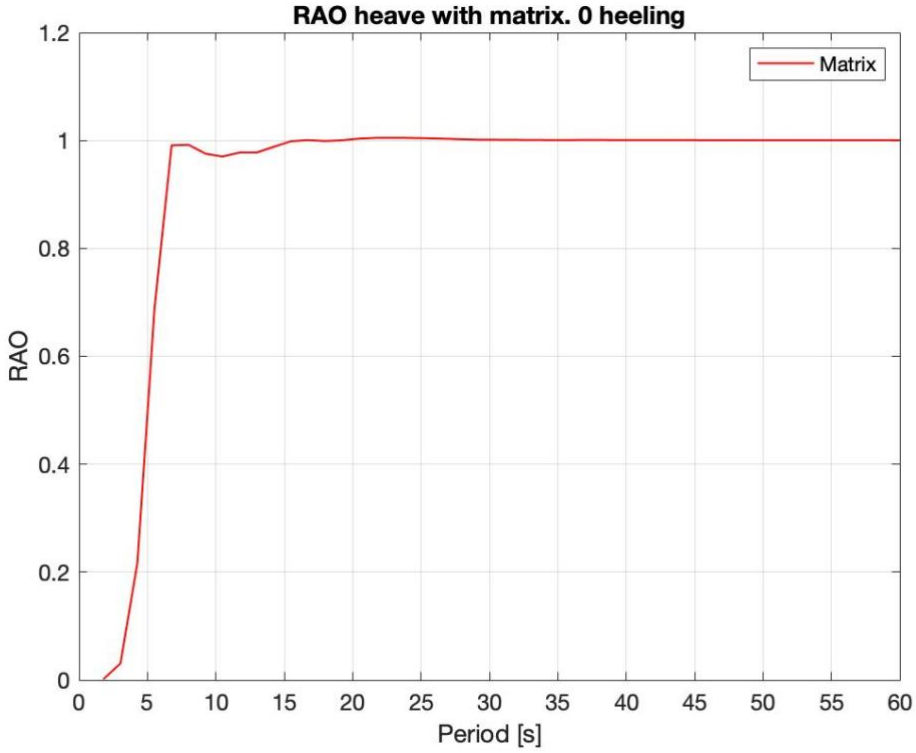

Figure 4.3 - RAO heave for 0 heeling, with additional matrix. 10 knots forward speed.

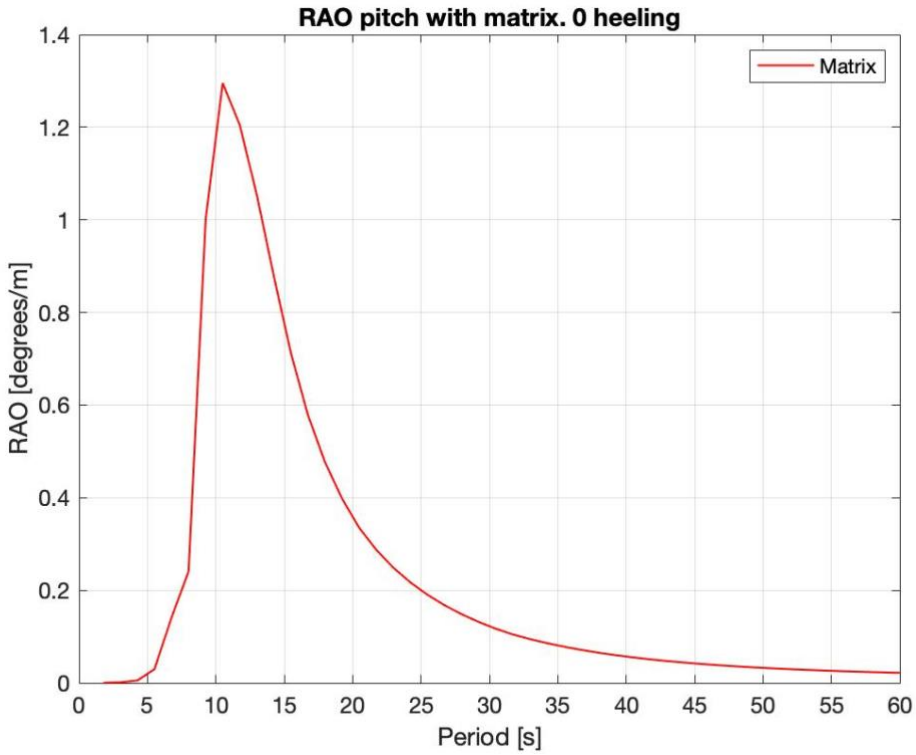

Figure 4.4 - RAO pitch for 0 heeling, with additional matrix. 10 knots forward speed.

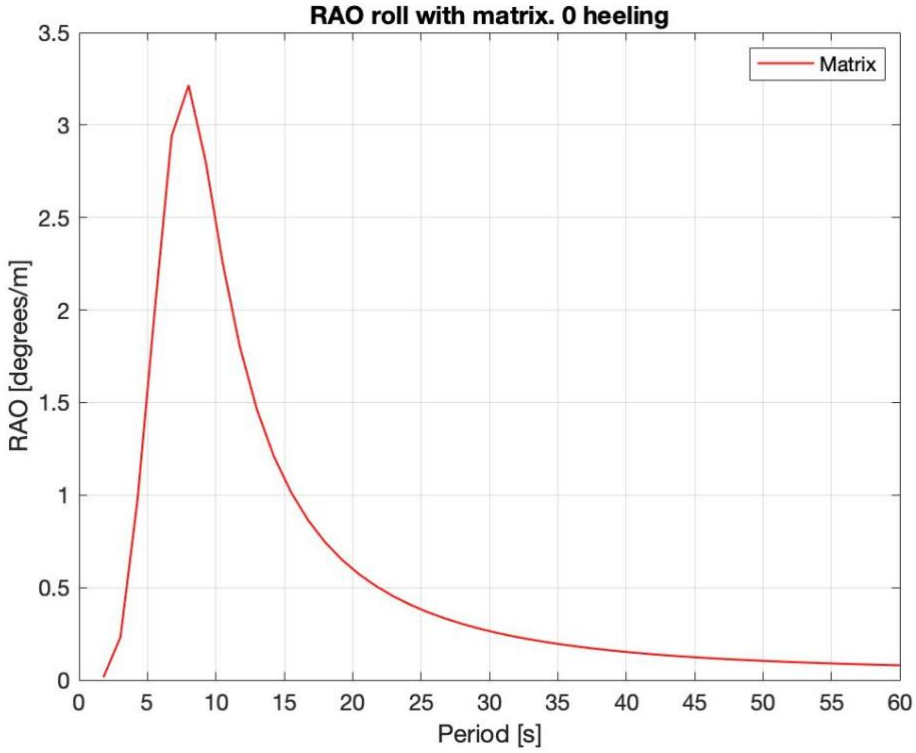

Figure 4.5 - RAO roll for 0 heeling, with additional matrix. 10 knots forward speed.

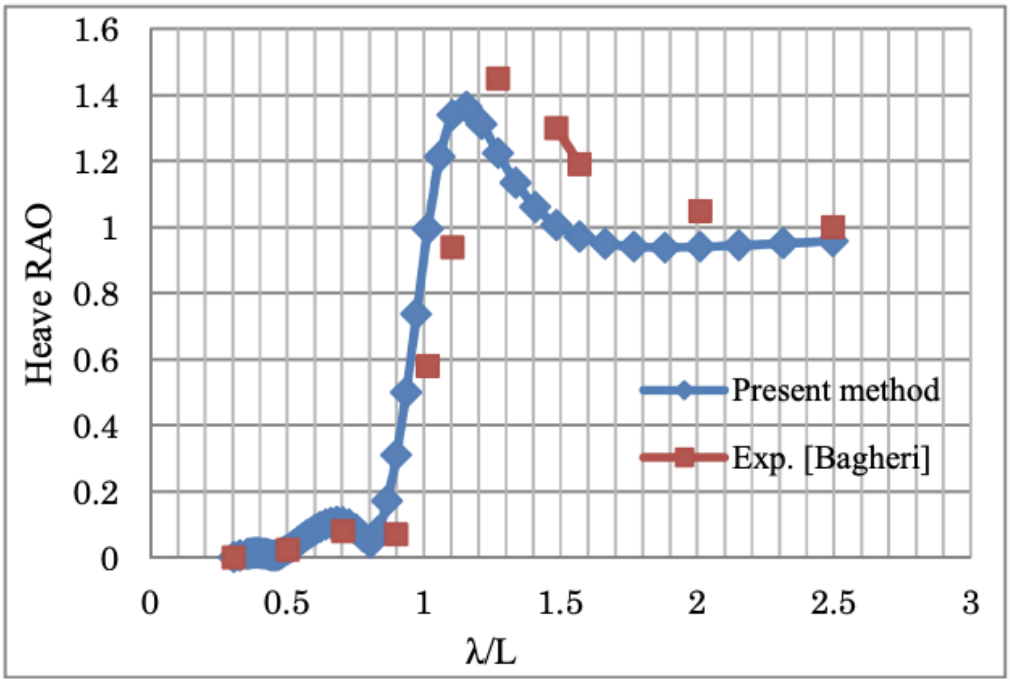

Figure 4.6 - Heave RAO for s60 at Fn = 0,2. Presented in [46].

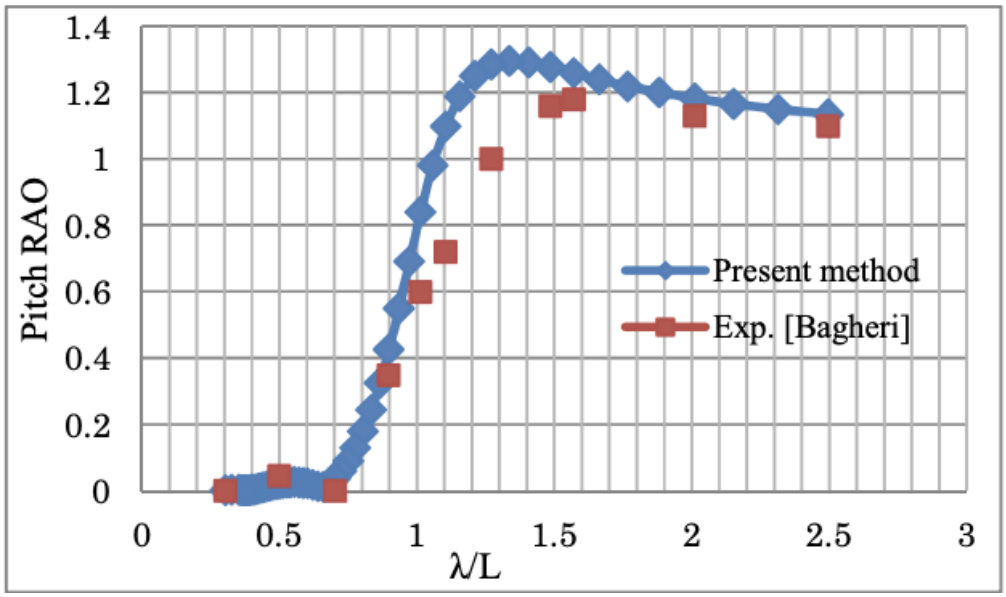

Figure 4.7 - Pitch RAO for s60 at Fn = 0,2. Presented in [46].

Both RAO for heave and pitch is quite similar for "ship hull" compared to the s60. Whereas the peak for s60 is 1,4 for heave, the peak is 1,005 for "ship hull." Regarding pitch, the peak is around 1,3 for the s60 and 1,295 for "ship hull." The values for pitch and heave are pretty similar. This gives reason to believe that the results obtained by the simulations are reasonable.

4.3. RAO without keel

First of all, simulations of the extreme values are run through AQWA. This means that the heeling angles of 0 degrees and 15 degrees are the first simulations to be presented. The graphs below compare the 0 degrees of heeling on the ship with the 15 degrees of heeling on the ship. These graphs have the additional damping matrix input and show the correct RAO.

The changes are minimal. The heave and pitch have increased slightly, while the RAO roll has decreased. The peak roll RAO has reduced from a peak angle of 3,215 degrees (0-heeling) to 3,152 degrees (15-heeling).

All the simulations done from this point and onwards are using the inputs stated in APPENDIX A.

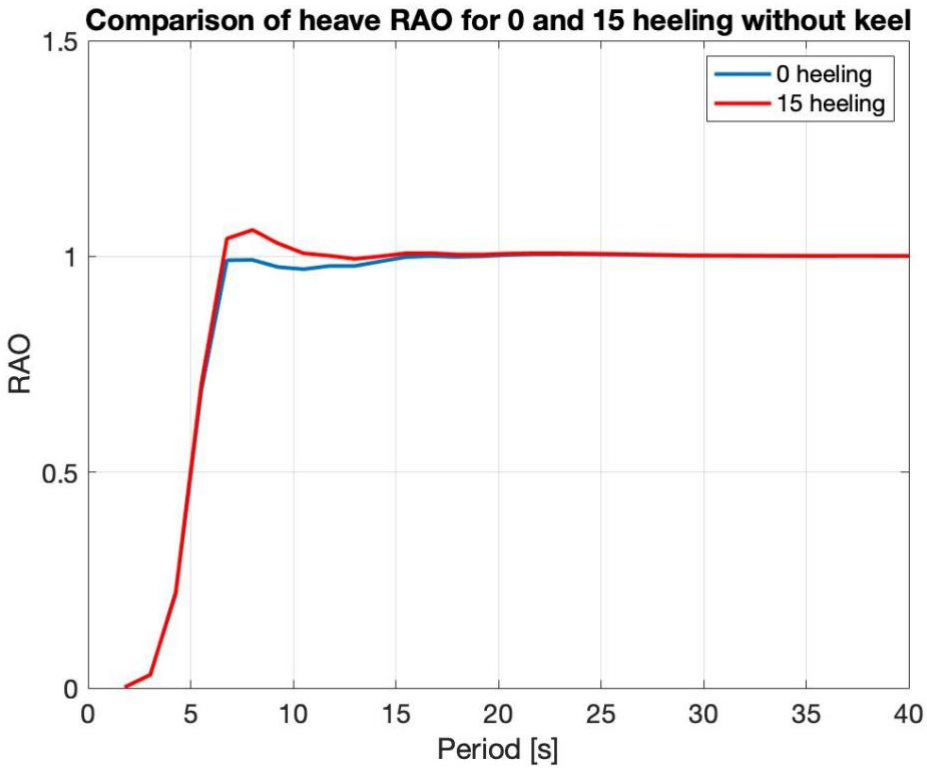

Figure 4.8 - Heave RAO for 0 and 15 heeling. Without keel and alpha = 0.01. Wave direction = -90 degrees. With additional matrix

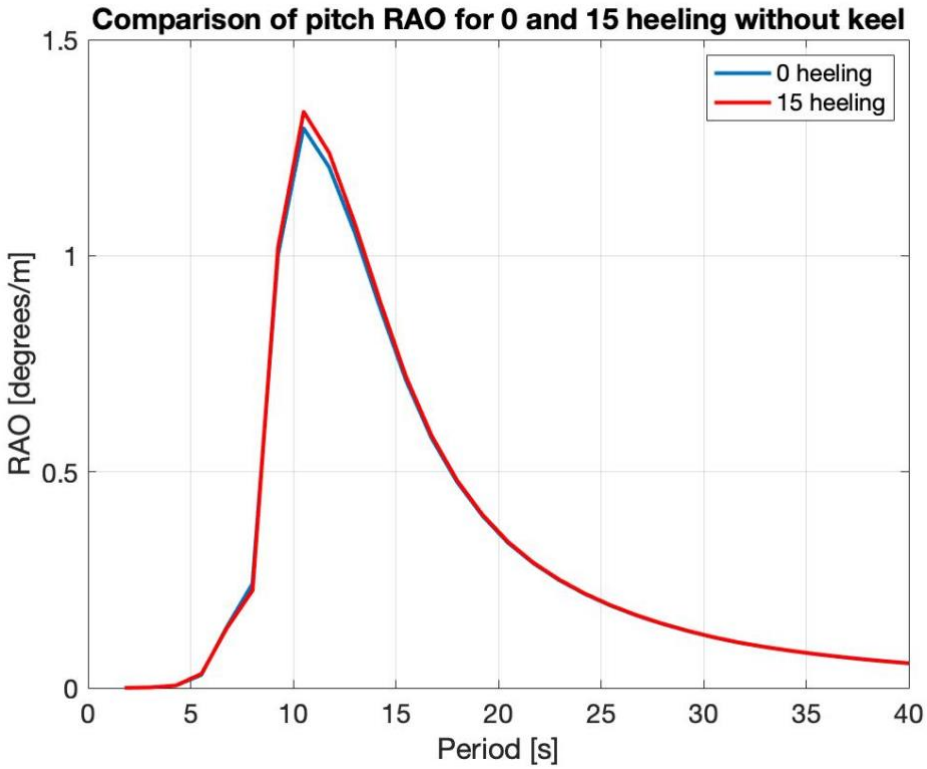

Figure 4.9 - Pitch RAO for 0 and 15 heeling. Without keel and alpha = 0.01. Wave direction = -135 degrees. With additional matrix

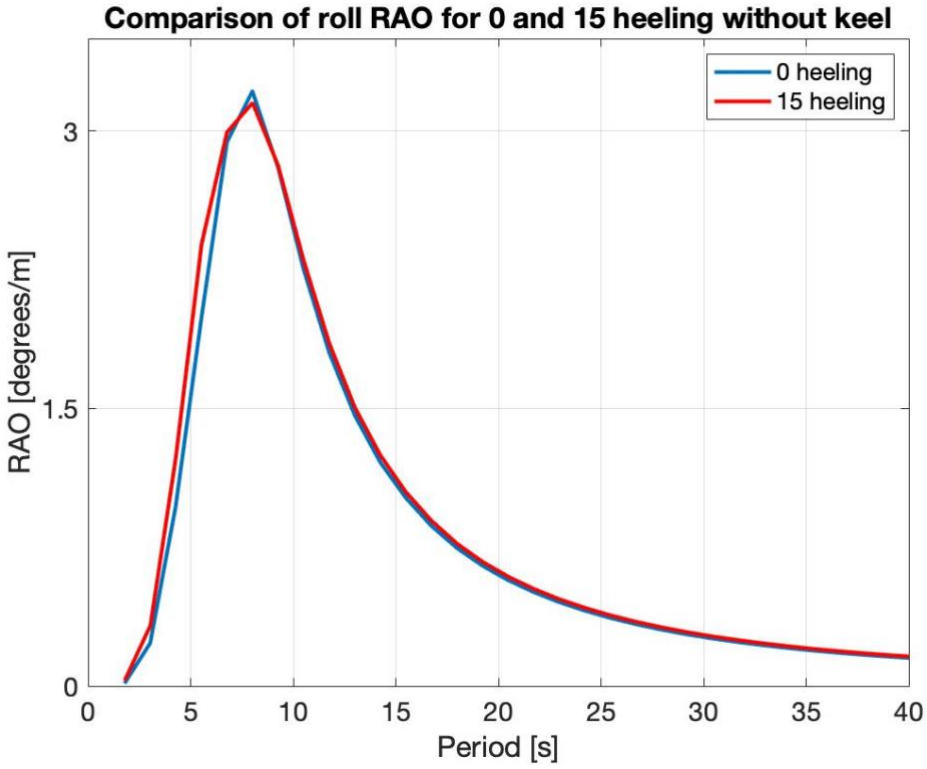

Figure 4.10 - Roll RAO for 0 and 15 heeling. Without keel and alpha = 0.01. Wave direction = 90 degrees. With additional matrix

The graphs above are extracted from the simulations, and the direction which created the highest peak is presented for each of the three motions; heave, pitch, and roll. An example of this is that waves coming from 90 degrees makes the highest roll peak, and the waves coming from –135 degrees create the highest pitch peak. This is due to the rotation of the ship towards port direction. If the vessel is rotated towards the starboard direction, the highest roll peaks would be at -90 degrees and pitch peaks at 135 degrees. This is due to the symmetry of the ship hull.

When rotating the ship 15 degrees to portside, the RAO for heave and pitch does not change significantly. The peak heave RAO changed from 1,005 to 1,061, and the peak pitch RAO changes from 1,295 to 1,333. The roll peak angle, however, is lower after rotating, although a minimal change. A peak roll angle at 3,215 degrees for a heeling angle of 0 decreased to 3,152 for a heeling angle of 15 degrees. This would result in the ship having a total peak roll angle of 18,152, as the original 15 degrees are added on top. Figure 4.11 demonstrates how a roll angle of 18,152 will be looking like with this ship hull. This amount of roll angle is not optimal and will require some reduction in roll motion.

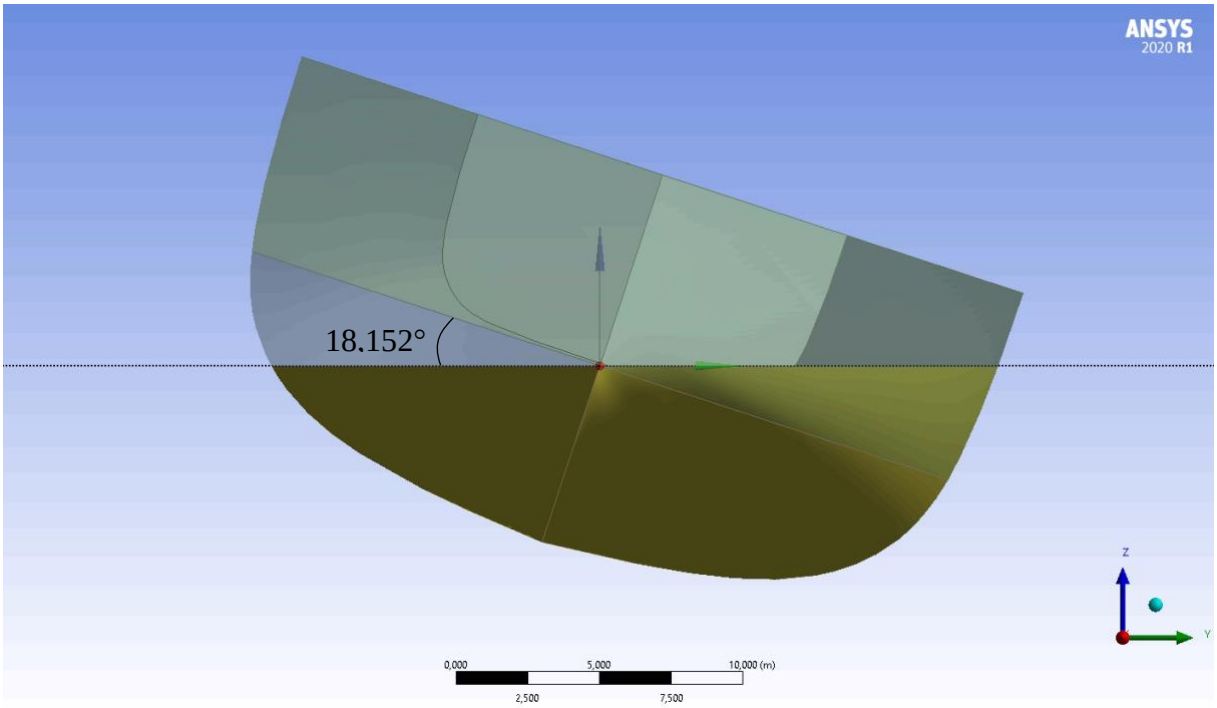

Figure 4.11 - Roll angle of 18,152 degrees, seen from the front (bow). Yellow area is the submerged volume.

The total area of the waterplane is decreasing when rotating the ship 15 degrees towards portside. This will affect the center of flotation, as the center of flotation equals the center of waterplane area.

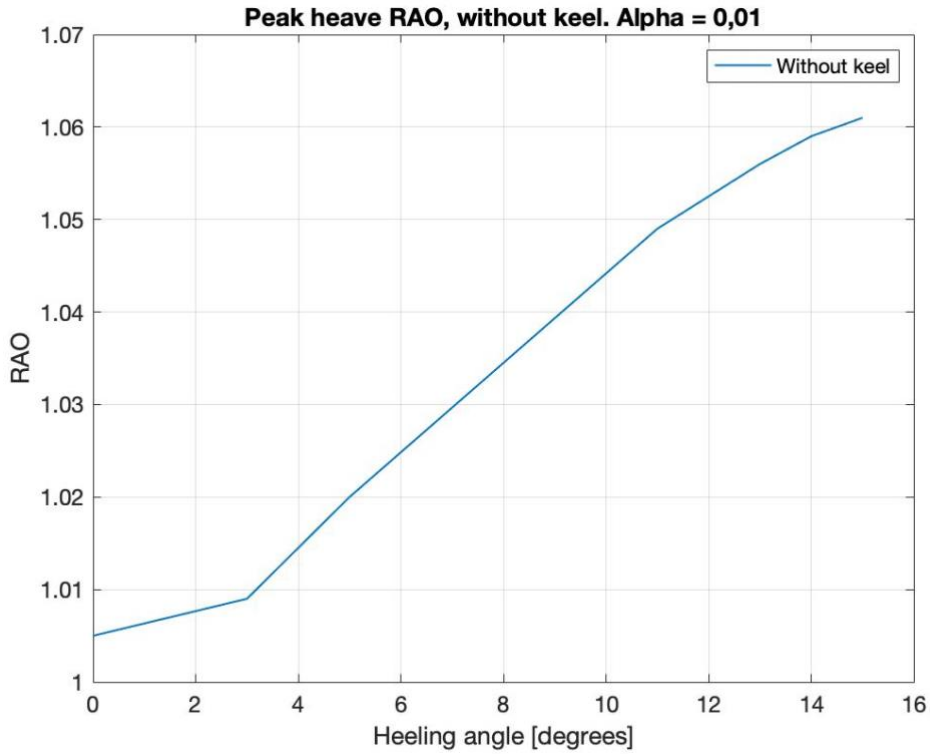

Figure 4.12 - Peak heave RAO, without keel. Alpha value 0.01 and waves coming from -90 degrees. With additional matrix

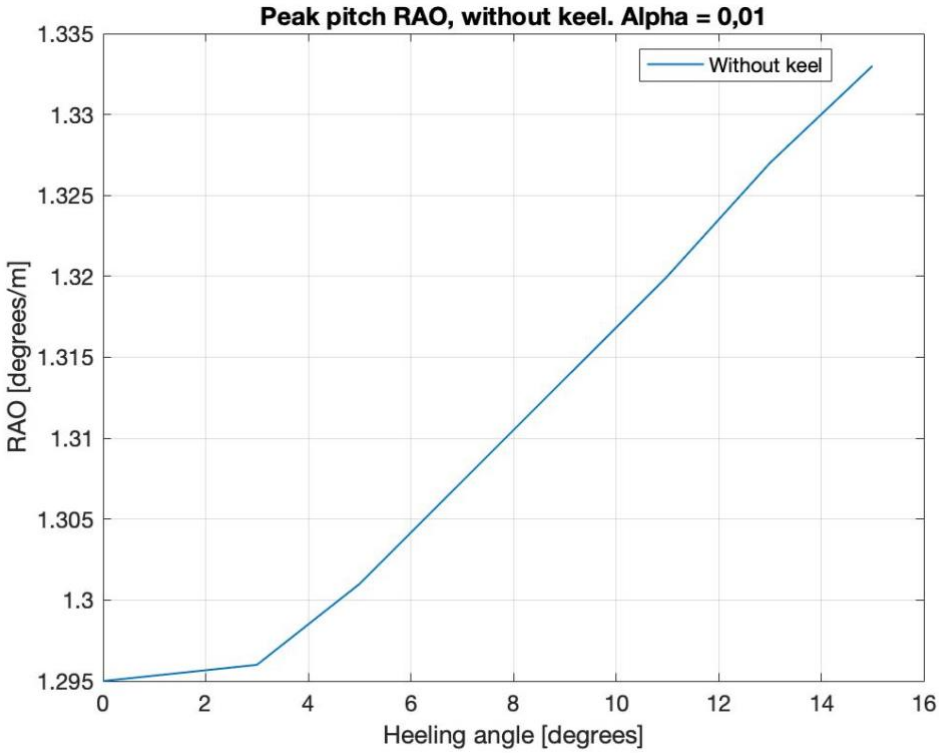

Figure 4.13 - Peak pitch RAO, without keel. Alpha value equals to 0.01 and waves coming from -135 degrees. With additional matrix

Heave and pitch values are increasing slightly with increased heeling. Although this is the case from the graphs in Figure 4.13 and Figure 4.12, it is essential to note that the values that will affect the heave and pitch motions are not included when adding the additional matrix. What is evident from this graph is that the heave and pitch will increase with more heeling as the geometry of the ship is not changed without adding the new keels.

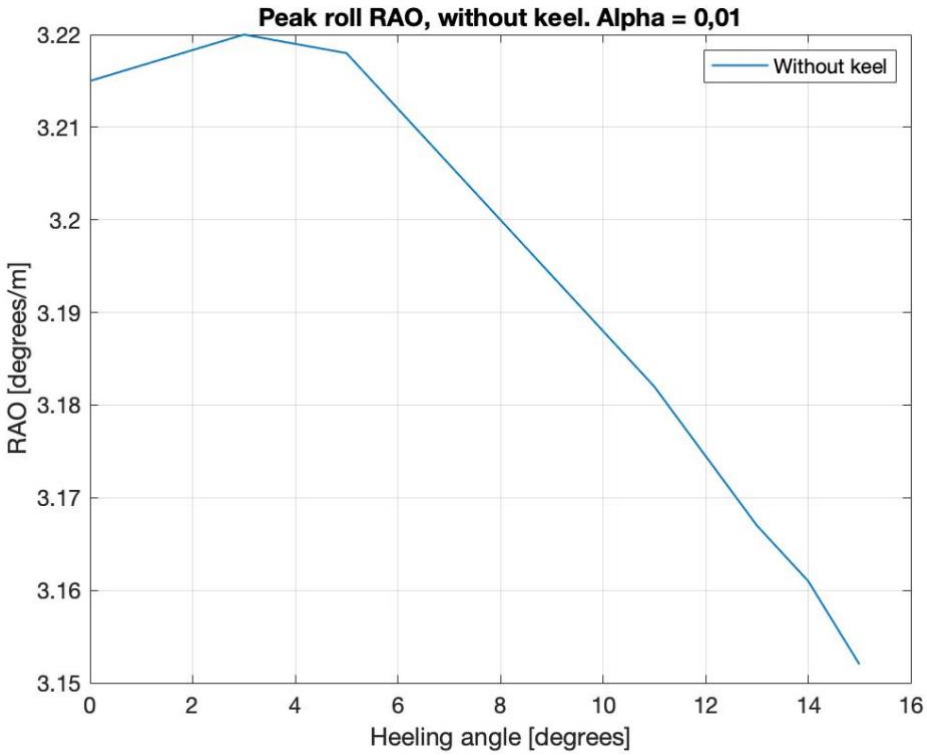

Figure 4.14 - Peak roll RAO, without keel. Alpha value equals to 0.01 and waves coming from 90 degrees. With additional matrix

From the simulations without keel, shown in Figure 4.14, the peak roll RAO occurs at 3 heeling. The peak corresponds to a RAO of 3,22 degrees. From 3 heeling, the ship's RAO roll motion decreases with larger heeling angles. The most prominent peak occurs at 15 heeling and corresponds to a RAO of 3,152 degrees. This will create a total roll angle of 15 heeling + 3,152 roll angle. This equals to an angle of 18,152 degrees. This graph is plotted using the additional matrix and is considered the correct RAO values.

4.3.1. Peak added mass for without keel scenario

The added mass of the structure is vital as this is one of the critical values that change the RAO when adding the additional matrix. Given the figures below, presenting added mass for different heeling angles, the conclusion is that the peak added mass is decreasing in heave, roll, and pitch when adding larger heeling angles to the ship hull. The lowest added mass is present when the ship is heeling 15 degrees. This is since the total area of the waterplane is being reduced when the vessel is heeling. More heeling means a smaller waterplane area.

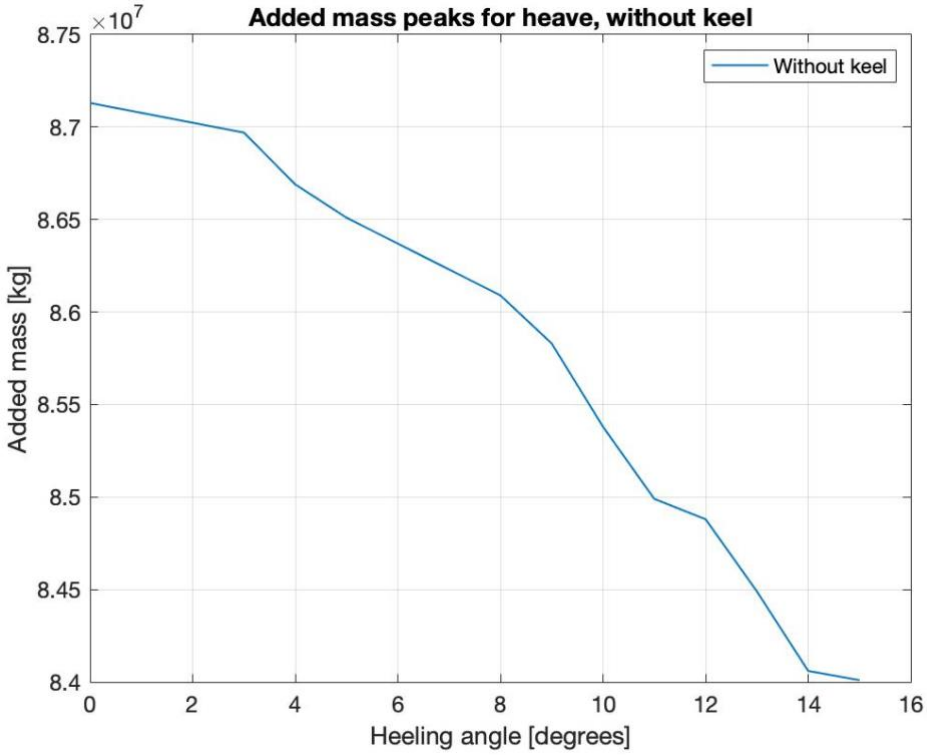

Figure 4.15 - Added mass peaks for heave, without keel. 10 knots forward

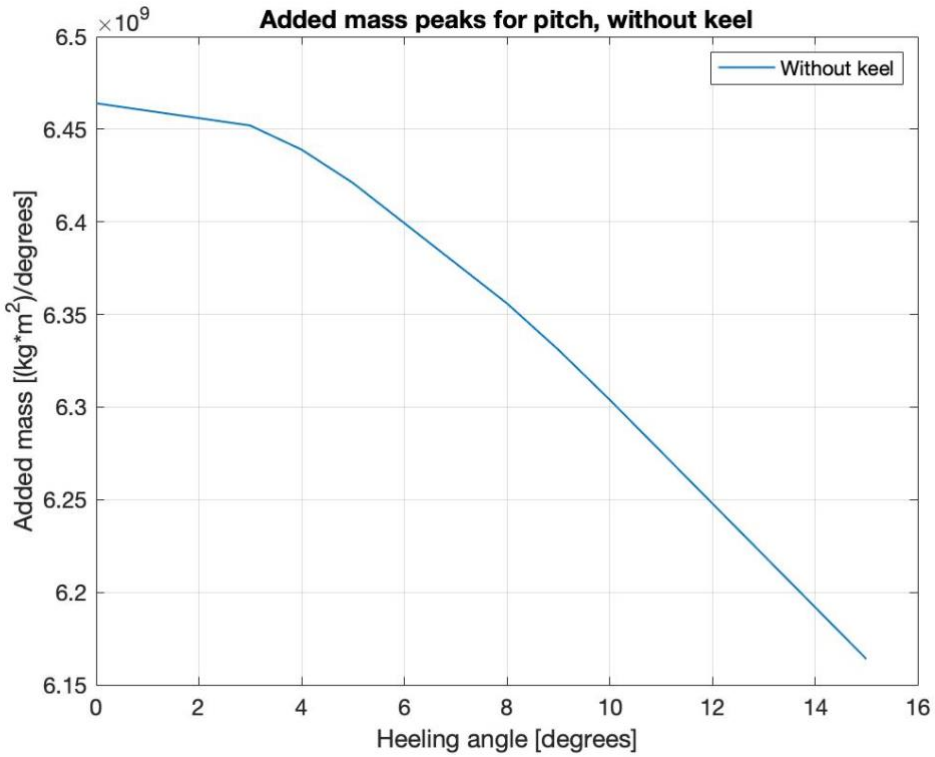

Figure 4.16 - Added mass peaks for pitch, without keel. 10 knots forward

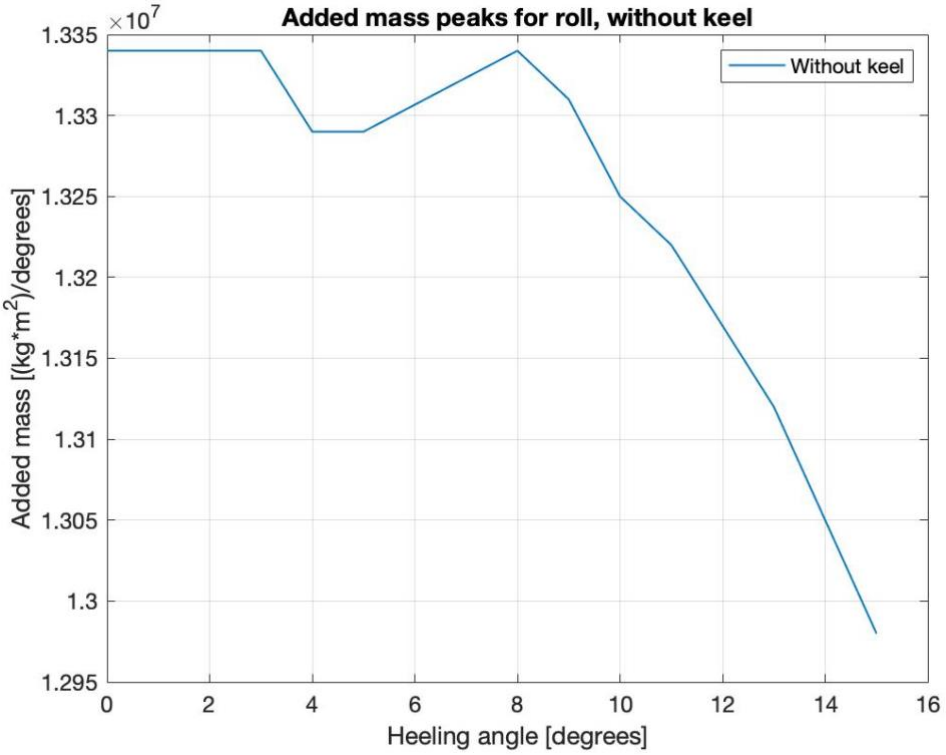

Figure 4.17 - Added mass peaks for roll, without keel. 10 knots forward

4.3.2. Damping calculations using Rayleigh and stiffness matrix

The damping method used to achieve the results in the chapter above is Rayleigh damping. This equation is given above in equation 23. Another way is also applicable when calculating the amount of damping. This uses the stiffness of the structure and also utilizes the alpha factor. This is also referred to as the critical damping. This factor is set to 0.01 in this case. This makes it possible to compare the value with the Rayleigh damping (0,01 alpha factor).

$$\alpha * 2 * \sqrt{k * M} \tag{24}$$

Where,

α = 0.01

k = Stiffness matrix

M = Total mass matrix

The stiffness matrix is gathered from the simulation results. The corresponding k44 value is extracted from this matrix and used in equation 24. The total mass matrix for the ship is generated from the mass matrix and the infinite added mass. These values are added together to obtain the total mass matrix. The infinite added mass is the added mass values at the lowest frequency.

$$M = (m + m_A)$$

To simplify the matrix, the stiffness matrix is reduced to only k44. This is done so that the total damping matrix is not a matrix consisting of complex values. The complete damping matrix will thus, only consist of 1 value, which is C44. This value can be compared with the damping matrix obtained with Rayleigh damping. The

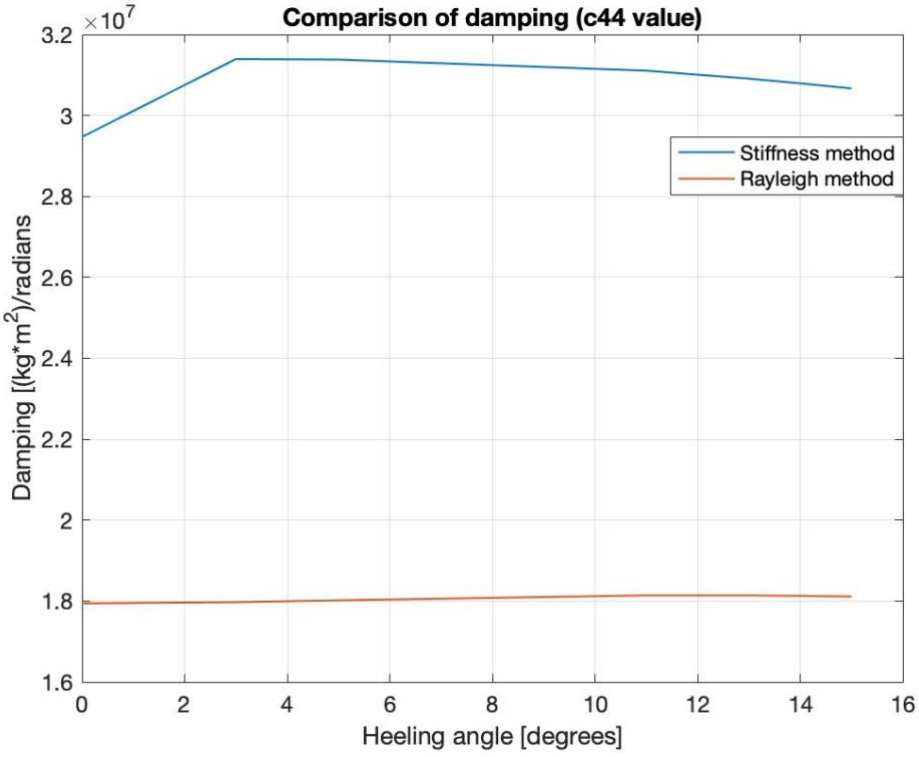

Figure 4.18 - Comparison of damping (c44 value) using stiffness and Rayleigh method. Alpha value equals to 0,01. 10 knots forward speed.

Figure 4.18 shows how the c44 value when using stiffness is higher than when using Rayleigh damping. If the stiffness is used to calculate the damping matrix, the roll RAO values will be lowered. The keels will then be more effective. The damping remains very stable throughout the different heeling angles. The damping calculated with stiffness deviates from 0 heeling to 3 heeling but stays consistent when increasing heeling further.

4.4. Roll stabilization

As the sails will create additional roll angles, it is crucial to create a reduction in this area. Reducing roll motion will be essential to keep the ship behaving relatively optimal. To do so, an analysis using non-identical roll stabilizers has to be performed. This will be done using AQWA software.

The procedure will implement some of the already designed roll stabilizer methods onto this ship, then use different solutions, and run simulations using these. To get a good result using fins/bilge keels, placement is important. If you were to have bilge keel and stabilizer fins, it is essential not to place the bilge keel behind the fins. If you were to have two fins and a bilge keel, the bilge keel could be placed in between the fins but in no circumstances behind the fin in the aft position[14][47][48].

When utilizing the bilge keel, analysis has shown that having a short but wide bilge keel is more effective than having a long but narrow bilge keel. This is true when operating with the same total area in both cases. This is presented in Figure 4.19, where a heading from 0 – 180 degrees is the case.

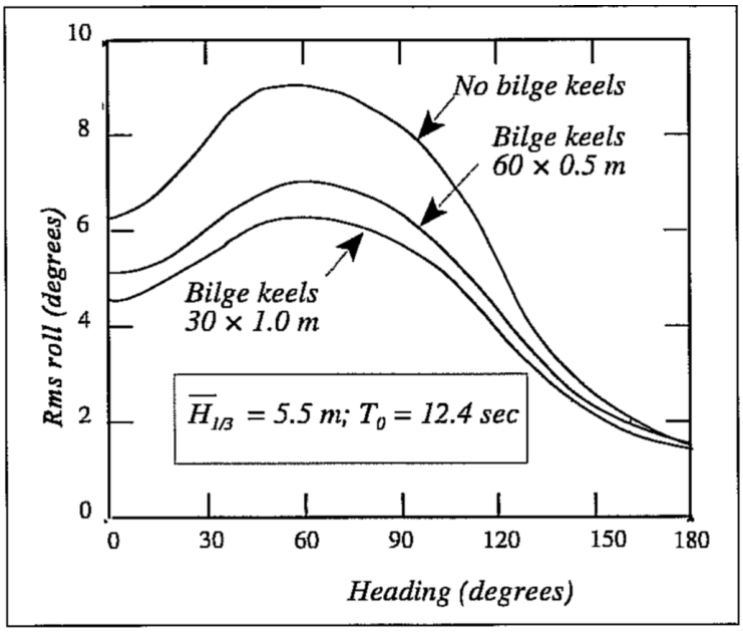

Figure 4.19 - Bilge keel effectiveness with respect to area (wide/narrow)[14].

As this ship will have a relatively low cruising speed, the optimal solution would be to utilize a roll stabilizing system that works efficiently with low speeds. As seen in Table 2.1, active fins are supposed to be less effective when traveling at low speeds. Hence, trying out non-identical bilge/non-active fins configurations would be the go-to solution.

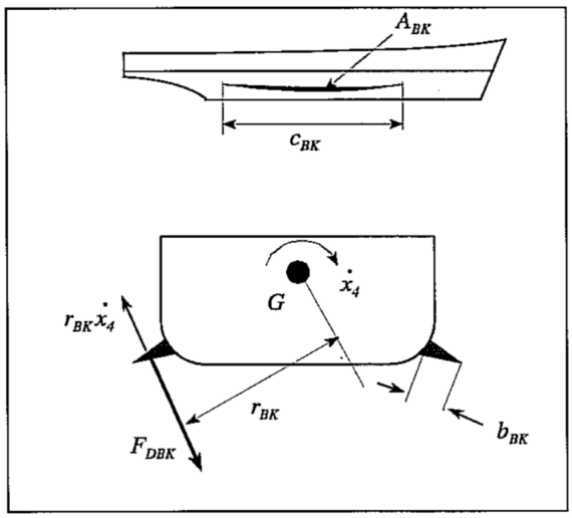

Figure 4.20 - Dimensions of bilge keel design[14]

Figure 4.20 shows the dimensions regarding the aspect ratio for the bilge keel.

The graph shown in Figure 4.21 displays how the aspect ratio of the bilge keel is more effective the higher the aspect ratio becomes[49]. This equation gives the aspect ratio:

$$\alpha_{BK} = \frac{2 * b_{BK}}{c_{BK}} \tag{25}$$

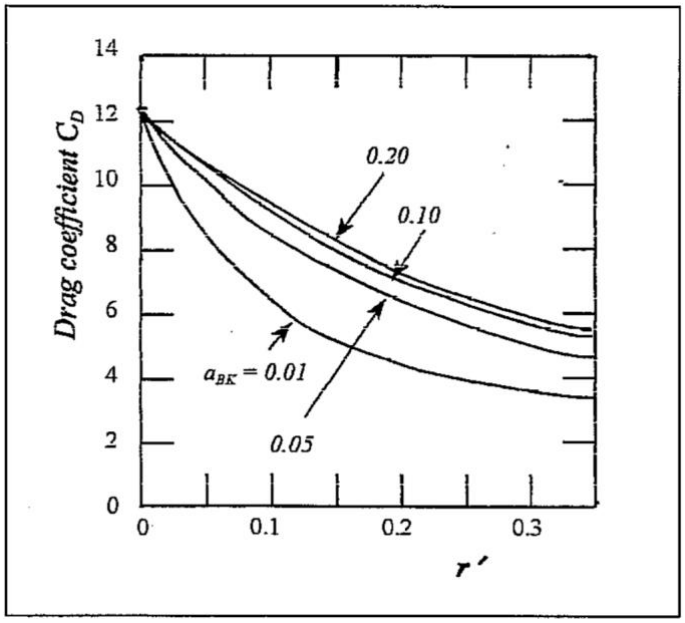

Figure 4.21 - Aspect ratio graph of bilge keel, at 20 knots [50][14].

The result of this is that the aim is to use a bilge keel that is as large as possible while still obtaining the highest aspect ratio possible. This will create the most possible drag in the roll direction and will mitigate the most roll motion. Note that this aspect ratio graph is constructed with a speed of 20 knots.

4.5. Simulations with bilge keels

As the roll motion from the original hull becomes too large, some roll motion reduction methods have to be performed.

Since the ship will use sails to create the forward motion, limited speed can be achieved. It is found out from previous testing that bilge keels become more effective when dealing with low speed. This is stated in Table 2.1, as it explains that a bilge keel is very effective at low speeds compared to fins. Hence, utilizing stabilizer fins on this ship would not be adequate. Bilge keels will, due to this, be the main focus when performing the analysis.

4.5.1. RAO for Keel1 with additional matrix using an alpha value 0,01

First, a simulation will be performed where the bilge Keel1 is attached to the hull. During this simulation, the ship hull will have a heeling angle of zero degrees. The results can then be compared to the previous simulations ran with 0-heeling angle and without bilge keels.

Alpha value of 0,01 means that 1% of the Rayleigh damping will be considered when importing the additional matrix to AQWA. This is assumed to be the lowest potential damping created by the keels and will later be compared will possible higher damping percentages.

These first simulations shown are RAO for heave, roll, and pitch without the additional matrix. One of the main reasons that it was apparent that the simulations showed wrong results was that the RAO roll without keel was lower than the RAO roll with a keel. This is against the theory that adding mass in the roll direction will reduce roll motion. The graphs of 0-heeling without a keel and 0-heeling with Keel1 are presented in the three figures below.

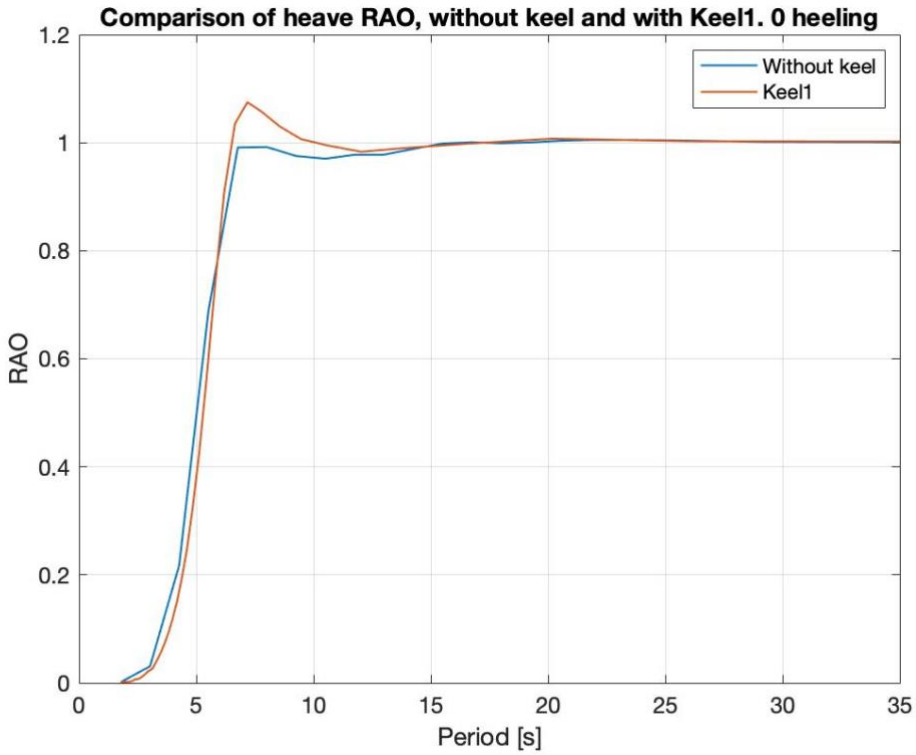

Figure 4.22 - Heave comparison of 0-heeling without keel and with Keel1. Without additional matrix. Not corrected RAO. Waves coming from -90 degrees.

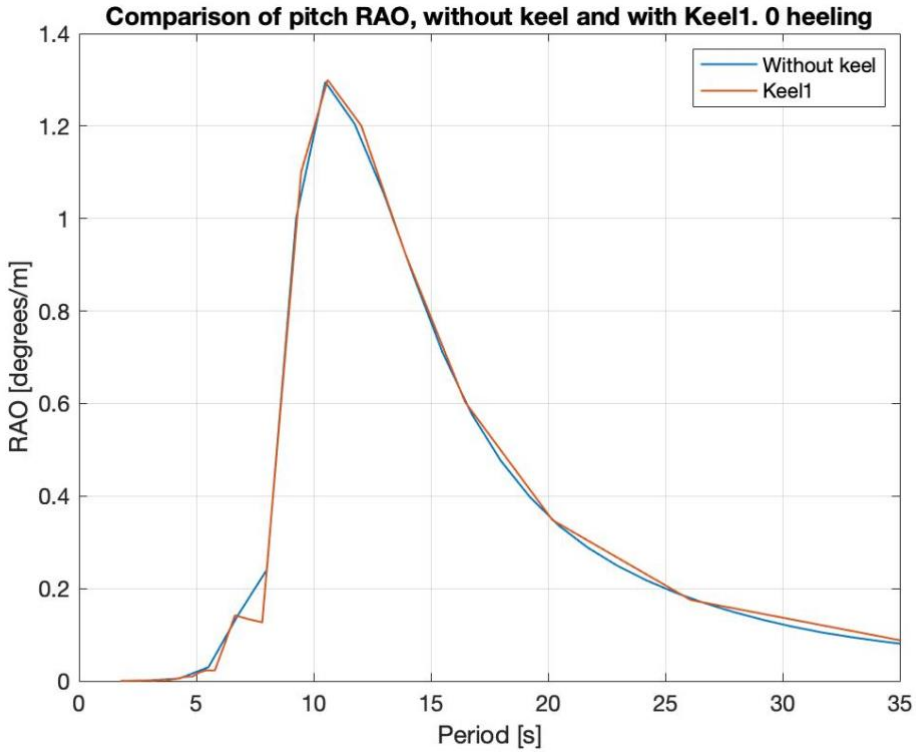

Figure 4.23 - RAO pitch comparison of 0-heeling without keel and with Keel1. Without additional matrix. Not corrected RAO. Waves coming from -135 degrees.

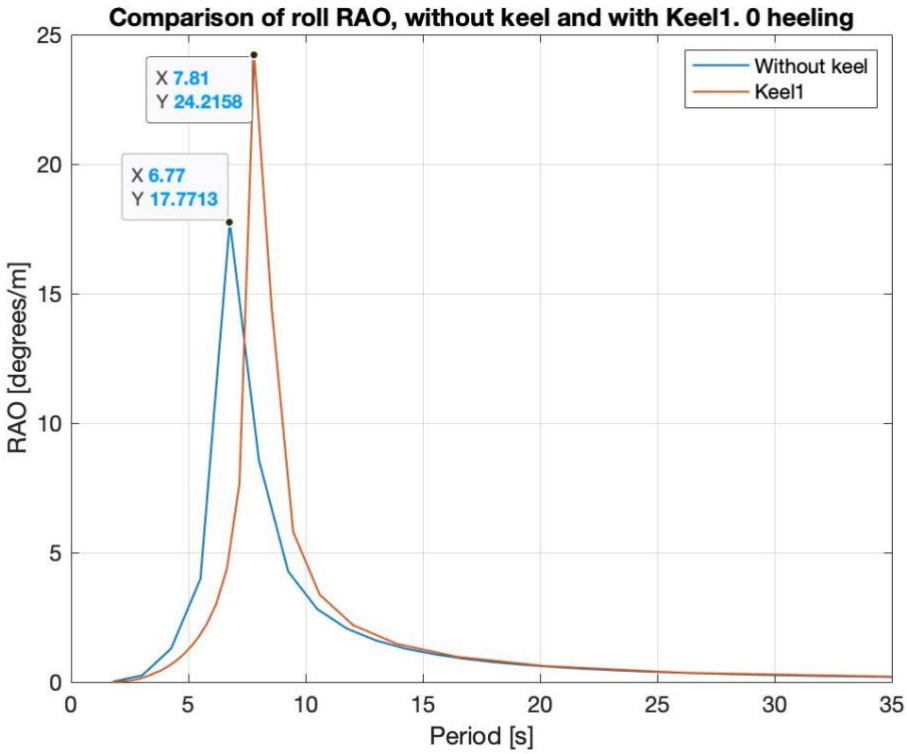

Figure 4.24 - RAO roll comparison of 0-heeling without keel and with Keel1. Without additional matrix. Not corrected RAO. Waves coming from 90 degrees.

As it is possible to see from the three figures above, the only real change when adding a bilge keel is increased roll motion. This is unexpected, and in theory, this should not be the case. When adding these keels, the roll motion should decrease, and the peaks should be significantly lower.

The most likely reason for this is that the default hydrodynamic diffraction option under the AQWA software does not include the non-linear roll damping created by the bilge keels. Hence, regular simulations are not valid when run with the bilge keels attached. The bilge keels create viscous damping, which is not added into the calculations in these linear simulations, as the viscous damping is second order.

To correct the RAO, the same procedure used to correct the simulations without keel is implemented here. Adding the additional matrix gives very promising results.

The first simulations run with Keel1 are also run with an alpha factor of 0.01, using the Rayleigh damping equation given in equation 23. Seven different heeling angles were used for these simulations, as they are very time-consuming. Heeling 0,3,5,11,13,14, and 15.

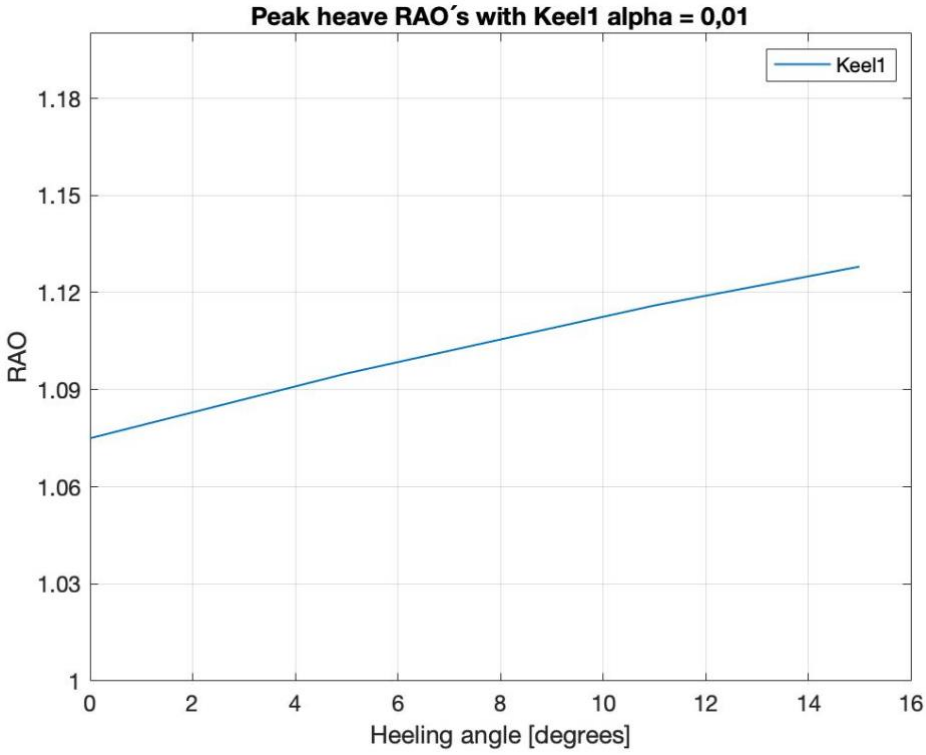

Figure 4.25 - RAO heave with Keel1 (additional matrix is added, alpha value equals to 0,01 and waves are coming from -90 degrees).

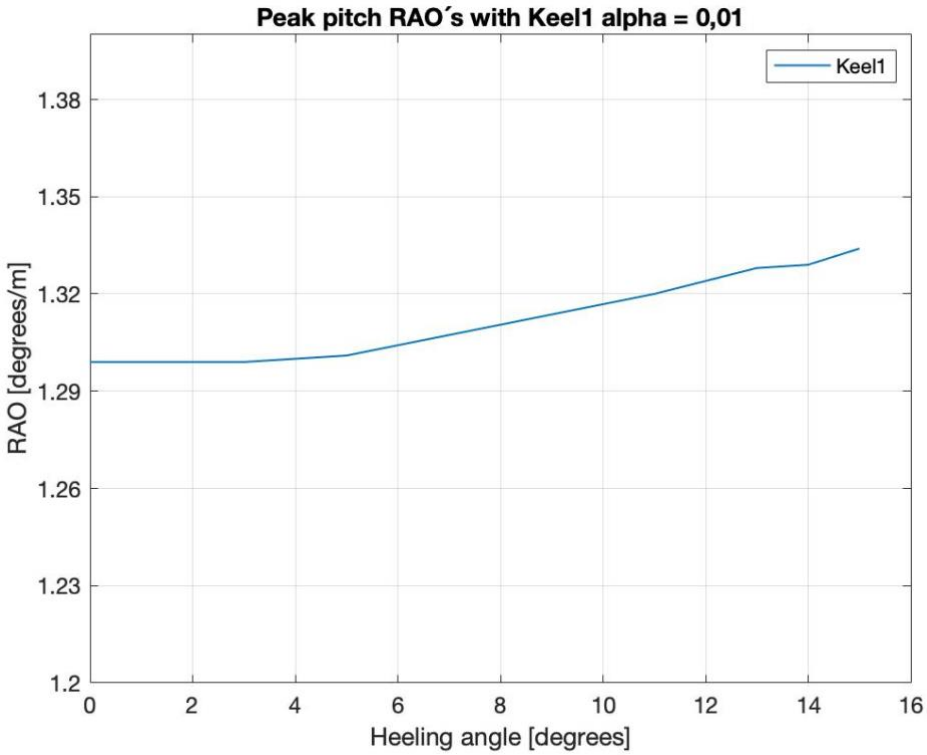

Figure 4.26 - RAO pitch with Keel1 (additional matrix is added, alpha value equals to 0,01 and waves are coming from -135 degrees).

The RAO heave and RAO pitch has a slight increase from 0-heeling to 15-heeling. The increase is very minimal, and these minimal changes will not affect the ship's seakeeping capabilities. It is important to note that the values that will affect the heave and pitch RAO are omitted when adding the damping matrix values. This is because, during this thesis, the focus is primarily on the roll motion.

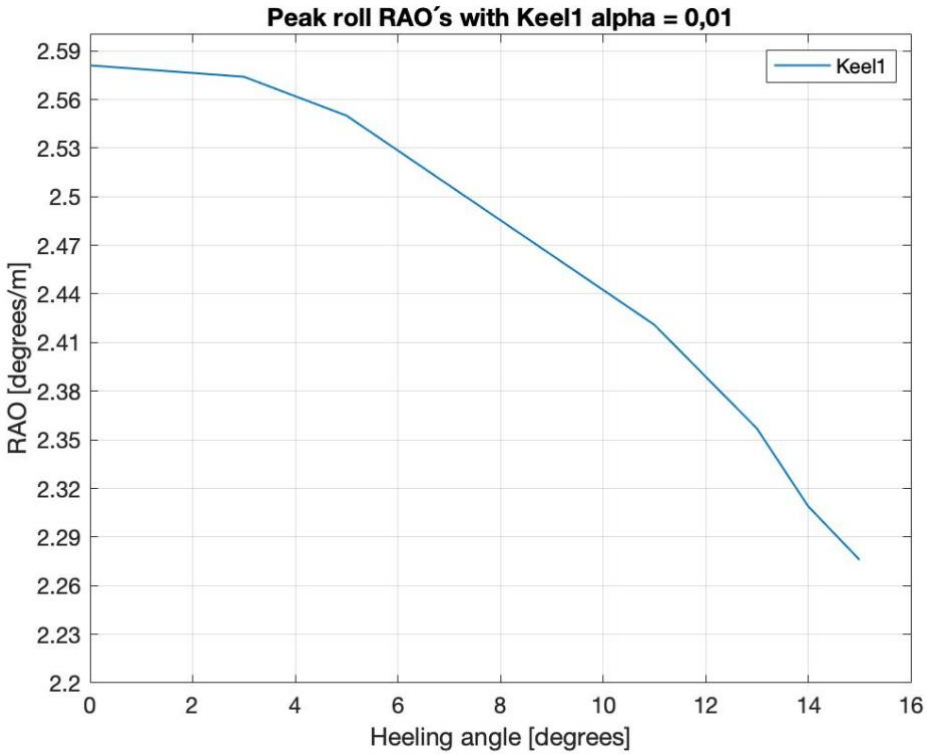

Figure 4.27 - RAO roll with Keel1 (additional matrix is added, alpha value equals to 0,01 and, waves are coming from 90 degrees).

When adding the additional matrix, the RAO roll changes drastically. From a roll angle of about 24 degrees without the additional matrix to a roll angle of 2,581 degrees with the additional matrix. This is because the added damping matrix has increased damping values in roll direction as the c22, c24, c42, and c44 values were included in the matrix when running the simulations. The RAO roll has the highest peak of 2,581 degrees, and this peak happens at 0-heeling. When increasing the initial heeling to the ship hull, the RAO roll decreases. The lowest peak is a roll angle of 2,276 degrees. This roll angle happens at a heeling angle of 15 degrees. This means that the total roll angle would be the 15-heeling angle + the additional 2,276 degrees. This results in a roll angle of 17,276 degrees. This keel is quite effective and shows a decrease in roll motion, as given in Table 4.2.

The effectiveness of the keel increases the more heeling angle the ship is exposed to. The lowest effectiveness is at 0 heeling angle with a 19,72% reduction, and the highest effectiveness is at 15 heeling angle with a 27,79% reduction.

Table 4.2 - Effectiveness of Keel1

Heeling	**Without keel peak roll angle [degrees]**	**Keel1 peak roll angle [degrees]**	**Decrease in peak roll RAO[%]**
0	3,215	2,581	19,72
3	3,22	2,574	20,062
5	3,218	2,55	20,76
11	3,182	2,421	23,92
13	3,167	2,357	25,58
14	3,161	2,309	26,95
15	3,152	2,276	27,79

4.5.2. RAO for Keel2 with additional matrix using an alpha value 0,01

The simulations are also run with an alpha value of 0.01 when adding the Rayleigh damping matrix. The same seven heeling angles were used during the simulations with keel2 as used for the simulations with Keel1. 0,3,5,11,13,14 and 15.

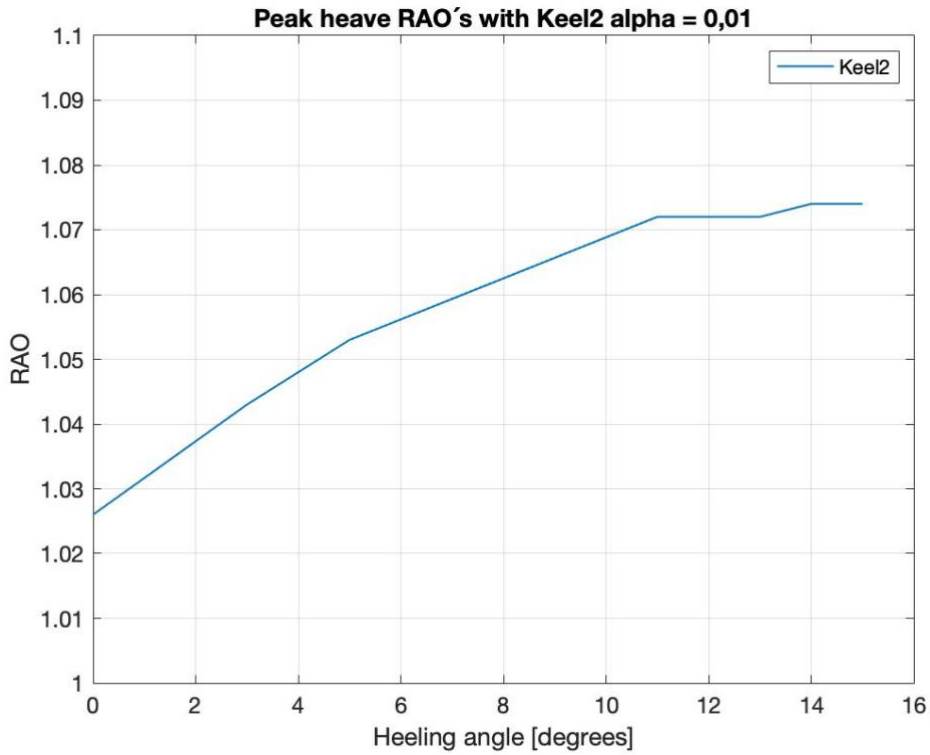

Figure 4.28 - Peak heave RAO, Keel2. Alpha value equals to 0,01. Waves coming from -90 degrees.

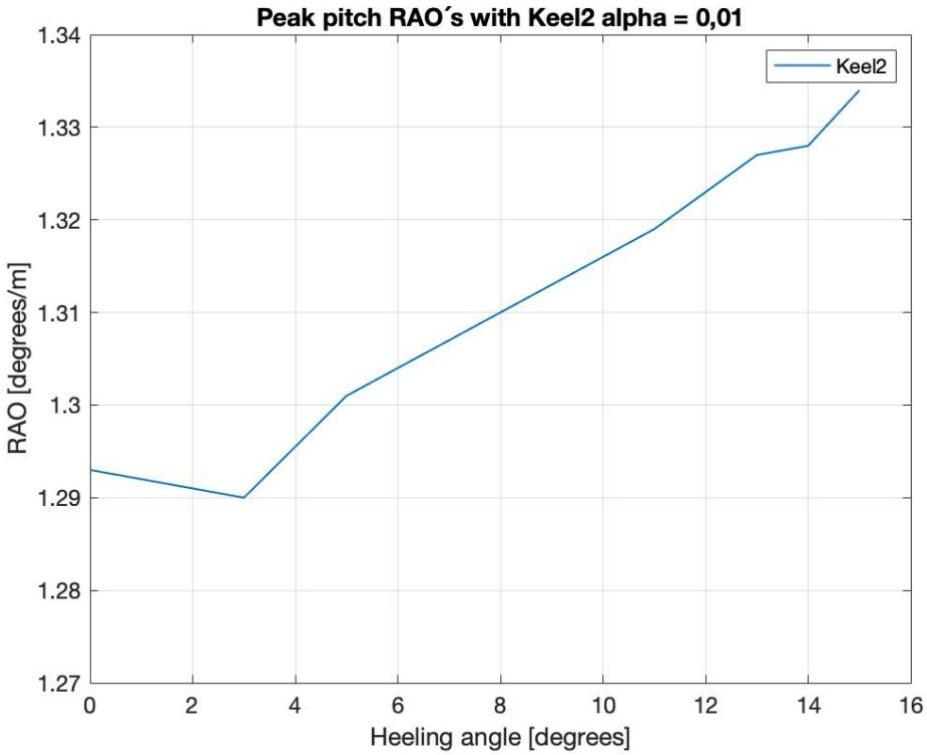

Figure 4.29 - Peak pitch RAO, Keel2. Alpha value equals to 0,01. Waves coming from -135 degrees.

Similar to what was said about heave and pitch with Keel1 simulations, the changes are minimal. This because the values in the damping matrix affecting the heave and pitch motion are neglected. Hence, these motions will not change much.

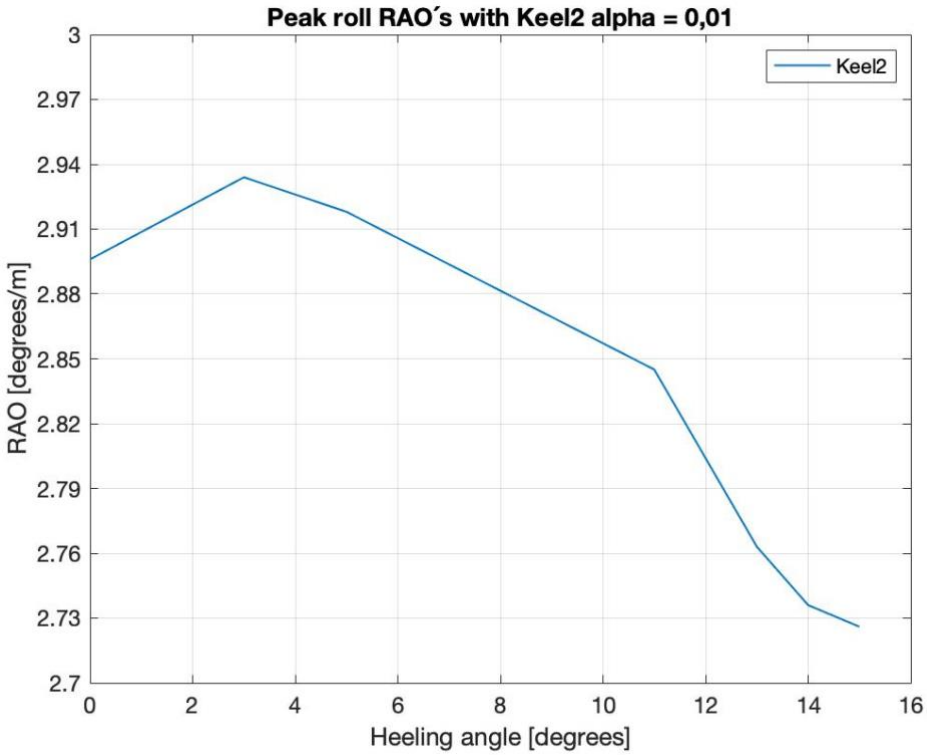

Figure 4.30 - Peak roll RAO, Keel2. Alpha value equals to 0,01. Waves coming from 90 degrees.

The peak roll angles when simulating with keel2 is presented in Figure 4.30. The peak, however, is not at 0 heeling but at 3 heeling. Even though it is slightly increasing initially, the decrease in RAO roll angle is present from 3 heeling and upwards. The highest peak of roll is, in this case, at 3 heeling, with a roll angle of 2,934 degrees. If the ship is to be heeling 15 degrees, where the lowest peak occurs, the highest potential roll angle will result in 15 degrees + 2,726 degrees. This equals to a heeling of 17,934 degrees. To show the effectiveness of keel2, Table 4.3 is presented below.

Table 4.3 - Effectiveness of keel2 in roll motion

Heeling	**Without keel peak roll angle [degrees]**	**Keel2 peak roll angle [degrees]**	**Decrease in peak roll RAO[%]**
0	3,215	2,896	9,92
3	3,22	2,934	8,88
5	3,218	2,918	9,32
11	3,182	2,845	10,59
13	3,167	2,763	12,76
14	3,161	2,736	13,45
15	3,152	2,726	13,52

Keel2 is least effective when the ship is heeling 3 degrees. The effectiveness of the keel is at this point reducing the roll RAO by 8.88%. The efficiency of the keel is increasing when the ship is exposed to a larger heeling angle. This is true, except for the anomaly when the vessel is exposed to a heeling of 3 degrees. The keel is most effective at 15 degrees of heeling with an efficiency of 13,52 degrees.

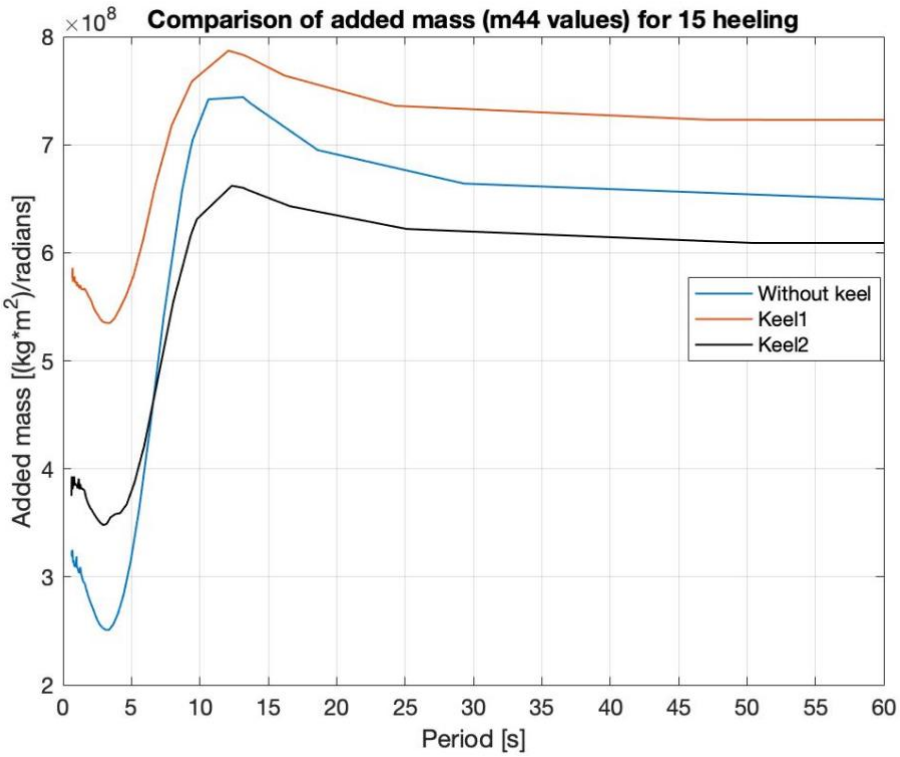

Figure 4.31 - Added mass for the three different configurations, alpha value equals to 0,01. Ship heeling 15 degrees.

Figure 4.31, presents the added mass values for the three configurations; Without keel, Keel1 and Keel2. The added mass values for Keel1 are noticeably more extensive than the two others. This is expected as Keel1 has a larger area affected by the added mass in the roll direction. Unexpectedly, no keel has a more considerable added mass value around a period of 10s compared to Keel1. The reason for this is unknown and might have to be investigated further.

The essential values to obtain from this graph is the infinite added mass for the three configurations. The infinite added mass is found at the lowest frequency and is the key factor to why the additional damping matrix changes so drastically. The lowest frequency in this graph is at a period of 0s. At this point, the lowest value is for the “No keel” scenario. For Keel1, the infinite added mass value is close to 25% higher, and for Keel2, the infinite added mass value is approximately doubled. This has a significant effect on the result of the additional damping matrix used when simulating the RAO. This is the key factor that reduces the RAO roll angles achieved in the simulations.

4.6. Comparison of damping values

To minimize the number of simulations, only a heeling angle of 15 degrees is considered when using the additional 0,02 and 0,05 alpha values. This is done so that the alpha values of 0,01, 0,02, and 0,05 can be compared and make it possible to determine the effect of potential higher damping. When an alpha value of 0,01 is considered, it means that 1% of the potential damping is imported into AQWA. 0,02 equals to 2% and 0,05 equals to 5%. 1% is assumed to be the lowest possible damping created by the keels.

4.6.1. Comparison of roll motion using an alpha value of 0,02

Using the Rayleigh damping equation given in equation 23 above, shown below for simplicity, changing the alpha value from 0,01 to 0,02 will double the additional damping obtained. The additional damping matrix will then be much more effective, and the roll RAO will act accordingly. The equation below is the same as presented in equation 23.

$$c = \alpha * (m * m_A)$$

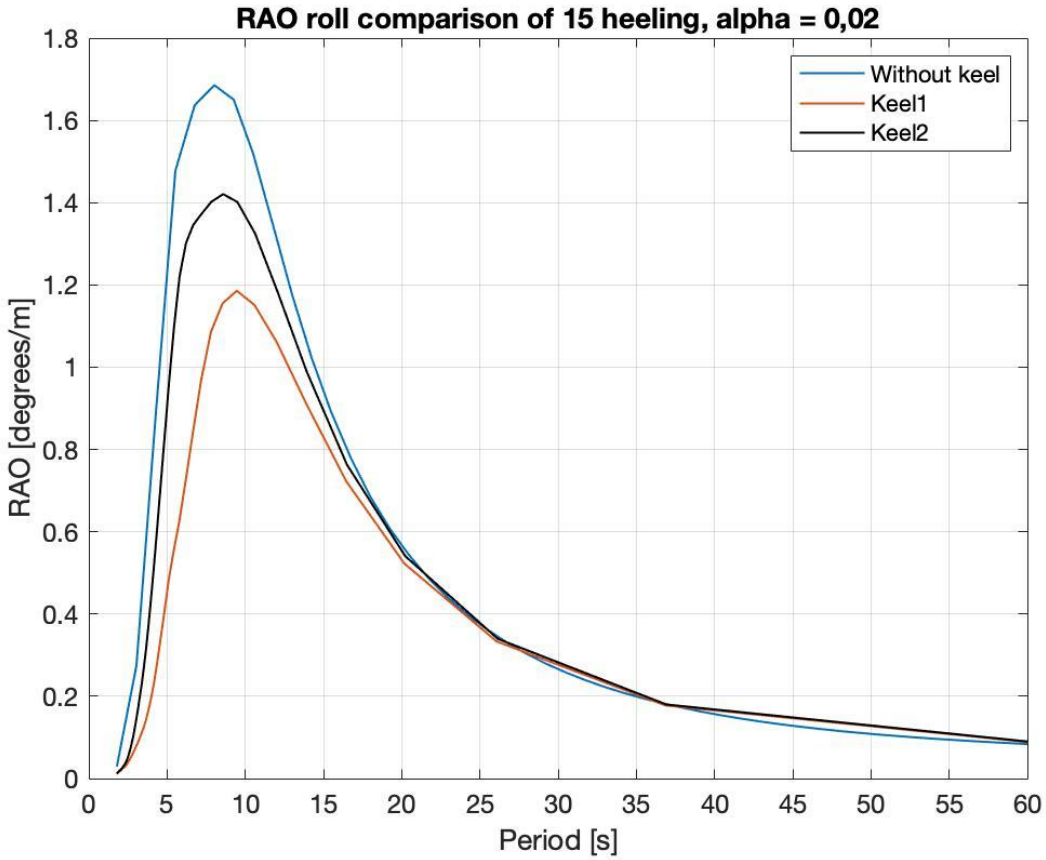

Figure 4.32 - Comparison of RAO roll of 15 heeling, with alpha value equal to 0,02. 10 knots forward speed.

- For no keel, the peak roll RAO is 1,685 and occurs at a wave period close to 8s.

- For Keel1, the peak roll RAO is 1,186 and occurs at a wave period just shy of 10s.

- For keel2, the peak roll RAO is 1,421 and occurs at a wave period close to 9s.

Table 4.4 - Comparison of roll RAO for the three different configurations with alpha value equal to 0,02

Configuration	**Heeling**	**Peak roll angle [degrees]**	**Decrease in peak roll RAO [%]**
Without keel	15	1,685	0
Keel1	15	1,186	29,61
Keel2	15	1,421	15,67

The configuration that consists of no keel is set as a standard. Hence, 0 decrease in roll RAO. As these simulations are very time-consuming, 15 heeling to the ship is the only instance simulated with an alpha factor of 0,02. Doing this makes it possible to compare the 15 heeling models and calculate the efficiency of the keels, Table 4.4.

- Keel1 is reducing the roll RAO by 29,61%.

- Keel2 is reducing the roll RAO by 15,57%.

4.6.2. Comparison of roll motion using an alpha value of 0,05

Using an alpha value equal to 0,05, the additional damping matrix is five times bigger than when using 0,01. This has a massive effect on the roll RAO as the damping matrix will result in a number 5 times larger than the original 0,01 matrix.

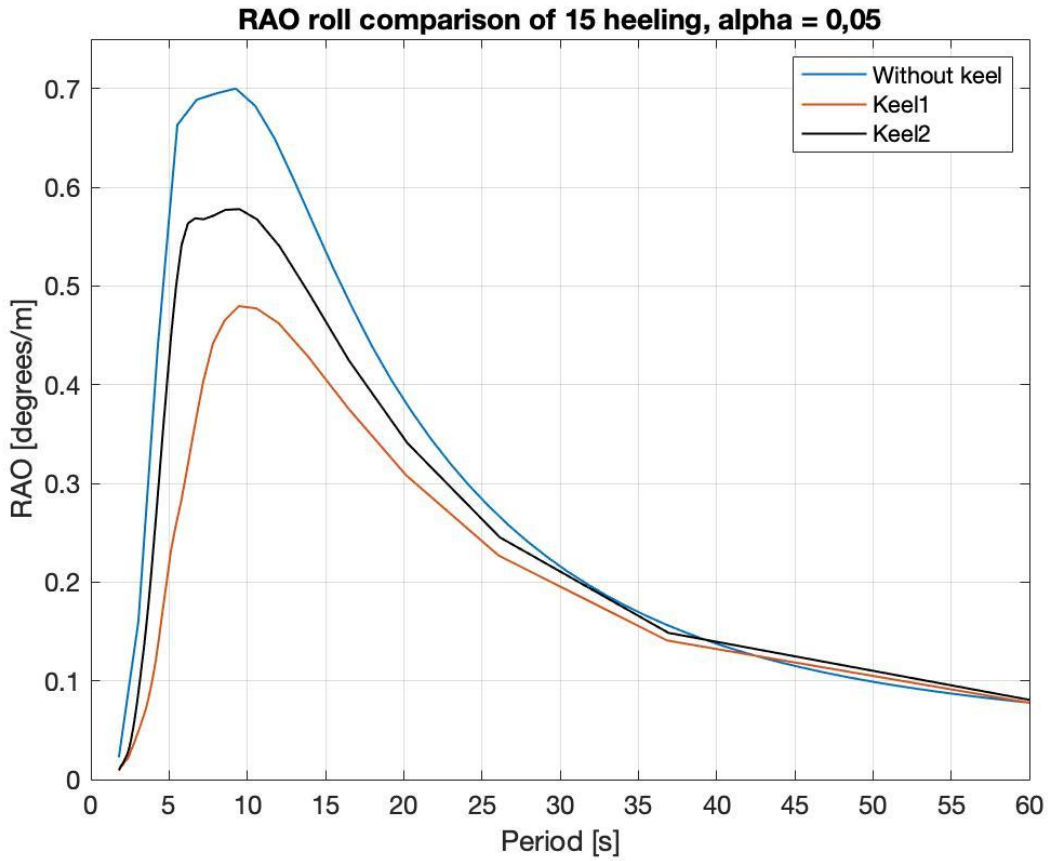

Figure 4.33 - Comparison of RAO roll of 15 heeling, alpha value equal to 0,05. 10 knots forward speed.

As seen from the simulations with an alpha value of 0,05, the RAO roll motion has significantly decreased.

- For no keel, the peak roll RAO is 0,699 and occurs at a wave period just shy of 10s.
- For Keel1, the peak roll RAO is 0,4795 and occurs at a wave period of 10s.
- For keel2, the peak roll RAO is 0,5778 and occurs at a wave period just shy of 10s.

Table 4.5 - Comparison of roll RAO for the three different configurations with alpha value equal to 0,05

Configuration	**Heeling**	**Peak roll angle [degrees]**	**Decrease in peak roll RAO [%]**
Without keel	15	0,6999	0
Keel1	15	0,4795	31,49
Keel2	15	0,5778	17,45

As the previous table stated, the "Without keel" scenario is set as the standard, hence 0%. 15 heeling to the ship is the only instance simulated with an alpha factor of 0,05. This makes it possible to compare the 15 heeling scenarios and calculate the efficiency. This is shown in Table 4.5.

- Keel1 is reducing the peak roll RAO by 31,49%
- Keel2 is reducing the peak roll RAO by 17,45%

4.7. Discussion of analysis

4.7.1. RAO comparison using an alpha value of 0,01

Most of the analysis has been done with an alpha value equal to 0,01. As there are multiple simulations run with this value, it is easier to compare the results.

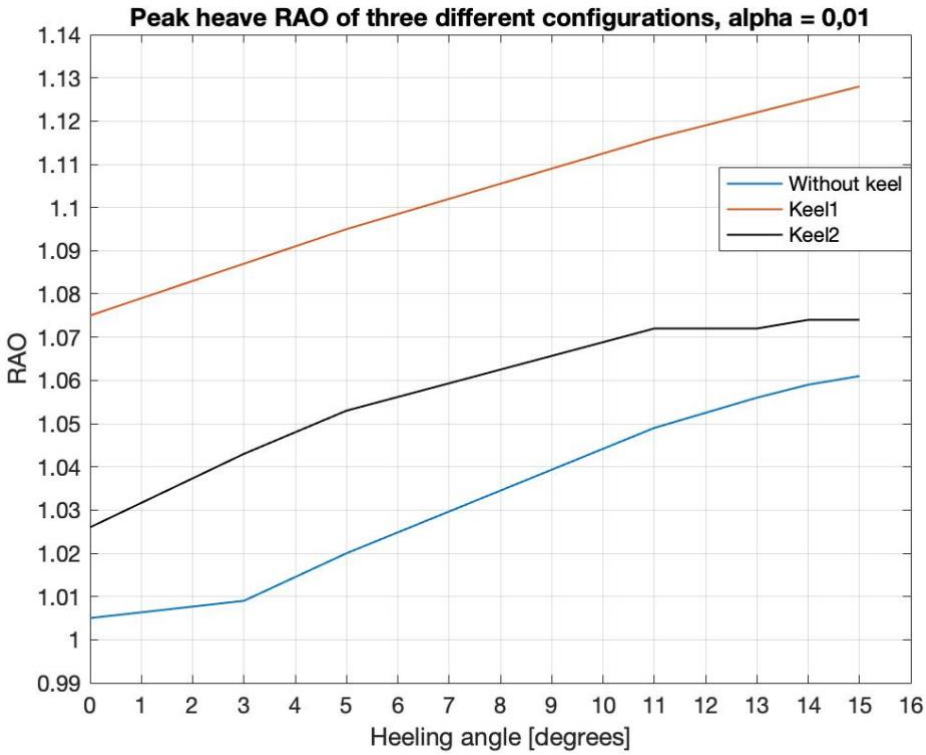

Figure 4.34 – Peak heave RAO comparison of the three different configurations. Alpha value equals to 0,01. 10 knots forward speed.

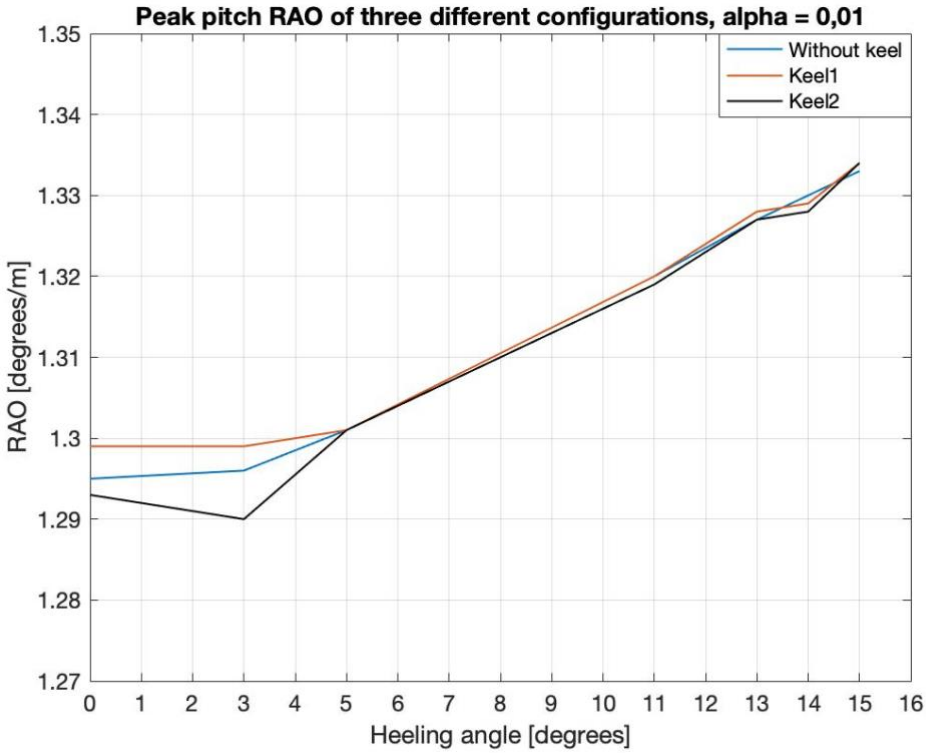

Figure 4.35 – Peak pitch RAO comparison of the three different configurations. Alpha value equals to 0,01. 10 knots forward speed.

As mentioned previously, the heave and pitch values stay stable throughout the whole process. It is possible to see a slight increase in heave due to keel2 and an even higher increase in heave from Keel1. The pitch RAO stays about the same throughout every different heeling angle given to the ship.

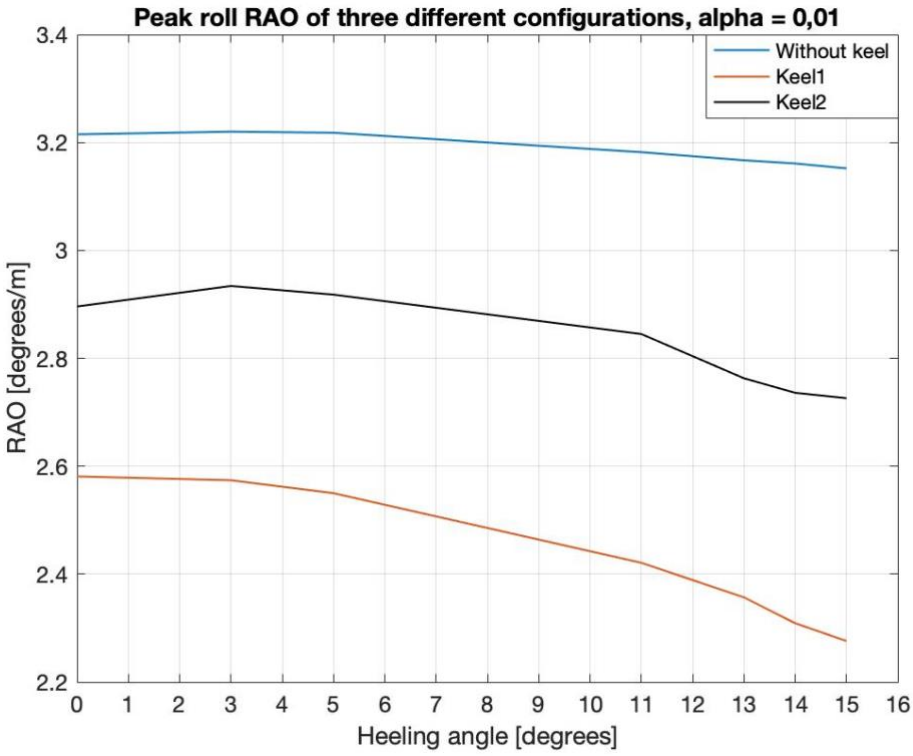

Figure 4.36 – Peak roll RAO comparison of the three different configurations. Alpha value equals to 0,01. 10 knots forward speed.

It is evident from this table that both of the keels are effective when it comes to reducing roll motion. In both cases, the efficiency increases when the ship is exposed to a larger heeling angle. This is valid in all cases, except the anomaly at 3 degrees of heel, where the roll RAO increases without keel and with keel2. The reason for this is most likely due to the geometry of the ship hull. The three different configurations have approximately the same curve in Figure 4.36, except that the curves regarding the keels become steeper due to the fact that the efficiency of the keels increases with heeling.

Table 4.6 - Comparison of keel efficiency

Heeling	**Without keel peak roll RAO [degrees]**	**Keel1 peak roll RAO [degrees] (% increase)**	**Keel2 peak roll RAO [degrees] (% increase)**
0	3,215	2,581 (19,72)	2,896(9,92)
3	3,22	2,574 (20,062)	2,934(8,88)
5	3,218	2,55 (20,76)	2,918(9,32)
11	3,182	2,421 (23,92)	2,845(10,59)
13	3,167	2,357 (25,58)	2,763(12,76)
14	3,161	2,309 (26,95)	2,736(13,45)
15	3,152	2,276 (27,79)	2,726(13,52)

.

Keel1 is by far the most effective keel. The area of this keel is more extensive and will generate more viscous damping. Keel1 is reducing the roll RAO by up to 27,79% at its most effective stage. This stage is when the ship is exposed to a heeling angle of 15. Keel2 is also at its most efficient at a heeling of 15 degrees with its efficiency of 13,52%. The difference from Keel1 to keel2 at this stage is considerable. Keel1 is 14,27% more effective at 15 heeling.

When creating keel2, the main focus was to make the keel such that it did not exceed the rectangle area created by the bilge of the ship hull, referring to Figure 3.5. Due to this, keel2 has a smaller effective area mitigating roll motion. This will make a configuration such as keel2 to be less desirable. Even though this is the case, Keel1 might cause issues when navigating shallow waters as the keel is further away from the original ship hull. This will "make" the ship's draft deeper and the beam wider.

A 3-heeling scenario is also set up with forward heeling. This is to check the efficiency of the keels when the ship is heeling forward. Giving the hull of the vessel a heeling of 3 degrees is quite drastic, and giving the ship increased heeling would result in the ship being underwater.

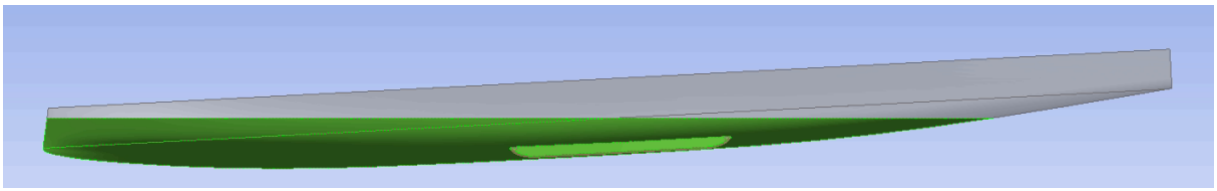

Figure 4.37 - Ship hull heeling 3 degrees forward

Figure 4.37 shows how the ship is presented when heeling 3 degrees forward. The green area is the submerged volume.

Table 4.7 - Comparison of the three different configurations with a heeling of 3 degrees. Alpha value equals to 0,01

Heeling	**Without keel peak roll RAO [degrees]**	**Keel1 peak roll RAO [degrees] (% increase)**	**Keel2 peak roll RAO [degrees] (% increase)**
3 degrees forward	2,789	2,088 (25,13)	2,348 (15,81)

The efficiency of the keels is increased when heeling the ship 3 degrees forward. The reason for this is likely to be that the 3 heeling forward is equivalent to a significantly steeper heeling angle to port/starboard side.

4.7.2. RAO comparison using an alpha value of 0,02 and 0,05

When increasing the alpha value to 0,02 and 0,05, the damping increased significantly. As a result of this, the peak roll RAO was drastically reduced.

Table 4.8 - Comparison of alpha values of 0,02 and 0,05

Alpha value	**Without keel peak roll RAO [degrees]**	**Keel1 peak roll RAO [degrees] (%increase)**	**Keel2 peak roll RAO [degrees] (%increase)**
0,01	3,152	2,276 (27,79)	2,726(13,52)
0,02	1,685	1,186 (29,61)	1,421 (15,67)
0,05	0,6999	0,4795 (31,49)	0,5778 (17,45)

Keel1 is still the most efficient configuration, both with 0,02 and 0,05 as alpha values. The difference that is worth noting from the simulations with these values is that the efficiency of the keels has increased.

- Increasing the alpha value from 0,01 to 0,02 increases Keel1´s efficiency with 1,82% and keel2´s efficiency with 2,15%.

- Increasing the alpha value from 0,01 to 0,05 increases Keel1´s efficiency with 3,7% and keel2´s efficiency with 3,93%.

This means that the viscous damping created by the keels is increased when using higher values of alpha. This is because the 0,01 increase in alpha value will increase the additional damping generated by the keels by 1%.

4.8. Estimating potential sail force

To give a perspective on how much wind force the ship will be able to hold, some calculations are performed. The equations used to calculate are presented in the theory chapter, equation 15 and 16. For simplicity, the equations are repeated below[29].

$$M_{thrust} = F_{thrust} * d$$

$$Heeling\ angle = \frac{M_{thrust}}{K_{44}}$$

Where,

d is the length from the center of sails to the center of buoyancy.

M_{thrust} is the moment of the thrust generated on the center of gravity, as the center of gravity is oriented at the ship's axis system.

K_{44} is the stiffness of the ship hull in the roll direction. The point of reference for this value is the center of gravity.

Assuming the sails are 80 meters tall.

$$d = \frac{80}{2} + (7{,}5 + 0{,}973) = 48{,}473\ m$$

The added values in the equation above are the height of the ship from the waterline (7,5m) and the length from the center of gravity to the waterline.
48,473 meters is the resulting length from the center of sails to the center of gravity.

When calculating the wind force, these equations are calculated backwards. Already having the heeling angles makes us able to back-calculate the potential wind force that could be acceptable on the ship hull. The first example will be done with a heeling angle equal to 15 degrees. This angle will be changed to radians.

$$0{,}259\ rad = \frac{M_{thrust}}{1298200000\ Nm} \qquad (26)$$

$$M_{thrust} = 336233800\ Nm \tag{27}$$

$$F_{thrust} = \frac{336233800\ Nm}{48{,}473\ m} = N = 6936{,}5kN \tag{28}$$

This means that to obtain a heeling angle of 15 degrees, the wind force has to be a total of 6266,4 kN. This force will be divided amongst the number of sails mounted on the ship. This is the worst-case scenario, and having this much sail force will most likely not be optimal.

Table 4.9 - Total sail force

	Total sail force [kN]		
Heeling angle	**Without keel**	**Keel1**	**Keel2**
3	1480,9	1302,3	1309,6
5	2459,8	2160,8	2173,3
11	5281,4	4611,2	4641
13	6158	5359,7	5396,1
14	6582,6	5718,8	5758,6
15	6937	6456,2	6058,1

From these calculations in Table 4.9, the total sail force that can be utilized at the different heeling angles is presented. This means that if a heeling angle of 15 degrees were acceptable, a total sail force of 6936,5 kN (without keel) would be possible as this will make the ship heel 15 degrees.

It is evident from the table that it is possible to have a more significant sail force when not utilizing the keels. This is surprising and might bring forward the question if a bottom keel is

necessary. This to potentially give a larger counterweight to when the ship is heeling due to the forces acting on the sails. This is commonly used for smaller sailing vessels.

5. Conclusion and future work

After doing plenty of simulations, it is evident that a bilge keel decreases the ship's roll motion while under seaway. As the vessel uses sails, the ship will not reach higher speeds, such as a traditional freighter ship. Thus, the bilge keels are a viable solution to reduce roll motion, as this is more effective when traveling at lower speeds. The keels are created with the knowledge that the higher aspect ratio gives higher efficiency. This means that the keel will be more beneficial if created as short as possible and as wide as possible. So, during the simulations, the limits are pushed when Keel1 is designed with a wide geometry and a high aspect ratio.
When comparing the efficiency of the different keel geometries, it is clear that Keel1 is more effective at reducing roll motion to the ship hull. Although this is the case, Keel2 is also effective at lowering roll motion, but Keel2 has been limited in terms of geometry size. The size has been limited such that the keel is inside the bilge of the hull and the hull's draft. This reduces the efficiency but increases the ship's mobility if navigating shallow waters becomes of interest. During the analysis, different alpha values were compared to display the effect of the viscous damping created by the keels. When increasing the viscous damping from 1% to 2%, the efficiency of the keels slightly increases. This is also the case when increasing the viscous damping from 1% to 5%. This compares the potential damping created by the keels, whereas 1% is assumed to be the lowest.

The reduction in peak roll RAO is showcased in Table 5.1. The additional damping matrix is added to these results, and the efficiency of the keels is presented.

Table 5.1 - Showing comparison of Keel1 and Keel2, peak roll RAO.

Heeling	**Without keel peak roll RAO [degrees]**	**Keel1 peak roll RAO [degrees] (% increase)**	**Keel2 peak roll RAO [degrees] (% increase)**
0	3,215	2,581 (19,72)	2,896(9,92)
3	3,22	2,574 (20,062)	2,934(8,88)
5	3,218	2,55 (20,76)	2,918(9,32)
11	3,182	2,421 (23,92)	2,845(10,59)
13	3,167	2,357 (25,58)	2,763(12,76)
14	3,161	2,309 (26,95)	2,736(13,45)
15	3,152	2,276 (27,79)	2,726(13,52)

It is clear that the roll RAO is decreasing when the ship has increased heeling. This is because of the geometry of the ship hull. When the hull is heeling, the waterplane area will change, and the resulting center of flotation will adjust.

As the simulations are very tedious, time-domain simulations were not included in this thesis. If this project is to be continued, a time-domain analysis will be beneficial. This will make it possible to analyze further the benefits of keels on such a large ship. After performing time-domain analysis, the project can be taken further by performing tests with a model version. This can be done using a water tank, and measurements will be obtained through practical testing. This will strengthen the analysis as the experimental testing will be more precise and can be compared with the theoretical results.

A CFD analysis should be performed to maximize the efficiency of the potential keels used to reduce the roll motion. This will improve the keel's hydrodynamic efficiency and the placement of the keel. This will reduce the resistance the keels will create.

Given the results obtained throughout this thesis, the most optimal solution to reduce roll motion on a large ship, such as used in this thesis, is using bilge keels. This is because the vessel will utilize sails and will, due to this, operate at lower cruising speeds. This will make the bilge keels more effective than the other alternatives as these other alternatives become more effective when increasing the speed. The bilge keels are proven to be easy to mount and easily maintained.

The additional matrix had to be added to the AQWA hydrodynamic diffraction simulations to obtain the correct results during the thesis. The approach to obtaining this matrix is clearly explained in this thesis and will make it easier for future work to be done using the AQWA hydrodynamic diffraction option.

References

[1] International Chamber of Shipping, “Shipping and world trade: driving prosperity.” https://www.ics-shipping.org/shipping-fact/shipping-and-world-trade-driving-prosperity/ (accessed Jan. 11, 2021).

[2] L. Blain, “Oceanbird’s huge 80-meter sails reduce cargo shipping emissions by 90%,” *New Atlas*, Sep. 14, 2020. https://newatlas.com/marine/oceanbird-wallenius-wing-sail-cargo-ship/ (accessed Jan. 12, 2021).

[3] Oceanbird, “Oceanbird.” https://www.oceanbirdwallenius.com/ (accessed Jun. 12, 2021).

[4] R. Spilman, “The Return of Commercial Sail - UT Wind Challenger & Retracting Rigid Wing Sails,” *Old Salt Blog*, Jul. 10, 2012. http://www.oldsaltblog.com/2012/07/the-return-of-commercial-sail-ut-wind-challenger-retracting-rigid-wing-sails/ (accessed Jun. 11, 2021).

[5] K. Ouchi, K. Uzawa, A. Kanai, and M. Katori, “‘Wind Challenger’ the Next Generation Hybrid Sailing Vessel,” p. 6.

[6] K. S. Youssef, S. A. Ragab, A. H. Nayfeh, and D. T. Mook, “Design of passive anti-roll tanks for roll stabilization in the nonlinear range,” *Ocean Engineering*, Feb. 2002, doi: 10.1016/S0029-8018(01)00021-X.

[7] A. F. A. Gawad, S. A. Ragab, A. H. Nayfeh, and D. T. Mook, “Roll stabilization by anti-roll passive tanks,” *Ocean Engineering*, vol. 28, no. 5, pp. 457–469, May 2001, doi: 10.1016/S0029-8018(00)00015-9.

[8] R. Moaleji and A. R. Greig, “On the development of ship anti-roll tanks,” *Ocean Engineering*, vol. 34, no. 1, pp. 103–121, Jan. 2007, doi: 10.1016/j.oceaneng.2005.12.013.

[9] “Anti-Roll Tank | Ship Stabilizer Manufacturer | DELIN.” http://dlmarine.com/2-anti-rolling-tank (accessed May 06, 2021).

[10] Norsepower, “Rotor Sail Technology | Norsepower.” https://www.norsepower.com/technology (accessed Jun. 12, 2021).

[11] USNA, “An Introduction to Seakeeping,” *United States Naval Academy*.

[12] K. J. Rawson, “Seakeeping.” https://www.sciencedirect.com/topics/engineering/seakeeping (accessed May 19, 2021).

[13] D. Hoffman, “The Impact of Seakeeping on Ship Operations,” *Marine Technology and SNAME News*, vol. 13, no. 03, pp. 241–262, Jul. 1976, doi: 10.5957/mt1.1976.13.3.241.

[14] A. R. J. M. Lloyd, “Seakeeping: Ship Behaviour in Rough Weather,” 1989, Accessed: Jan. 25, 2021. [Online]. Available: http://resolver.tudelft.nl/uuid:f9315ebe-acbb-4b22-81a9-

a2a340090ebd

[15] R. A. Barr and V. Ankudinov, “Ship Rolling, Its Prediction and Reduction Using Roll Stabilization,” *Marine Technology and SNAME News*, vol. 14, no. 01, pp. 19–41, Jan. 1977, doi: 10.5957/mt1.1977.14.1.19.

[16] “slingrekjøl,” *Store norske leksikon*. Dec. 31, 2020. Accessed: Apr. 26, 2021. [Online]. Available: http://snl.no/slingrekj%C3%B8l

[17] M. DiFrangia, “Electrohydraulic controls improve ship stability,” *Fluid Power World*, Apr. 18, 2016. https://www.fluidpowerworld.com/electrohydraulic-controls-improve-ship-stability/ (accessed Jan. 25, 2021).

[18] Engineering Toolbox, “Lift and Drag.” https://www.engineeringtoolbox.com/lift-drag-fluid-flow-d_1657.html (accessed Jun. 12, 2021).

[19] C.-Y. Tzeng and C.-Y. Wu, “ON THE DESIGN AND ANALYSIS OF SHIP STABILIZING FIN CONTROLLER,” *Journal of Marine Science and Technology*, vol. 8, no. 2, p. 8, 2000.

[20] Wartsila, “Active-fin stabilisers.” https://www.wartsila.com/encyclopedia/term/active-fin-stabilisers (accessed Mar. 18, 2021).

[21] K. J. Rawson and E. C. Tupper, *Basic Ship Theory*. Elsevier, 2001. doi: 10.1016/B978-0-7506-5398-5.X5000-6.

[22] C. B. Barrass and D. R. Derrett, “Initial Metacentric Height - an overview | ScienceDirect Topics.”

[23] A. Biran and R. L. Pulido, *Ship Hydrostatics and Stability*. Butterworth-Heinemann, 2013.

[24] C. D. R. Derrett and B. Barrass, *Ship Stability for Masters and Mates*. Elsevier, 1999.

[25] S. Chakraborty, “Ship Stability - Introduction to Hydrostatics and Stability of Surface Ships,” *Marine Insight*, Apr. 05, 2019. https://www.marineinsight.com/naval-architecture/ship-stability-introduction-hydrostatics-stability-surface-ships/ (accessed Jun. 12, 2021).

[26] “Aqwa Theory Manual - [PDF Document].” https://cupdf.com/document/aqwa-theory-manual.html (accessed Mar. 22, 2021).

[27] J. Excell, “The rise of the wind ships,” *The Engineer*, Feb. 19, 2020. https://www.theengineer.co.uk/wind-ships-marine-propulsion/ (accessed Jun. 12, 2021).

[28] Y. Ma, H. Bi, M. Hu, Y. Zheng, and L. Gan, “Hard sail optimization and energy efficiency enhancement for sail-assisted vessel,” *Ocean Engineering*, doi: 10.1016/j.oceaneng.2019.01.026.

[29] A. Ghigo, L. Cottura, R. Caradonna, G. Bracco, and G. Mattiazzo, “Platform

Optimization and Cost Analysis in a Floating Offshore Wind Farm," *Journal of Marine Science and Engineering*, vol. 8, no. 11, Art. no. 11, Nov. 2020, doi: 10.3390/jmse8110835.

[30] "Sea Fastening - an overview | ScienceDirect Topics," *Kingdom Drilling training*.

[31] Cult of Sea, "Stresses in Ships," *Cult of Sea*, May 18, 2016. https://cultofsea.com/ship-construction/ship-stresses/ (accessed Jun. 12, 2021).

[32] Freight Forwarder, "Ship motions at sea and their effects on cargo ships," *FFQO US*, May 31, 2019. https://www.freightforwarderquoteonline.com/news/six-types-of-cargo-ship-motions-at-sea-and-their-effects/ (accessed Jan. 18, 2021).

[33] Y. J. Yang and S. H. Kwon, "Prediction for Irregular Ocean Wave and Floating Body Motion by Regularization: Part 1. Irregular Wave Prediction," *undefined*, 2016. /paper/Prediction-for-Irregular-Ocean-Wave-and-Floating-by-Yang-Kwon/3dd2b15e6fb18fb96e99a4d8ff89bb192f0cebd3/figure/0 (accessed Sep. 22, 2020).

[34] J. J.M.J and M. W.W, "OffshoreHydromechanics." Delft University of Technology, 2001. [Online]. Available: https://ocw.tudelft.nl/wp-content/uploads/OffshoreHydromechanics_Journee_Massie.pdf

[35] "How to Write a Research Methodology in Four Steps," *Scribbr*, Feb. 25, 2019. https://www.scribbr.com/dissertation/methodology/ (accessed May 03, 2021).

[36] S. Savov, "Big Boat Hull | 3D CAD Model Library | GrabCAD." https://grabcad.com/library/big-boat-hull-1 (accessed May 03, 2021).

[37] ANSYS, "ANSYS Fluent User´s Guide".

[38] ANSYS, "DesignModeler User Guide," *ANSYS*.

[39] J. M. J. Journée, "Theoretical Manual of SEAWAY-M.Journee.pdf," *Delft University of Technology*.

[40] Brown University, "EN4: Dynamics and Vibrations." https://www.brown.edu/Departments/Engineering/Courses/En4/notes_old/Forcedvibes/Forcedvibes.html (accessed Apr. 27, 2021).

[41] E. W. Weisstein, "Reciprocal." https://mathworld.wolfram.com/Reciprocal.html (accessed Apr. 28, 2021).

[42] O. M. Faltinsen, "Sea Loads on Ships and Offshore Structures," *Cambridge Ocean Technology Series Cambridge University Press*.

[43] "Aqwa quadratic damping," *Boat Design Net*. https://www.boatdesign.net/threads/aqwa-quadratic-damping.42432/ (accessed May 05, 2021).

[44] Orcaflex, "Rayleigh damping." https://www.orcina.com/webhelp/OrcaFlex/Content/html/Rayleighdamping.htm (accessed

Apr. 26, 2021).

[45] D. T. Sen and T. C. Vinh, “Determination of Added Mass and Inertia Moment of Marine Ships Moving in 6 Degrees of Freedom,” *International Journal of Transportation Engineering and Technology*, Art. no. 1, Apr. 2016, doi: 10.11648/j.ijtet.20160201.12.

[46] H. Ghassemi, S. Majdfar, and V. Gill, “Calculations of the Heave and Pitch RAO ’ s for Three Different Ship ’ s Hull Forms,” *International Society of Ocean, Mechanical and Aerospace Scientists and Engineers*.

[47] M. Brendlinger, D. Gonzalez, P. Miguel, and S. Rutledge, “Sailboat Stabilization System,” *Faculty of Worcester Polytechnic Institute*.

[48] A. F. Molland, *The Maritime Engineering Reference Book: A Guide to Ship Design, Construction and Operation*. Elsevier, 2011.

[49] M. Martin, “Roll Damping Due to Bilge Keels,” *Iowa University Institute of Hydraulic Research (1958)*.

[50] M. Ridjanovic, “Drag coefficients of flat plates oscillating normally to their planes,” *Mechanical, Maritime and Materials Engineering*.

APPENDIX A

Input values for AQWA simulations are displayed in the figures below.

Details of Wave Frequencies	
Name	Wave Frequencies
Intervals Based Upon	Frequency
Encounter Frequencies Options	
Encounter Frequencies (Target)	40
Encounter Frequencies (Actual)	54
Display Encounter Frequencies	In Hydrodynamic Analysis Only
Incident Wave Frequency/Period Definition	
Range	Program Controlled
Total Number of Frequencies	50

Details of Wave Directions	
Name	Wave Directions
Visibility	Visible
Type	Range of Directions, Forward Speed
☐ Forward Speed	5,144 m/s
Required Wave Input	
Wave Range	-180° to 180°
Interval	45°
Number of Intermediate Directions	7
Optional Wave Directions A	
Additional Range	None
Optional Wave Directions B	
Additional Range	None
Optional Wave Directions C	
Additional Range	None
Optional Wave Directions D	
Additional Range	None

Details of Analysis Settings	
Name	Analysis Settings
External Operation before Solving	None
External Operation after Solving	None
Parallel Processing	Program Controlled
Generate Wave Grid Pressures	Yes
Wave Grid Size Factor	2
Common Analysis Options	
Ignore Modelling Rule Violations	Yes
Calculate Extreme Low/High Frequencies	Yes
Include Multi-Directional Wave Interaction	No
Near Field Solution	Program Controlled
Linearized Morison Drag	No
QTF Options	
Calculate Full QTF Matrix	No
Output File Options	
Source Strengths	No
Potentials	No
Centroid Pressures	No
Element Properties	No
ASCII Hydrodynamic Database	No
Example of Hydrodynamic Database	No
Generate AHD Pressure Output	No

Advanced Options	
Generate Internal Lid	Yes
Lid Element Size Definition	Program Controlled
Current Calculation Position	At Fixed Depth
Current Calculation Depth	0.0 m
Submerged Structure Detection	Program Controlled
Override Calculated GMX	No
Override Calculated GMY	No
Fixity Options	
Structure Fixity	Structure is Free to Move
Force Multiplying Factors	
Drag Multiplying Factor	1
Mass Multiplying Factor	1
Slam Multiplying Factor	0.0
Shear Force/Bending Moment Options	
Calculate Shear Force/Bending Moment	Yes
Neutral Axis	Global X
Neutral Axis Position Definition	Through Center of Gravity
Neutral Axis Y Position	1,79069993464509E-05 m
Neutral Axis Z Position	0.0 m

Details of Point Mass	
Name	Point Mass
Visibility	Visible
Activity	Not Suppressed
Point Mass Properties	
Mass Definition	Program Controlled
X	9,41359922289848E-02 m
Y	1,79071448656032E-05 m
Z	0.0 m
Mass	16175253,7353516 kg
Inertia Properties	
Define Inertia Values By	Radius of Gyration
Kxx	8,87 m
Kyy	66,525 m
Kzz	66,525 m
Ixx	1272618820,61088 kg.m²
Ixy	0.0 kg.m²
Ixz	0.0 kg.m²
Iyy	71584808659,3621 kg.m²
Iyz	0.0 kg.m²
Izz	71584808659,3621 kg.m²